A MATHEMATICAL MODEL
FOR
THE DESIGN AND EVALUATION
OF A
SOUND NAVIGATION
AND
RANGING (SONAR) SYSTEM

BY

EDMUND P. O'REILLY

A Design Thesis

Submitted to the Faculty of Graduate Studies

in Partial Fulfilment of the Requirements

for the Degree

Master of Engineering

McMaster University

September 1969

MASTER OF ENGINEERING (1969) McMASTER UNIVERSITY
(Design Engineering) Hamilton, Ontario

TITLE: A MATHEMATICAL MODEL to aid in the Design and Evaluation of a Sound Navigation and Ranging (SONAR) System

AUTHOR: Edmund Patrick O'Reilly, M.Sc.(Physics)

Agra University

SUPERVISORS: Dr. M. A. Dokainish

Dr. N. K. Sinha

NUMBER OF PAGES:

SCOPE AND CONTENTS: The literature on relevant parameters used in the model is reviewed.

A Rigid Mathematical Model and a Stochastic Model are developed to describe acoustic propagation in the medium.

The two models are used to determine bounds on the design parameters for a hypothetical shipborne SONAR System.

The System so designed is evaluated on the basis of measurements made at sea.

ACKNOWLEDGMENTS

The author benefitted greatly from the help and interest of a number of people. He would like especially to express his appreciation to Professors M. A. Dokainish and N. K. Sinha who, in supervising his studies, provided much stimulating guidance and encouragement. The author is grateful, too, for the interest shown by Mr. W. Chick and Mr. H. Webber in discussing many aspects of the work. Finally, the author wishes to express his deepest gratitude to his wife, Glenda, for her patient assistance and efficient typing of the manuscript.

Financial assistance was provided to the author by the Ford Foundation of Canada and by Canadian Westinghouse Company Limited, of Hamilton, Ontario.

TABLE OF CONTENTS

CHAPTERS Page

ABSTRACT

A Sonar System is usually designed to give a 50% Probability of Detection with a False Alarm rate of 1×10^{-3} at some specified Maximum Detection Range. The actual performance will be dependant upon the nature of the target and upon the Oceanographic conditions existing at the time of the trial.

Several constraints are automatically placed upon the System Designer. Cavitation usually places a peak power limitation on any shipborne system. Transducer size and weight are also constrained by ships' size, and hence an automatic upper bound is placed upon the beamwidth obtainable and Power output.

A model has been developed, in this Thesis, for the propagation of Sound Energy in the Ocean. This model consists of two portions in series with each other. The first portion is a Rigid Mathematical Model which is used to predict the mean values for Background Interference and Echo energy. The second portion is a Statistical model which attempts to predict the fluctuations, of interference and echo energy, about their mean values.

The Rigid Model is based upon Ray acoustics. The Statistical Model is based upon the Linear Time Varying Filter model developed by T. Kailath in [2].

A literature search has yielded parameters which can be associated with oceanographic conditions in the case of the Rigid Model. A thorough literature search of the unclassified literature failed to yield any values for parameters which could be used in the Statistical model.

The Rigid Model has also been related to System parameters such as Power output, Beamwidth, Pulse length and Frequency. This enables a Sonar System to be designed if its mean performance is first specified. It also enables a System with known parameters to be evaluated on paper for a given set of Oceanographic conditions.

The Rigid Mathematical model has been used to design a Shipborne Sonar System and the System so designed has had its performance assessed for three sets of oceanographic conditions which were measured in the North Atlantic.

NOMENCLATURE

m	Backward scattering coefficient, subscripts b,s,v refer to bottom, surface and volume respectively
C_o	Average Sound Velocity along a Ray Path
C	Velocity of Sound under stated conditions
τ_o	Standard Ping Duration
R^1	The dB equivalent of reverberation intensity
τ	Ping duration
r	slant range in yards
A	Transmission anomaly
$J(\theta)$	Reverberation index for the angle Subscripts b,s,v refer to bottom, surface and volume respectively
α	Absorbtion factor
S	Scattering strength. Subscripts b,s,v refer to bottom, surface and volume respectively
$(\frac{S}{I})$	Signal to interference ratio at the transducer face
R.D.	Recognition differential
G_1	Gain due to beamforming
G_2	Gain due to signal processing in the Receiver
p	Sound pressure level in dynes/cm^2 measured relative to one microbar at a distance of one yard from the source

NOMENCLATURE (contd.)

T.S.	Target strength
t_e	Duration of echo pulse
N_o	Noise spectral level in a 1 Hz bandwidth
DI	Directivity Index
ψ	Plane angle of the transducer beamwidth
ϕ	Solid angle beamwidth at the transducer
λ	Wavelength of transmitted energy
NF	Noise figure of array
$g_k(t)$	Time varying gain of the k th tap
F^*	Complex conjugate of F
*F	Convolution with F
L	Time delay spread of the medium
B	Frequency shift spread of the medium
W_o	output bandwidth of Receiver
	amount of variation of transmission function
η_d	Target Doppler shift
$a(\tau,\eta)$	Spreading function of medium filter model
$H(f,t)$	instantaneous transfer function of medium filter model
$g(\tau,\eta)$	interaction function of medium filter model
$\chi\|\tau,\eta\|$	cross ambiguity function of transmitted signal and receiving filter

LIST OF ILLUSTRATIONS

LIST OF ILLUSTRATIONS (contd)

LIST OF ILLUSTRATIONS (contd)

LIST OF TABLES

1. INTRODUCTION

A Sound Navigation and Ranging (SONAR) System can be defined and evaluated by the following parameters:-

1. Frequency of operation
2. The transmitted signal
3. Signal Processing in the Receiver
4. The transducer
5. Accoustical Power radiated.

The purpose of this Thesis is to develop a mathematical model for Acoustic propagation in the Ocean. The model shows the relationships which exist between the design/ performance parameters listed above and physical properties of the Ocean. This mathematical model is used to aid in the design of a Shipbourne Sonar System and the performance of the system has been derived under conditions which have been measured in the Ocean.

In order to analyze a system by modelling, we must consider both the system itself and a mathematical model which brings together in a formal and orderly manner all of the information which describes the behaviour of the system. The mathematical model may be composed of many parts, in many forms, including discrete states which the system may acquire under certain boundary conditions.

The model for each part of the system can often be formulated independantly of other parts of the system.

It is customary to divide mathematical models into two classes. In class I we have the Analytical Rigid Model and in class II we have the Numerical Probability Model. In most cases, when physical processes are involved, it is possible to formulate the system model in both of these forms and the one chosen will depend on the ease of solution. The Analytical Rigid Model is generally used when the various operations can be described without referring to statistical distributions. This type of model can be applied to probabilistic phenomena if we are prepared to deal with the mean values rather than with the distributions themselves. When the system is only describable in statistical terms, or if we are unwilling to tolerate the deviations from the mean which must be expected when using a rigid model, a probability model is necessary. In complex situations probability models can be easily handled by numerical methods such as the Monte Carlo method.

It must be noted here that two very definite

classes of probability models exist viz. time invariant models and time variant models. For time invariant models the Ergodic hypothesis is satisfied and hence the moments of the statistical distributions being modelled can be measured in the physical world as time averages. For time variant processes it has been shown [1], [2], [3], that the process may be modelled as closely as we wish by a tapped delay line filter with time varying tap gains. Such a model is shown in Fig.1.

Let us consider the mechanics of Echo Ranging in the Ocean. Every Echo Ranging system has two operational modes - a TRANSMIT mode and a RECEIVE mode. In the TRANSMIT mode a carrier is modulated with some intelligence and a power amplifier is used to transmit energy into the ocean via a suitable transducer. This transducer is usually made up of a number of elements arranged in a suitable mechanical configuration. Immediately after transmission the Echo Ranging system goes into the RECEIVE mode to enable it to pick up the energy scattered back to the transducer from any reflecting objects in the Medium. In the RECEIVE mode the transducer output is processed in a temporal signal processor the output of which is presented to a human

operator as an optical display together with an audible signal. The function of the signal processor is to conserve the modulation and destroy the background interference. It should be noted that, in general, the carrier itself plays no part in the target detection process. A target is generally said to be detected [4] when the operator has a 50% probability of correctly recognising it in the interference background with a specified false alarm rate. In both the RECEIVE and the TRANSMIT modes it is customary to make use of the elements of the transducer to synthesize an array. This array allows the transmission and reception to be concentrated in beams [5], [6] which can usually be rotated by the operator. This spatial beam forming enables the direction of the echo to be roughly located.

In deriving a model for the evaluation of systems' performance in the Ocean the following points have been considered:-

1. The velocity of sound in the sea is variable and is a function of depth. One result of this is that strong ducts are usually present.

2. For a point source radiating sound energy equally in all directions, larger volumes of water are insonified as we move farther away from the source.

The intensity of the propagated wave decreases as a function of range.

3. The echo from a target will be delayed by an amount which is a function of the velocity of sound in the water and the distance of the target.

4. The target is generally in motion and hence the returned echo will exhibit the Doppler effect.

5. The ocean is bounded, stratified, turbulent and contaminated. Reflections from these boundaries and contaminations will give rise to an interfering signal at the receiver. This interfering signal will be dependant on the nature of the transmitted signal.

6. There is always a broadband ambient noise background due to wind, wave motion, ocean fauna and shipping traffic.

A desirable model [7] is one which can be used to predict the results of echo ranging in the Ocean. Such a model will be used to predict the echo to interference ratio at the receiver output. Of necessity the model must involve all the parameters that determine how a signal, which returns as an echo from some reflecting object, is related to the signal which was originally transmitted. The model must show the relationship between all the parameters

affecting propagation and must involve expressions for all the effects and processes which the research scientist can measure under practical situations.

In this Thesis the echo is modelled by an analytically rigid model in series with a stochastic model. The rigid model describes the average echo energy at the transducer face as the outcome of several factors viz.

1. Source energy per unit solid angle
2. Transmission losses in the medium
3. Time delay
4. Doppler effect.

The stochastic echo model describes the variations in target reflectivity in the form of a time invariant model.

The interference energy is derived as the sum of two models - one signal dependant and the other a function of ambient sea noise and sonar platform noise. The signal dependant interference is again made up of a rigid model in series with a stochastic model. The rigid model describes average losses due to reflections from boundaries and inhomogenities in the medium, while the stochastic model will be of the time variant form in order to describe multipath and dispersive scattering in the medium. The model for ambient sea noise and

sonar platform noise is a time invariant stochastic model.

The gain due to beam forming of the transducer elements is modelled [5] by an additive array which is described on the basis that the noise background is uncorrelated from element to element of the array while the signal has perfect correlation along some direction.

In Section 4 the mathematical model is used to design a Shipbourne Sonar System to an intuitively developed specification.

As part of the author's work at Canadian Westinghouse he was permitted to make certain oceanographic measurements. These oceanographic measurements are used in Section 5 to evaluate the performance of the System designed in Section 4.

1.1. Literature Search on Reverberation

General Background

An attempt will be made to summarize the present experimental knowledge of under sea reverberation as recorded in the unclassified literature.

Reverberation is energy which is scattered back to the source by irregularities in the medium. If these irregularities extend over a large volume of the medium then the sound beam may only change direction and lose little energy. However, small inhomogenities in the medium may cause an energy loss from the beam. Some of this "lost" energy will return to the source in the form of an echo.

Reverberation is therefore caused by such discontinuities as air bubbles, suspended solid matter, marine life, thermal patches, and density fluctuations in the ocean. The amplitude of the resultant reverberation follows a Rayleigh distribution [9] and the phenomena is characterised by being narrow band and similar to those displayed by a target echo and therefore effectively masks a 'wanted' target return.

1.1.1. Definitions of terms

Undersea reverberation

According to Naval tradition reverberation is classified into three categories according to the part of the ocean from which the sound is thought to return.

A) Surface reverberation is caused by scattering from the irregular sea surface and from bubbles and other inclusions near the sea surface.

B) Bottom reverberation is due to reflection from rough bottom topography, from the specular nature of the bottom material, and to scattering from inhomogenities in soft silts which are penetrated by the sound.

C) Volume reverberation occurs when the sound pulse reflects from marine organisms, from turbulence, and from temperature or salinity gradients distributed through the body of the ocean.

Reverberation limited condition

A reverberation limited condition is one in which detection is limited by the reverberation part of the sonar background noise.

Echo

An echo is a returning sound wave which has sufficient magnitude and delay to be identified as a

wave distinct from the original transmission which gave rise to the echo.

1.1.2. The Classic of Underwater Reverberation Literature:- "Physics of Sound in the Sea"

"Physics of Sound in the Sea", was written at the end of World War II as a result of a program designed to accumulate information which would be directly useful in submarine operations. This document is remarkable for the care with which the assumption used are stated and justified.

Chapter 12 of "Physics of Sound in the Sea", is devoted to the mathematical formulation of the theory of reverberation. The assumptions utilised in the formulation of this theory are enumerated below:-

I) Reverberation is scattered sound.

II) Scattering from an individual scatterer begins the instant sound energy begins to arrive at the scatterer and ceases at the instant sound energy ceases to arrive at the scatterer.

III) Multiple scattering has a negligible effect on the intensity of the received reverberation i.e. the major portion of reverberation is made up of sound which has been scattered only once.

IV) The intensity of the sound scattered backwards from a small element of volume dv is directly proportional to each of the following three quantities:-

a) the volume occupied by dv

b) the intensity of the incident sound

c) a backward scattering coefficient m which depends only upon the properties of the ocean near dv

d) The average reverberation intensity, which is a function of the time elapsed since the emission of the ping, is the sum of the average intensities received simultaneously from the individual scatterers in the ocean.

Besides the basic assumptions listed above there are also other assumptions which are implied by the mathematical development. These assumptions are:-

i) Fermats principle applies i.e. the sound which returns to the origin from the insonified volume traverses the same ray path traced out by the sound incident on the volume.

ii) The transmission loss on the path from the source to the scattering volume is equal to that in the return direction.

iii) The extension of a sound ray between the leading and following bounding surfaces of the

insonified volume is equal to $c_o \cdot \frac{\tau}{2}$ where c_o is the average sound velocity along the ray and τ is the ping duration.

iv) The transmission loss in the ocean depends only on the distance traversed by the ray entering or leaving the transducer and not at all on the direction of the ray.

v) Scattering in the ocean is independant of the initial ray direction.

vi) Sound travels from the source to the insonified volume along only one path.

1.1.3. Definition of Terms used in "Physics of Sound in the Sea".

a) Reverberation

Reverberation is a component of the background noise heard in echo ranging gear. It is distinguished from the general noise background by the fact that it is directly due to the pulse put in the water by the gear. The travelling ping meets not only the desired target but also many small scattering centers, each of which returns a tiny echo. These tiny unwanted echoes combine to make up reverberation.

b) Reverberation intensity

The strength of the reverberation sound depends not only upon the intensity of the backward scattered

sound in the water near the receiver but also on the nature of the receiver. The intensity of the reverberation actually heard or recorded after the sound in the water, has been converted to electrical energy, by the receiver, amplified, and passed on to the observer, is called the reverberation intensity.

c) Reverberation level

The reverberation level R' is the decibel equivalent of the reverberation intensity, expressed relative to some arbitrary standard.

Reverberation intensities are proportional to the ping duration. We define the standard ping duration as $\tau = 100$ m.seconds and the standard reverberation level R as

$$R = R' + 10 \log \frac{\tau_0}{\tau}$$

d) Backward scattering coefficients

Backward scattering is sound scattered back along the incident ray path. If there is only one ray path from the projector to the scatterers, only sound which is scattered directly backward gives rise to reverberation. The efficiency of a small volume of the ocean in scattering sound backward is specified in terms of the backward scattering coefficient. This value is defined by:-

$$E = \frac{m_v}{4\pi}$$

where E = the average energy scattered by the volume per second per unit of incident intensity per unit solid angle in the backward direction. The factor 4π ensures that the average energy scattered in all directions per second per unit incident intensity will be m_v for the case of isotropic scattering.

e) Deep water reverberation levels

In deep water the reverberation heard at ranges past 1,500 yards is almost always volume reverberation. At shorter ranges surface reverberation may exceed volume reverberation if the sea state is sufficiently high and the transducer beam is horizontal. Pointing a directional transducer downwards will usually cause surface reverberation to be less than volume reverberation at all ranges past 100 yards.

f) Volume reverberation levels

The expected volume reverberation level $R_v(t)$ at a time τ seconds after midsignal is

$$R_v(t) = 10 \log\left(c_o \frac{\tau}{2}\right) + 10 \log m_v + J_v - 20 \log r - 2A$$

c_o = sound velocity in yds./sec.

τ = ping duration in seconds

m_v = volume scattering coefficient

J_v = volume reverberation index

r = range in yards of the reverberation

A = total one way transmission anomaly to range

A_1 = one way transmission anomaly to range due to the effect of refraction.

Surface reflections will increase the reverberation levels predicted by the above equation by about 30 dB.

If the transmission anomaly terms can be neglected and is constant throughout the relevant portion of the ocean, then the intensity of volume reverberation should drop 20 dB for each tenfold range increase (Inverse - square law). It should be noted that in general the transmission anomaly terms cannot be neglected beyond 1000 yards.

The only frequency dependant terms in the above equation are J_V and m_V. J_V can be determined from the directivity function of the transducer. m_V can very roughly be estimated from the results of transmission studies. Chapter 14 in "Physics of Sound in the Sea", concludes that 10 log m_V varies from about -50 dB to -81 dB without -71 dB being typical.

g) Surface reverberation

The expected surface reverberation level at a time τ seconds after midsignal is given by the formula:-

$$R_s(t) = 10 \log\left(c_o \frac{\tau}{2}\right) + 10 \log m_s + J_s(\theta) - 30 \log r - 2A$$

m_s = backward scattering coefficient of the surface scattering layer

θ = angle between the sound returning at time and the horizontal plane

$J_s(\theta)$ = surface reverberation index for the angle θ

A = transmission anomaly along actual ray path to surface.

Measured values of surface reverberation levels with a horizontal beam are usually 6 dB higher than those predicted by the equation.

At short ranges $R_s(t)$ should be proportional to the inverse cube of range provided that m_s and $J_s(\theta)$ also change negligibly with increasing range. This simple inverse cube relationship is observed only rarely because of the following factors:-

I) Refraction bends the sound path away from the surface

II) The scattering coefficient itself is a function of grazing angle

III)There is appreciable attenuation in the near surface layer

IV) The surface sea waves tend to produce a sound shadowing effect

V) Interference takes place between direct and

surface reflected waves.

At ranges beyond 1,500 yards the received reverberation does not depend upon wind speed and is usually ascribed to being due to volume reverberation. At a range of 100 yards, however, as the wind speed increases from 8 mph the reverberation level rises sharply in a manner roughly described as the seventh power of wind velocity. There is little increase in level due to wind speeds of 0 mph to 8 mph when the ship's speed exceeds twenty knots.

h) Bottom reverberation levels

Bottom reverberation only plays a prominent part in the case of horizontal transmissions in shallow water.

The expected bottom reverberation level at a time t seconds after midsignal is:-

$$R_b(t) = 10\log\left(c_o \cdot \frac{\tau}{2}\right) + 10\log\left(\frac{m_b}{2}\right) + J_b(\theta) - 30\log r - 2A$$

m_b = scattering coefficient

$J_b(\theta)$ = bottom reverberation index

θ = angle of depression to the horizontal.

With beams and transducers near the surface the observed bottom reverberation levels will average about 6 dB higher than the levels predicted by the above equation (due to surface reflections).

Because of the distance between the transducer and the bottom, bottom reverberation does not set in until a significant time has elapsed after the ping. Usually the reverberation then quickly builds up to a peak corresponding approximately to the time when the edge of the beam strikes the bottom. After the peak the reverberation falls off rapidly (usually as the fourth power of the range).

The range to the bottom reverberation peak depends on refraction conditions and the water depth. In isothermal water the peak is expected at about twelve times the water depth. m_b and $J_b(\theta)$ are only slightly dependant upon range for ranges past the reverberation peak.

$J_b(\theta)$ and m_b are dependent upon frequency. $J_b(\theta)$ can be determined from the pattern function of the transducer and m_b can be estimated from tabulated measurements.

Bottom reverberation levels are not the some over all types of bottoms. The highest reverberations are observed over rock, lower values over mud or sand and mud and the smallest values over sand bottoms.

i) Fluctuation

There is always some variation between reverberation from successive pings. This short time fluctuation is

measured by the variance of the reverberation intensity at a time τ seconds after midsignal.

If we regard reverberation as the resultant of a large number of small amplitudes of random phase, then the probability P that the reverberation intensity will exceed the value I is

$$P = \exp\left(I/\bar{I}\right)$$

$\bar{I}$ = the average intensity

$(\bar{I})^2$ = the variance.

j) Coherence

Over here the term coherence refers to a tendency of the reverberation in the form of pulses or blobs about the length of the ping. The degree of coherence can be described mathematically in terms of ρ, the correlation coefficient between the reverberation intensities at two different times on the same record. For square top pings and the intensity distribution defined by

$$P = \exp\left(-I/\bar{I}\right)$$

we have

$$= \left(1-\frac{\alpha}{\tau}\right)^2 \text{ for } \alpha \leq \tau$$

$$= 0 \quad \text{for } \alpha \geq \tau$$

where $\alpha = |\tau_1 - \tau_2|$

τ = ping length.

k) Frequency spread

It is assumed that reverberation has the same

spectrum as the ping.

1.1.4. Recent research

In the mid 1950's there began what can only be described as a "research explosion" in undersea reverberation. Most of the experimental papers published within the last decade are concerned with obtaining quantitative evaluation of scattering strengths. These papers form the basis of the summary which is to follow. Two comments are relevant at this stage.

(1) In attempting to adhere to the theoretical foundation laid down in "Physics of Sound in the Sea", many researchers have been forced by the inadequacy of their sonar equipment to introduce new (and largely undefined) parameters to describe the scattering process.

(2) Other researchers have abandoned completely the concepts of "Physics of Sound in the Sea", and redefined terms which are far easier to measure with existing Sonar equipment.

As a consequence of the above two facts some of the fundamental definitions will now be closely examined and some of the newly adopted parameters will be defined.

1.1.5. Definition of terms used by modern Researchers

The scattering properties of the body of the ocean were traditionally described in terms of a scattering coefficient 10 log$m$. The quantity m was defined to be the total power that would be scattered by unit area or volume, per unit intensity of an incident plane wave, if the scattering in all directions were equal to that in the direction of observation. For volume reverberation the definition may be illustrated with reference to Fig.2. A plane wave of intensity I_i is incident upon a small volume dv centered at Q. If I_s is the intensity of the scattered sound at P which is distant one yard from Q then the total power scattered by the volume Δv is $4\pi \cdot I_s$ and m_v is defined by:-

$$10 \log m_v = 10 \log \frac{4\pi \cdot I_s}{\Delta v \cdot I_i}$$

where m_v has the dimension yards^{-1}.

Similarly for surface and bottom we have

$$10 \log m_{s,b} = 10 \log \frac{2\pi \cdot I_s}{A_{s,b} \cdot I_i}$$

Modern researchers have found it easy to get an estimate of the ratio of echo strength to the reverberation interference. It would therefore be handy to define reverberation in terms of a parameter

which can be compared directly with the target strength of a known target. Thus, reverberation can be expressed in terms of scattering strength which is the ratio, expressed in dBs, of the scattered intensity at unit distance from unit volume (or unit area), to the incident intensity i.e.

$$S = 10 \log \frac{I_s}{I_i}$$

I_s = scattered intensity at 1 yd

I_i = incident intensity.

We therefore have the relationship between S and m defined by the equations:-

$$S_v = 10 \log \frac{m_v}{4\pi}$$

$$S_{b,s} = 10 \log \frac{m_{s,b}}{4\pi}$$

Volume reverberation excited by explosions

The use of a non directional explosion to study the vertical distribution of volume scattering coefficients is described in [9]. The merit in this method lies in the fact that such an explosion is very intense over a wide range of frequencies.

The experiment is analysed in terms of the time curve of received reverberation intensity I(t). The source strength is defined in terms of E, and an integral over the solid angle of the energy flux per

unit solid angle of the omnidirectional shock wave. The analysis problem resolves itself into finding the $m(z)$ which best fits the echo trace in time. It was found that the depth distribution of scatterers is given by the curve $t^2 \cdot I_t$ multiplied by the slope of the curve $t^{(n+3)} \cdot I_t$ plotted against t on a logarithmic scale.

For research done on the deep scattering layer Chapman and Harris [10] fitted the expression

$$I(t) = \frac{2E}{c^2 \cdot t^3} \int_D^{D+\Delta} m(z) \cdot dz$$

to a reverberation trace which falls off as $\frac{1}{t^3}$ and have reported the results in terms of the integral

$$\int m(z) \cdot dz$$

The average scattering strength in this case is

$$10 \log \bar{m} = 10 \log \left(\frac{m_v}{4\pi} \right)$$

where $\bar{m}$ is given as

$$\bar{m} \Delta = \int_D^{D+\Delta} m(z) \cdot dz$$

Δ = thickness scattering layer.

Thus the average deep scattering layer strength is:-

$$10 \log \int m(z) \cdot dz - 10 \log \Delta$$

where Δ has to be estimated. Chapman and Harris [10]

report that for a scattering layer thickness of 100 yards to 300 yards

$$10 \log \Delta = 20 \text{ dB to } 25 \text{ dB}.$$

Similar results are also reported in [11] and [12].

1.1.6. Surface backscattering strength using explosive charges

Models similar to the mathematical model described in 1.1.5. have been adopted in [13], [14], [15], [16], [17] to derive equations for surface scattering strength. These papers and subsequent work described in [18] successfully extended the study of surface scattering to very low frequencies.

1.1.7 Non specular scattering

A very exhaustive theoretical treatment of non specular scattering of underwater sound based upon (assumed) spectrum statistics of surface roughness has been developed in [19] and [20], [21]. Elegant though this treatment may be it is very difficult to relate the assumed spectral statistics to observable phenomena such as wind velocity, wave height or sea state.

1.1.8. A summary of present knowledge of reverberation

The available experimental data have been collected on supplementary curves from which certain

broad conclusions can be drawn. All the data has been reduced to common parameter, namely scattering strength. In spite of this however there is still a wide range of observed values for the scattering coefficients. This scatter is most possibly due to the fact that the scattering strength is really a function of several parameters such as sea state, grazing angle, bottom roughness etc.. When we attempt to plot scattering strength as a function of a single factor alone (say bottom roughness in the case of bottom reverberation) then the affect of the other contributing factors is to produce a scatter in the graph. This is better expressed by saying that scattering strength depends on a number of quantities and plotting the data against any one of them leaves the variability due to the others to appear as scattered data.

It should also be noted here that the scattering coefficient is calculated from the equation.

Reverb level = Source level + 10 log (reverberating volume) + volume scattering strength - two way transmission loss .

Local properties of the ocean govern not only the attenuation suffered over a given distance but also the

length of the distance itself (curvature of the ray path due to temperature gradients). The uncertainties in being able to guess accurately the two way transmission loss contribute directly to the spread in observed scattering strengths. In practice most experimenters use:-

$$\text{Transmission loss} = 20 \log r + \alpha \cdot r$$

r = range

α = absorbtion factor

This formula only applies to straight line transmission along a single path in a homogeneous medium due to spherical divergence. The actual transmission loss is known to vary from this by as much as 15 dB for simple short paths and by considerably more for paths involving multiple reflections.

1.1.9. Volume reverberation

The assumption has been made [22] that the distribution of scatterers is uniform in the ocean. Measurements indicate that scattering strength decreases slowly with depth as a direct result of the decrease in the density of marine life with depth. In the absence of (or above and below) the deep scattering layer, the scattering strength diminshes as the rate of approximately 0.5 dB per 100 feet having a value of -77 dB at 300 feet and -91 dB at 3,000 feet.

A summary of the data on volume scattering strength is given in Fig.3 as a function of depth. Despite considerable scatter there is a trend to decreasing scattering strength at greater depth. There is approximately 26 dB scatter over the data. Fig.4 gives a summary of the data on scattering strength as a function of frequency. There is some indication of increased scattering with increasing frequency but the information is too sparseto enable this to be confirmed.

1.1.10. Volume scattering from a near surface layer

The near surface layer has been postulated to account for scattering which is relatively constant with increasing range for grazing angles of $\leq 10^{\circ}$. The scattering strength of this layer is dependant upon wind speed and sea state. Except in very calm seas, the scattering in the near surface layer tends to mask [23] and [24] the true surface roughness scattering which according to theory [13] and some observations [17], [25], [13] and [19], drops sharply for low values of grazing angle. This surface layer is less than 200 feet thick and reverberation in it is mostly due to air bubbles caused by wind and waves and by floating debris stirred into the water by wave motion.

1.1.11. Volume scattering from the Deep scattering layer

The term deep scattering layer is used to describe [26] the concentration of marine animals which make an appreciable vertical diurnal migration, moving closer to the surface at sunset and away from it at dawn. The concentration of these marine animals is not uniform over the entire volume of the ocean and experiments [26], [27] have established the existence of sudden increases in reverberation level limited to specific depths. This increased scattering is universally accepted to be due to the swimbladders of several different types of bathypelagic fish. The layers of concentration of these fish vary from 150 feet to 600 feet thickness.

The deep scattering layer is the most striking feature of reverberation from the ocean volume. There has been careful documentation of the reverberation properties of these layers in [22], [26], [27], [28], [9] and [12].

a) Diurnal depth migration

The deep scattering layers migrate in depth in a diurnal cycle moving between depths of less than

400 feet to depths of 2000 feet. The rate of ascent is of the order of 600 feet per hour. There is considerable evidence to suggest that the fish which cause the scattering are photophobic so that the speed of the migrations depends to some extent on the number of hours of twilight.

b) Frequency migration

According to 11 the scattering from layers in the western North Atlantic is strongly frequency dependant. In the North Atlantic three classes of layers have been found:- a high frequency layer (20 - 24KHz), an intermediate frequency layer at (8 KHz - 16 KHz), and a low frequency layer in the neighbourhood (2 KHz - 4 KHz). Some high frequency layers show a 5/6 power dependance of resonant frequency on pressure but other high frequency layers neither migrate nor exhibit this power dependance on resonant frequency.

Some intermediate frequency layers migrate in depth with corresponding frequency migration changing as the square root of pressure. On the other hand a layer has been observed which migrates through a considrable depth range without changing its peak

frequency at all. Some intermediate frequency layers do not migrate at all.

The study of low frequency scattering layers in the region 2.5 KHz to 5 KHz has been constrained by the inadequate resolving power of the equipment used to study them.

c) Variation with depth

The scattering strength within the deep scattering layer is relatively constant irrespective of the position of the layer i.e. close to the surface at night or deep down during the day. Fig.5 shows a plot of scattering strength vs. frequency of the deep scattering layer at the depth it was encountered.

d) Variation with frequency

There is inconclusive proof to indicate that scattering strength increases according to Rayleigh scattering as the fourth power of frequency up to about 5 KHz, above which there is no further dependance on frequency.

e) Variation with season

There is considerable evidence of seasonal variations in the observed volume reverberation levels. It is plausible to postulate that this seasonal

variation is caused by to some extent by seasonal variations in the production of phytoplankton. No conclusive proof however exists.

1.1.12. Bottom reverberation

The nature of the bottom profoundly effects the scattering coefficient. In [29] it has been shown that it is possible to divide ocean bottoms into the following groups:-

(1) silt and mud

(2) sand

(3) rock and gravel.

Within any one of the groups ennumerated above there is no evidence of correlation between scattering coefficient and particle size.

a) Variation with grazing angle

For grazing angles up to the critical angle scattering increases with grazing angle according to $\sin\theta$ or $\sin^2\theta$ depending upon the type of sediment. For θ greater than the critical angle, attenuation within the bottom decreases the available energy and the apparent scattering strength is stabilized.

The formula below was postulated in [30] and [31]

$$S_b = 10 \log \mu \sin^k \theta$$

where

μ = bottom scattering strength = $\frac{m_b}{2\pi}$

at the normal incidence for a given type of bottom. Mackenzie [30], [31], [32] reports that $\mu = -28$ fits all the mud data reasonably well.

b) Variation with frequency

[31] and [34] report that no observable dependancy on frequency exists for scattering from a mud bottom. In [29], and [33] it is reported that backscattering increases with frequency according to the 1.6 power for sand bottoms. No one has reported any frequency dependancy in scattering from rock bottoms.

1.1.13. Surface reverberation

As in the case of bottom reverberation surface scattering is a function of the angle of incidence. Near normal incidence specular reflections from wave facets and sea swell are the cause of the reverberation. At angles between 10° and 40° roughness scattering is the major cause of reverberation. At angles less than 10° the scattering depends upon sea state and is usually small compared with volume scattering from the surface layer if the sea is relatively calm. Total reverberation is largely independant of surface conditions beyond 1,500 yards.

a) Dependancy on grazing angle

In [34] the surface scattering strength is

determined as a function of grazing angle, and wind speed. Similar results have also been produced in [13].

The equation:-

$$S_s = -36 + 40 \log(\tan\theta)$$

is derived in [19].

This formula yields results which appear to be valid only for data taken in very low sea states.

In [10] R. P. Chapman and J. Harris have fitted an empirical equation to surface scattering in octave bands from 400 Hz to 6,400 Hz. They noted that at low grazing angles volume reverberation from biological scatterers in the subsurface layer frequently masked the surface reverberation. At grazing angles of the order of 40° the surface scattering appears to be independant of frequency. The Chapman and Harris formula is:-

$$10 \log S_s = 3.3\beta \cdot \log\left(\frac{\theta}{30}\right) - 42.4 \log\beta + 2.6$$

where

$$\beta = 158\, v \cdot f^{-\frac{1}{3}} - 0.58$$

v = wind speed in knots

θ is in degrees

f is in Hz.

In a later work [17] Chapman and Scott prove that at low wind speeds, surface scattering strengths are

independant of acoustic frequency. This is presumably due to the fact that the scale of roughness of the oceans surface is appreciably greater than the wavelength of the radiation. At low wind speeds therefore, the predominant source of surface scattering is ocean swell. In this paper it is also pointed out that for grazing angles greater than 60° specular reflections from wave facets form the major portion of the surface scattering.

b) Variation with frequency

In [10] the formula used to fit the experimental data was:-

$$= 3.38\beta \cdot \log\left(\frac{\theta}{30}\right) - 4.24 \log\beta + 2.6$$

where $$\beta = 158\, f^{-1/3} - 0.58$$

i.e. there is some dependancy on frequency. The range of frequencies used during the experiment is so small that it is not possible to verify this dependancy on frequency.

c) Variability of surface scattering

The scattering can directly be deduced from the statistics of the roughness of the surface velocity to the second or third power for both low and high frequencies. See [10], [24], [35], [36] and [37] and [16].

1.1.14. Frequency spreading

The widening of the reverberation spectrum can be caused by several factors [38]. These factors are:-

a) own ship Doppler [52]

b) Finite transducer beamwidth

c) Random motion of the scatterers.

The observed spectral spreading is so small that it can be assumed to be negligible except in the cases of very long pulses. Theoretical analyses of frequency spreading have been given in [39], [40], [41], [42] and [43].

1.1.15. Fluctuation

Reverberation returns do not decay smoothly with time. Very rapid changes are noted within intervals of the same duration as the ping. These rapid swings of amplitude are thought to be due to the following causes:-

(1) interference from different scatterers

(2) range dependancy in the mechanism producing the scattering

(3) changes in transmission loss

(4) movements in the transducer platform.

[44] shows that a Rayleigh distribution best fits the short term fluctuations in reverberation amplitude.

An expression has been developed in [45], [46] and [47] for a coefficient of amplitude variation as a function of fluctuations in refractive index. The continous movement of these patches of inhomogenity will cause amplitude fluctuations by focussing and de-focussing the incident sound. Mathematical expressions for the average fluctuation magnitude and it's distribution as a function of system and medium parameters are necessary to affect any quantitative description of the process.

An experiment designed to study long term fluctuation in the reverberation amplitude is described in [48] and [51]. The experiment established that long paths in the ocean remain remarkably stable over rather long periods.

1.1.16. Coherence

The envelope of the reverberation trace changes very gradually. These slow changes are usually described by saying that the reverberation coheres in blobs. This reverberation coherence is less pronounced than that experienced in the case of target echoes.

The spatial coherence of the reverberation signal was investigated in [49]. It was found that the volume reverberation returns received on pairs of vertically separated hydrophones are substantially uncorrelated.

The highest correlation is obtained [50] for bottom returns at normal incidence. This correlation is degraded by increasing the spacing between the hydrophones.

1.1.17. The effects of ice

Measurements have been made in the Arctic circle to study the effect of ice on reverberation. These measurements are described in [52], [53] and [54].

1.1.18. Theoretical treatments of Reverberation based upon Wave Theory

Several papers [55], [56], [57] and [58], have attempted to explain the reverberation theory in terms of wave theory and Lame' parameters. In general these papers do not identify the phenomena in terms of parameters which yeild readily to experimental verification.

1.2. A literature search on Ambient Sea Noise

General Comments

Ambient noise is the interference that is due to natural conditions or sources in the medium. It is a property of the medium itself at the time and place of observation, irrespective of the hydrophone and the platform that is used to observe it. The ambient noise level is expressed in terms of the level of an equivalent isotropic noise field at the observing transducer. Such an equivalent field is one that would produce, at

the transducer output, a response equal to the actual noise present. In [59] it is shown that in any given region of the frequency spectrum, one or more noise sources are dominant and the combination of the other sources can usually be ignored.

The following list has been compiled to show the commonly recognised sources of ambient noise.

1. Thermal noise due to molecular agitation of the medium [60]. This is most important in deep water at frequencies above 50 KHz.

2. Surface noise which is a result of wave height and wind speed. This source of noise dominates the frequency band 100 HZ to 50 KHz.

3. Biological noise caused by marine life [61] and [62].

4. Man made noise from other ships [63] and from industrial noise from other ships and from industrial noise in and near busy harbours. This source of noise is restricted to frequencies below 1 KHz.

5. Rain noise [64].

6. Flow noise as a result of current flow. This source is generally restricted to very low frequencies.

7. Terrestrial noise from earthquakes, wind storms.

1.2.1. Thermal noise

Thermal agitation due to molecular motion in the water is dominant in the frequency range of 50 Hz to 200 KHz. depending upon the Sea State. By assuming that the average energy per degree of freedom is KT and that the number of degrees of freedom in a large volume of water is equal to the number of compressional modes in that volume, R. H. Mellen has shown in [65] that the equivalent noise spectrum level is

$$N = 115 + 20 \log f$$

in dB s relative to one microbar in a 1 Hz bandwidth at a temperature of about 15°C when f is in KHz.

This noise is the same as the Nyquist noise developed in the radiation resistance of the hydrophone in water and has been measured experimentally by Ezrow [60]. The spectrum level obviously decays at a rate of 6 dB/octave with frequency due to the 20 log (f) term.

1.2.2. Surface noise

Surface noise predominates in the frequency range 1 KHz to 50 KHz the major source of ambient noise appears to be the wind and the wave height. Extensive measurements of ambient noise in the frequency range of 1 KHz to 50KHz were made during World War II and have been summarized in [65] by V.O. Knudsen. In this report and in [66]

the spectrum of deep sea water noise is plotted as a function of frequency and sea state. The scale commonly used to define sea state along with distinguishing characteristics has been reproduced in Table 1. The Knudsen curves are reproduced in Fig.16 and they show clearly that at all sea states the spectrum level decreases about 5 dB/octave and that the intensity varies approximately as the 1.8 power of wind speed - which seems to imply that the noise originates at the surface.

Wenz in [66] and [67] has developed a theory that the wind dependant ambient noise is largely caused by bubbles in the ocean i.e. the wind causes the bubbles to oscillate or collapse. Wenz also considers the possibility of the noise being due to the pressure save at a depth which is caused by oscillations of the fluid surface. He concluded however that noise due to the latter source would be restricted to frequencies below 10 Hz.

1.23. Biological noise

Biological noise is important only in shallow coastal waters. The noise produced by marine organisms has been studied and summarized by M. D. Fish in [61] & [62]. Two types of marine organisms in particular are known to be a source of noise. These are the snapping shrimp and croakers.

1.2.4. Man made noise

Man made noise predominates in busy harbours and shipping lanes. Fig.20 shows typical measurements taken from [66]. For comparison Fig.20 also shows the deep water ambient sea noise for Sea State No.2.

1.2.5. Rain noise

In [64] and [68] an increase of 12 dB in a 1 Hz bandwidth as a result of steady rain is reported. Rain noise is shown in Fig.18.

1.2.6. Correlation

Measurements [69] on the correlation of ambient sea noise indicate that the noise is truly Gaussian and "white" over the spectrum 10 Hz to 100 KHz.

1.2.7. Directionality of ambient noise

Studies [70], [71] on the directional properties of ambient sea noise show some relationship with depth [70].

The Analytical Rigid Models

2.1. The Analytical Rigid Models

General Comments

In the following sections a series of analytical rigid models will be derived following the proceedure outlined in [71], [72] and [73]. The overall rigid model will be in the form:-

$$\left(\frac{S'}{I'}\right).G_1' G_2' = R.D'. \quad \ldots\ldots\ldots\ldots(1)$$

where

$\left(\frac{S'}{I'}\right)$ = echo - to - interference ratio at the transducer face

G_1' = gain in $\left(\frac{S'}{I'}\right)$ due to beam forming

G_2' = gain in $\left(\frac{S'}{I'}\right)$ due to signal processing in the Receiver

$R.D'.$ = the $\left(\frac{S'}{I'}\right)$ ratio which is required at the receiver output for a 50% probability of detection at a specified False Alarm rate.

Because of the large numbers that are involved it is easier to work with the logarithms of the quantities defined in Eqn.1. The rigid model is therefore developed in the form:-

$$S - I + G_1 + G_2 = R.D. \quad \ldots\ldots\ldots\ldots(2)$$

where

$$S = 10 \log \left(S'\right)$$

$$I = 10 \log (I')$$
$$G_1 = 10 \log (G_1')$$
$$G_2 = 10 \log (G_2')$$
$$R.D. = 10 \log (R.D.')$$

In order to derive a model for the mean echo energy S we will first derive a model for the average source energy transmitted by the transducer. By subtracting the two way propagation losses in the medium and adding the gain produced by reflection from a target we can obtain the mean returned energy (echo energy) at the transducer face. The model for echo energy is shown conceptually in Fig.7.

When the transducer radiates energy into the water some fraction of this energy is scattered from the medium boundaries and from the many inhomogenities that are always present in the volume of the medium itself. The portion of the scattered energy which returns to the transducer can be regarded as interference which is dependant upon the transmitted signal energy. This form of interference is known as reverberation. In addition to the reverberation there will also be interference due to the following causes:-

1. Ambient sea noise caused by wave motion, breakers, distant shipping and marine life.

2. Sonar platform noise caused by propeller noise, machinery noise, turbulence and water movement within the transducer dome. The rigid model for interference energy is shown conceptually in Fig.8.

2.2. Average Source energy at the Transducer

The source energy of the transmitted signal is a function of several parameters. For easy manipulation we follow Urick [71] and express the source energy in terms of the energy density which is produced by the source in the direction being considered at a distance of one yard. The energy density is usually represented in dB relative to the energy density of a plane wave of r.m.s. pressure one dyne/cm for an interval of one second. For sinusoidal square topped pulse we have:-

$$E = I_o + \log t_o \quad \text{dB's} \quad ..(3)$$

where

E = energy density relative to the energy density of a plane wave of rms pressure one dyne/cm

I_o = intensity level of the source at a distance of one yard

t_o = duration of the pulse in seconds.

For an isotropic radiating point source the radiated power will flow through successively larger areas as the distance between the point of observation

and the source increases. The intensity I_r of the sound wave at any range r is defined as the sound power flowing through unit area situated at range r from the source. By considering the intensity of sound I_r at the surface of a sphere of radius r drawn about the source, we obtain

$$I_r = \frac{P}{4\pi \cdot r^2}$$

where

P = power in ergs/sec

r = radius of the sphere in cms.

It should be obvious that if P is measured in watts then I will be in watts/cm^2.

When a source radiates sound energy into the water it generates an alternating pressure. This alternating pressure is easily measurable and hence it is usual to specify [74] the pressure. Sound power is given by

$$P = \frac{p^2 \cdot A}{\rho \cdot c}$$

where

A = area through which sound flow is measured in cm^2.

p = sound pressure in dynes/cm^2

ρ = density of the medium in

c = velocity of sound in the medium.

If I is measured in watts/cm , p in dynes/cm^2 and the

product $\rho.c$ is in gms/cm^2 · sec then

$$I = \left(p\,10^{-7}\right)^2 / \rho.c \quad \text{watts/cm}^2 \quad \ldots\ldots\ldots(6)$$

where 10^{-7} converts the ergs/sec into watts. The above equation exemplifies the inconvenient mixture of units commonly encountered in underwater acoustics. I is measured in watts/cm^2, p in dynes/cm^2, ρ in grams/c.c. and c in feet/sec. In addition it is customary to measure the temperature profile of the ocean in feet and the range to the target in yards. It is therefore essential to use the necessary conversion factors in order to maintain consistency amongst the units being employed.

A logarithmic scale is commonly used for underwater acoustic calculations. Such a decibel scale is only meaningful when the reference standard is clearly defined. In the case of sound pressure the reference sound pressure usually adopted is one dyne per cm^2 or one microbar. Thus when a particular sound pressure is referred to as being n dB we mean that

$$n = 10 \log p$$

where p is the sound pressure in dynes/cm^2 // 1 microbar

For a specified pressure wave of n dB the equation giving the required acoustic intensity in watts/cm^2 is

$$I = \frac{\left(\Psi \cdot 10^{7}\right)^2}{\rho \cdot c} \quad \text{watts/cm}^2$$

where

I = acoustic intensity in watts/cm

n = specified pressure wave in dB's relative to $1\ \mu$ bar

$= 15 \times 10^{4}$ gms/cm^{2} -sec

Ψ = anti log$\left(\frac{n}{10}\right)$

2.3. Average Transmission losses in the Medium

Transmission loss is defined as the reduction in magnitude of the signal energy level between two reference points. A general model for transmission loss must include the following physical effects

a) Divergence loss

b) Transmission anomaly

c) Loss due to reflection from the boundaries of the medium

d) Absorbtion loss.

2.4. Divergence loss

This model takes into account the fact that as the energy travels away from the source the energy per solid angle will remain a constant. Thus the divergence loss model accounts for the geometrical spreading of the energy and not for any conversion of the transmitted

energy to some other form. In the absence of any information regarding the temperature structure of the medium we are forced to make the unwarranted assumption that the energy is undergoing spherical spreading through isovelocity water. For isovelocity water the spherical spreading loss is given by

$$D = -20 \log \left\{ (\text{slant range}) \right\} \quad \ldots\ldots\ldots(9)$$

D = divergence loss in dB's.

In general the medium is always stratified in temperature. The velocity of sound in each of these layers is a function of temperature. If a bathythermograph record can be obtained of the medium temperature profile then we make the (valid) assumption that the change in velocity with depth is far greater than in the other two dimensions. Due to this radical difference in the velocity gradients it is reasonable to assume that the sound ray is curved in the vertical plane in much the same manner that a ray of light would be bent when passing through a medium with a varying refractive index. The simple model for divergence loss must therefore be modified to take into account the additional losses due to curved paths. These added losses are allowed for by including an expression for transmission anomaly in the simple spherical spreading divergence loss model.

2.5. Transmission anomaly

The transmission anomaly A is defined as the ratio of the intensity predicted by the inverse square law and the actual sound intensity I, both quantities being measured in dBs. When the acoustic pressure can be determined at a particular spot in the medium, the sound intensity at that spot can be calculated. It is possible to calculate the acoustic pressure produced by a radiating source by solving the wave equations for propagation in the medium. There is however considerable difficulty in solving the wave equations when the boundary conditions involve reflections from the ocean boundaries. Under these conditions ray acoustics provide a more manageable solution.

We now make use of the ray theory to derive a model for transmission anomaly.

2.5.1. Ray Theory

This section follows very closely the outline and derivations given in [75], [76], and [77].

An acoustic 'ray' is defined as a line drawn in the direction of propagation so that it is everywhere $\perp r$ to the wavefront. The concept of a sound ray therefore refers to the direction of propagation of actual wave fronts and not to the propagation of a

narrow beam with sharp edges. Ray theory is based upon the assumption that the sound energy is propagated along curved paths, or rays. These rays paths are straight lines in all parts of the medium where the velocity of sound is constant and curved where the velocity of sound is changing. For reasons of symmetry the energy flow from the source takes place along the radial sound rays and there will be a definite number of rays inside a unit solid angle.

In the ocean the velocity of sound depends only on the vertical depth coordinate z. Thus we are justified in making the assumption that we can ignore horizontal variations in sound velocity and concentrate on the vertical velocity profile. For this assumption it can be shown that the entire path of an individual ray lies in a plane determined by the vertical line through the transducer and the initial direction of the ray.

Since the water depth increases in the downward direction, we shall take the z axis positive downwards. We will consider only those rays which move in the direction of increasing x viz. from the LHS to the RHS in Fig.9. If the ray is gaining depth with increasing range then the angle between the ray path and the horizontal is taken as positive. If the ray is losing

depth with increasing range then the angle between the horizontal and the ray path is negative. This convention is shown clearly in Fig.10.

The curvature of a ray path is determined by examining the angle through which the ray path tangent turns as one moves through unit distance along the ray path. If the ray is curving downwards then the tangent will rotate through a positive angle and the curvature is considered to be positive. We can now ennunciate a general rule [75] for the direction taken by rays when they pass from one layer to another:-

"A ray entering a layer of higher sound velocity is bent away from the layer, and a ray entering a layer of lower sound velocity is bent into the layer."

2.5.2. Derivation of equations for ray paths

Let P in Fig.10 be any point on the wave front at time t. The equation of this wave front is

$$W(x,y,z) = c\,(t - t_o)$$

c = velocity of sound at certain designated standard conditions

t_o = a term which has different values for the different wave front but is a constant in space and time for any specific wave front.

Let the coordinates of P be (x,y,z); let PP' be the ray

element from P at the end of a time interval dt and let α,β,γ, be the direction cosines of PP'. It can be shown that:

$$\left(\frac{dW}{dx}\right)^2 + \left(\frac{dW}{dy}\right)^2 + \left(\frac{dW}{dz}\right)^2 = \frac{c_o^2}{c^2(x,y,z)} \qquad (9)$$

if we define μ, the index of refraction by:-

$$\mu(x,y,z) = \frac{c_o}{c(x,y,z)}$$

then equation(9) becomes

$$\left(\frac{dW}{dx}\right)^2 + \left(\frac{dW}{dy}\right)^2 + \left(\frac{dW}{dz}\right)^2 = \mu^2(x,y,z) \qquad (10)$$

Equation (10) is the fundamental equation of ray acoustics and once the solution of W has been found the ray pattern can be drawn.

Let us consider the special case when the sound velocity is constant in the xy plane and varies only in the z plane i.e.the velocity is a function of depth only. For this case equation (10) reduces to:

$$\left(\frac{dW}{dx}\right)^2 + \left(\frac{dW}{dz}\right)^2 = \mu^2(z)$$

where

$$\frac{d}{ds}(n\alpha) = \frac{d\mu}{dx} = 0$$

$$\frac{d}{ds}(n\beta) = \frac{d\mu}{dz} = 0$$

$$\frac{d}{ds}(n\gamma) = \frac{d\mu}{dz}$$

and

$$\alpha = \cos\theta$$

$$\beta = 0$$

$$\gamma = \sin\theta$$

It follows that if ds is a small elemental area which is perpendicular to the ray path, then

$$\frac{d}{ds}(\mu \cos\theta) = 0 \qquad (11)$$

$$\frac{d}{ds}(\mu \sin\theta) = \frac{d\mu}{dz} \qquad (12)$$

From eqn.(11) it follows that n cos θ has a constant value along a single ray i.e. if P_0 and P_1 are two points as shown in Fig.10.b.

$$\frac{c_o}{c} \cos\theta_o = \frac{c_o}{c_1} \cos\theta_1$$

or if $c_o = c(z)$ and $\theta_o = \theta$ at point P

$$\frac{\cos\theta}{\cos\theta_o} = \frac{c}{c_o} = \frac{1}{\mu} \qquad (13)$$

which is Snell's law.

From equations 12 and 13 we can derive

$$\frac{d\theta}{ds} = \frac{\cos\theta_o}{c_o}\left(\frac{dc}{dz}\right)$$

where $c = c_o$ at the point of ray emmission

θ_o = the initial angle of ray

When the velocity has a constant gradient i.e.

$$c = c_o + g.z$$

we have at all points on the ray

$$\frac{d\theta}{ds} = -\frac{g \cos\theta}{c_o}$$

i.e. the ray is an arc of a circle of radius

$$r_A = \left| \frac{c_o}{g \cos\theta} \right|$$

if 'g' is positive then the curvature is negative and the ray bends upward; but for negative 'g' the circular arc bends downwards: In practice the path of the ray cannot be plotted as a sum of semicircular arcs because the depths of water are usually in thousands of yards. For this reason it is customary [75], [76] to perform the calculation as shown in Fig.10b. The ray leaves the projector at angle θ_o, enters the layer at angle θ_1 and leaves the layer at angle θ_2. From eqn.13 we have:-

$$\theta_1 = \text{arc cos} \frac{c(z_1) \cos\theta_o}{c_o}$$

$$\theta_2 = \text{arc cos} \frac{c(z_2) \cos\theta_o}{c_o}$$

where $c(z_1)$ and $c(z_2)$ are calculated from

$$c(z_n) = c_o + g_n z$$

From Fig.10b it follows that

$$P_1P_2 = \frac{h}{\sin(\frac{\theta_1 + \theta_2}{2})}$$

or the horizontal range in the layer is:-

$$r_h = h \cot(\frac{\theta_1 + \theta_2}{2}) \qquad (15)$$

2.5.3. Calculation of Transmission anomaly from Ray pattern

We make the assumption that energy always travels outward along the rays even when the sound velocity is not constant and the rays are curves. We also restrict ourselves to the case where the sound velocity is a function only of the depth coordinate z. The ray pattern can be computed by dividing the medium into a large number of infinitely thin horizontal layers, each of which can be considered homogenous with a constant (though different) velocity of propagation within it. Snell's law can then be applied to the boundaries between each of these layers. We can get the entire ray pattern in space by rotating the ray pattern of the xy plane about the y axis.

Consider the case of a point source of energy located on the z axis at depth z_o . Let this source radiate energy at a rate of E energy units per unit solid angle per second. Then, energy will be projected into the solid angle $d\Omega$ at the rate of $E \cdot d\Omega$ energy units per second. The rays bounding this solid angle will curve in some fashion depending upon the refractive index and the angle of emmission. At some point P somewhere out along the ray bundle, the cross sectional

area of the bundle is ds and the intensity at P' will equal the energy crossing ds in one second. i.e.

$$\text{Intensity at } P = E\frac{d\psi}{dS} \tag{16}$$

For convenience we define our small solid angle as shown in Fig. 10c. From this figure we see that

$$d\Omega = 2\pi\psi_o \cdot d\psi_o \tag{17}$$

From equations (9) and (10)

$$I = E \cdot 2\pi \cos\psi_o \cdot \frac{d\psi_o}{ds} \tag{18}$$

where ds = the area swept out by rotating PP' about the z axis in Fig. 10d. From Fig. 10d we can show that

$$ds = -2\pi r \frac{dr}{d\theta_o} \sin\theta_h \, d\theta_o \tag{19}$$

from which we get

$$\frac{I}{E} = \frac{\cos\theta_o}{\frac{dr}{d\theta_o}\sin\theta_h} \tag{20}$$

We can calulate the range r_h from

$$r_h = \int_{z_o}^{h} \cot\theta \, dz$$

$$= \int_{z}^{h} \cot\theta \, \frac{dz}{dc} \cdot \frac{dc}{d\theta} \, d\theta$$

From Snell's law $c = c_o \frac{\cos\theta}{\cos\theta_o}$

$$\frac{dc}{d\theta} = \left(\frac{c_o}{\cos\theta_o}\right)\sin\theta_o$$

$$r = -\frac{\cos\theta}{\cos\theta_o} \int_{\theta_o}^{\theta_h} \cos\theta \cdot \frac{dz}{dc} \, d\theta$$

$$\frac{dr}{d\theta} = -c_o \frac{\sin\theta_o}{\cos\theta_o} \left\{ \frac{\cos^2\theta_h}{\sin\theta_h}\left(\frac{dz}{dc}\right)_h - \frac{\cos^2\theta_o}{\sin\theta_o}\left(\frac{dz}{dc}\right)_o \right\}$$

Making the small angle assumption that

$$\sin\theta = \theta$$

$$\cos\theta = 1$$

where

$$\frac{dr}{d\theta} = c_o\left(\left(\frac{dz}{dc}\right)_o - \frac{\theta_o}{\theta_h} \left(\frac{dz}{dc}\right)_h \right)$$

$\left(\frac{dz}{dc}\right)_o$ = velocity gradient at layer entrance.

$\left(\frac{dz}{dc}\right)_h$ = velocity gradient at layer exit.

The transmission anomaly A is defined as the ratio of the intensity predicted by the inverse square law and the sound intensity I also in dB's.

$$A = 10 \log \frac{E/r^2}{I} = 10 \log \frac{E}{I \cdot r^2}$$

substituting we have

$$A = 10 \log \frac{\frac{dr}{d\theta_o} \sin\theta_h}{r \cdot \cos\theta_o} \qquad (21)$$

making the small angle approximation

$$A = 10 \log\left(\left(\frac{dr}{d\theta_o} / r \right) \right)$$

where

$$\frac{dr}{d\theta_o} = c_o\left(\left(\frac{dz}{dc}\right)_o - \text{——} \left(\frac{dz}{dc}\right)_h \right)$$

2.5.4. Transmission anomaly for a reflected beam in a linear gradient

Consider Fig.11 which shows a ray which has suffered several bottom reflections. If the ray hits the bottom at angle θ_b it will be reflected at $-\theta_b$ We have shown that the horizontal range is given by:-

$$r = -c_o \cdot \int_{\theta_o}^{\theta_h} \frac{dz}{dc} \cdot d\theta$$

If the sound gradient is given by

$$g = \frac{dz}{dc}$$

we can obtain for the horizontal range through a layer of thickness h

$$r_h = \frac{c_o}{g}(\theta_h - \theta_o)$$

so that

$$\frac{dr}{d\theta} = \frac{1}{g}\left(1 - \frac{\theta_o}{\theta_h}\right)$$

When the ray path is made up of several arcs as in Fig.11 we have

$$r = -c_o \int_{\theta_o}^{\theta_b} \frac{dz}{dc}\, d\theta - c_o \int_{\theta_b}^{\theta_h} \frac{dz}{dc}\, d\theta$$

$$= \frac{c_o}{g}(2\theta_b + \theta_h - \theta_o)$$

whence

$$= \frac{c_o}{g}\left(2 - \frac{\theta_o}{\theta_b} + \frac{\theta_h}{\theta_b}\right)$$

Substituting into the expression for transmission anomaly A

$$A = 10 \log \left| \frac{h(2 - \theta_o/\theta_b + \theta_h/\theta_b)}{2\theta_b + \theta_h - \theta_o} \right| \quad (22)$$

For the case of the ray which suffers (n+ 1) reflections the calculated transmission anomaly for a ray which leaves the source at angle θ_o and suffers (n + 1) bottom reflections before striking target T at inclination θ_h is

$$A = 10 \log \left| \frac{\theta_h\left(2(n+1) - \frac{\theta_o}{\theta_b} + \frac{\theta_b}{\theta_h}\right)}{2(n+1)\theta_b + \theta_h - \theta_o} \right| \quad (23)$$

2.5.5. Ray paths in a combination of linear gradients

Consider a ray which passes through (n + 1) layers in which the velocity gradients are g_0, g_1, g_2 ....g_n respectively. The velocity at the transducer depth is c_0, c_1 at the top of layer 1 and c_2 at the top of layer 2 and so on. The direction taken by the ray is θ_0 at the source, θ_1 at the bottom of layer 1 and at the top of layer 2 and so on ending with θ_n at the bottom of the (n + 1) layer. The horizontal range covered in the first layer is r_0, r_1 is the horizontal range in the second layer and so on until the horizontal range in the (n + 1)th layer is r_n.

Consider Fig.12 which shows the ray path in the i th layer. The small ray element ds is inclined at the angle θ. In traversing the distance ds the horizontal distance dr travelled by the ray is ds $\cos\theta$ But we have shown in Section 2.5.3. that:

$$ds = -\frac{c_i}{g_i}\frac{d\theta}{\cos\theta_i}$$

giving

$$dr = \frac{c_i}{g_i}\frac{d\theta}{\cos\theta_i}\cos\theta$$

whence

$$r = \frac{c_o}{\cos\theta_o}\cdot\frac{\sin\theta_i - \sin\theta_{i+1}}{\theta_i}$$

The total horizontal range from the source to the point

in Fig.12 is given by:

$$r_h = \sum_{i=0}^{n} r_i$$

i.e.

$$= \frac{c_o}{\cos\theta_o} \sum_{i=0}^{n} \frac{\sin\theta_i - \sin\theta_{i+1}}{g_i}$$

differentiating with respect to

$$\frac{dr}{d\theta} = \frac{c_o \sin\theta_o}{\cos^2\theta} \sum_{i=0}^{n} \left(\frac{\sin\theta_i - \sin\theta_{i+1}}{g_i} + \frac{\cos\theta_i \cdot \cos\theta_o}{\sin\theta} \left(\frac{d\theta_i}{d\theta_o} \right) - \frac{\cos\theta_{i+1} \cdot \cos\theta_o}{\sin\theta_i} \left(\frac{d\theta_{i+1}}{d\theta_o} \right) \right)$$

$$\frac{dr}{d\theta_o} = \frac{c_o \sin\theta_o}{\cos^2\theta_o} \sum_{i=0}^{n} \left(\sin\theta_i - \sin\theta_{i+1} + \frac{\cos\theta_i \cdot \cos\theta_o}{\sin\theta_o} \left(\frac{d\theta_{i+1}}{d\theta_o} \right) - \frac{\cos\theta_{i+1} \cos\theta_o}{\sin\theta_o} \left(\frac{d\theta_{i+1}}{d\theta_o} \right) \right)$$

From Snell's law we have:

$$\frac{c_i}{c_o} = \frac{\cos\theta_i}{\cos\theta_o}$$

or

$$\frac{d\theta_i}{d\theta_o} = \frac{c_i \sin\theta_o}{c_o \sin\theta_i}$$

and hence

$$\sin\theta_i - \sin\theta_{i+1} + \frac{\cos^2\theta}{\sin\theta_{i+1}} - \frac{\cos^2\theta_{i+1}}{\sin\theta_{i+1}} = \left(\frac{-1}{\sin\theta_{i+1}} + \frac{1}{\sin\theta_i} \right)$$

whence

$$\frac{dr}{d\theta} = \frac{c_o \sin\theta}{\cos^2\theta} \sum_{i=0}^{n} \frac{1}{g_i}\left(\frac{1}{\sin\theta_i} - \frac{1}{\sin\theta_{i+1}}\right)$$

$$= \frac{\sin\theta_o}{\cos\theta_o} \sum_{i=0}^{n} \frac{r_i}{\sin\theta_i \sin\theta_{i+1}}$$

Substituting this expression into eqn.21

$$A = 10 \log\left(\frac{\sin\theta_o \cdot \sin\theta_{n+1}}{r \cos^2\theta_o} \sum_{i=0}^{n} \frac{r_i}{\sin\theta_i \sin\theta_{i+1}} \right) \qquad (24)$$

To make use of the above equation we calculate the angles from Snell's law

$$\frac{1}{\mu} = \frac{c}{c_0}\left(\frac{\cos\theta}{\cos\theta_o}\right)$$

and the r_i from

r = $h_o \cot\left(\frac{\theta_1 + \theta_2}{2}\right)$

h = thickness of layer

θ_1 = angle at which ray enters layer

θ_2 = angle at which ray leaves layer.

2.6 Cylindrical spreading

A special model is required to cover the case when the transducer is situated in a thermal layer having a negative velocity gradient. This case is shown in Fig.13. When the transducer is situated in region II a sound channel is formed. Rays leaving the source at angles less than that of the limiting ray

pass into region I and never return to region II. Rays leaving the transducer with angles greater than that of the limiting ray are refracted downward into region III where the positive velocity gradient bends them upwards and back into region II. Thus these rays (with angles greater than that of the limiting ray) are constrained to travel in a channel and suffer cylindrical spreading instead of spherical spreading. The model for cylindrical spreading is:

$$D_L = -10 \log(r) \qquad (25)$$

2.7. Absorbtion Losses

General

At the frequencies commonly used for echo ranging, absorbtion becomes the chief effect modifying the inverse square law of simple geometrical spreading. Absorbtion is a form of loss which involves the conversion of acoustic energy to the medium. It is thought that the attenuation due to absorbtion is a function of the following factors:-

a) Sea State

b) Depth

c) Temperature

e) Frequency

No one has yet performed measurements to try and isolate the effects of (a) and (b) above. A fair amount of both theoretical and practical work has been done on (c) and (d) and (e).

Energy is absorbed and scattered by sea water. This absorbtion represents a process of conversion of acoustic energy into heat and is hence a true 'loss' of energy into the medium. Losses also occur due to scattering in the medium itself. It is customary to lump the losses due to both absorbtion and scattering into a single model. We derive an expression for the logarithmic absorbtion coefficient α to the base 10. α is expressed in dB's per kiloyard. For each kilo-yard travelled the intensity is diminshed by absorbtion by the amount α dB i.e.

$$\text{Absorbtion losses} = \alpha \cdot (\text{slant range}) \qquad (26)$$

If the acoustic intensity at slant range r from the source is I_r and the intensity absorbed per yard is $\alpha' I$ then we have:

$$\frac{d}{dr}(\tilde{I}) = -\left(\frac{2\tilde{I}_r}{r} + \alpha'\tilde{I}\right)$$

where $\alpha' \cdot \tilde{I}$ is the intensity absorbed per yard

$\frac{2\tilde{I}_r}{r}$ is the loss in intensity per yard due to spherical divergence.

Solving the above equation

$$I = \Psi(\theta,\psi)\exp(-\alpha' r)$$

where $\Psi(\theta,\psi)$ is the power per unit solid angle.

Converting into dB's

$$I_r = P - 20 \log r - \alpha' r$$

where

$$I_r = 10 \log \tilde{I}_r$$

$$P = 10 \log \Psi(\theta,\psi)$$

$$= (10 \log_{10} e) \cdot \alpha'$$

From emperical studies α is given by

$$\alpha = \frac{40f^2}{4100 + f^2} + 0.000275f^2 \text{ dB/kyd}$$

where f is in KHz.

Horton [79] has shown that when the propagation involves multiple reflections, the attenuation due to boundary reflections are greater than those due to volume absorbtion. For this case the total attenuation below 10 KHz may be approximated by:

$$\alpha = 0.2f \text{ dB/Kyds} \qquad (27)$$

where f is in KHz.

Fig.14 is taken from [7] and shows the absorbtion coefficient in sea water of salinity 35 parts per thousand as a function of frequency at three temperatures.

2.7.1. Effect of Depth

R. H. Fisher in [80] has investigated the effect

of pressure on absorbtion by studying the decay of sound in a glass sphere of sea water excited into vibration in one of its natural modes. In the range of hydrostatic pressure found in the sea the relationship between the absorbtion coefficient and hydrostatic pressure is:

$$\alpha_p = \alpha\left(1 \cdot 654 \cdot 10^{-4} P\right)$$

α_p = value of α at pressure P.

By taking 1 Atmosphere as the equivalent of 33.9 feet of water at 39 degrees Fahrenheit the absorbtion coefficient at depth d feet is:

$$\alpha_d = \alpha_o(1 - 1.93 \cdot 10^{-5} d)$$

α_d = absorbtion coefficient at depth d

α_o = absorbtion coefficient at depth d = 0.

2.7.2. Effects of Frequency and Temperature

The definitive work in this area was done by Schulkin and Marsh [81] and [82]. These two researchers have derived an empirical formula based on several thousand measurements. Their empirical formula is:

$$\alpha = 1.86 \times 10^{-2} \cdot \frac{S \cdot f_t \cdot f^2}{f_t^2 + f^2} \times 2.68 \times 10^{\frac{f^2}{f_t^2}} \text{ dB/Kyd}$$

where

S = salinity in parts per thousand

f = frequency in KHz

f_t = relaxation frequency

i.e. $f_t = 21.9 \times 10^6 - \frac{1520}{T}$ in KHz.

where T is the Absolute Centigrade.

It can be seen from the above formula that at both extremes of temperature the absorbtion coefficient is strongly temperature dependant while at intermediate frequencies the coefficient varies in a complicated way with both frequency and temperature.

2.8. Target strength

In order to predict the usefulness of a Sonar Set it is necessary to have an estimate of the range at which a submarine can be detected. It is therefore necessary to derive a model which connects the energy returned by the target to the energy incident upon the target from a given direction.

In keeping with the terminology already used in the analytical rigid model we define target strength by the equation:-

$$T.S. = 10 \log_{10}\left(\frac{I_r}{I_i}\right) \qquad (28)$$

where

I_r = intensity of the reflected energy at one yard from the target centre

I_i = intensity of energy incident from a particular direction.

We now express equation (28) in terms of energy density i.e.

$$T = 10 \log_{10}\left(\frac{E_r}{E_i}\right)$$

where E_r = scattered energy density

E_i = incident energy density

It follows that:

$$T.S. = 10 \log I_r/I_i = 10 \log E_r/E_i + 10 \log t_o/t_e \qquad (29)$$

where t_o and t_e are the duration of the incident pulse and the echo respectively.

In general submarine target strength will depend upon the target's orientation with respect to the echo ranging beam. The orientation of an irregular target is most conveniently described in a system of rectangular coordinates with the origin 0 as the centre of the submarine. The aspect angle is defined as the angle between the X axis and the projection of the incident beam on the XY plane. The angle between the echo ranging beam and its projection in the XY plane is called the altitude angle. Fig.15 shows how the aspect and altitude angles are measured.

2.8.1. Realistic target model

We have seen that target strength is proportional to the logarithm of the pulse length for point targets and a function of target length for target which are more than twice the pulse length. For a given pulse

length the relative echo length is a function of aspect.

The target strength can therefore be expressed as:-

$$T.S. = (T.S.)_{aspect} + (T.S.)_{TL} \qquad (30)$$

$(T.S.)_{aspect}$ = Relative target strength as a function of aspect

$(T.S.)_{TL}$ = Relative echo length as a function of target length.

Thus, for point targets

$$T.S. = 30 + 10 \log(S_o/S_p) + (TS)_{aspect} \qquad (31)$$

and for targets longer than $\frac{1}{2}$ pulse length

$$E = 30 + 10 \log(L_p/2L_t) + 10 \log(S_o/S_p) + (T.S.)_{aspect} \qquad (32)$$

where

S_o = constant average power of transmitted signal

L_p = length of pulse in seconds

L_t = target length in seconds

S_p = source level for the duration of the pulse.

2.8.2. Aspect angle

The strongest echo from a submarine [75] is between 70° and 110° as shown in Fig.23. For these aspects the target strength has been measured as 19.7 dB± a standard deviation of 2.5 dB.

At other aspects the target strength is much smaller and averages between 5 dB and 15 dB. A typical figure for stern target strength is 13 dB$\pm$ a standard deviation of 6 dB.

2.8.3. Variation due to frequency

No variation due to frequency is expected nor has it been observed.

2.8.4. Effect of Altitude angle

There does not appear to be much practical importance to the variation of target strength with altitude angle. In general the transducer is always above the target so that negative altitude angle can be ignored. For altitude angles greater than 20 degrees and a target which is at a depth of less than 400 feet a narrow beam transducer will not fully illuminate the submarine at near beam aspects. For such a condition it can be expected that the target will show less aspect dependance.

2.9. General comments on Rigid Model for Average Interference Energy

This model will be developed in two distinct portions. The first model will predict interference

energy which is independant of the Sonar transmission itself i.e. it will predict the interference energy which can be observed at the transducer output at all times before the transmitter has been switched on. The second model will predict the interference that arises as a result of the actual transmission i.e. this model will be concerned with background interference caused by reflections from the medium boundaries. This source of interference is commonly known as reverberation.

2.10. Ambient Sea noise

Ambient noise is defined as the interference noise that is due to natural conditions or sources in the medium. It is considered to be a property of the medium itself at the time and place of observation irrespective of the transducer and the sonar platform used to observe it. It is the composite noise from all sources present in a given environment, desired signals and noise inherent in the measuring equipment and platform being excluded.

The ambient noise level, as a sonar parameter is the intensity, in decibels, of the ambient noise measured with an omnidirectional transducer and referred to the intensity of a plane wave having an rms pressure of 1 microbar. Although measured in different frequency

bands, ambient levels are always reduced to a 1 Hz frequency band and are then called ambient noise spectral levels.

By means of the component spectra of Fig.16 the level of the deep sea ambient noise can be estimated with a degree of assurance. The noise for shallow water conditions in the neighbourhood of bays and harbours is less easy to estimate accurately but Fig.17 can be used to gain a rough estimate. Noise due to rain and biological sounds can be estimated from Fig.18.

Every receiver has its input noise bandwidth limited by a tuned filter. As far as the receiver is concerned the only relevant noise level is the noise spectrum level at the centre frequency of this filter.

The thermal noise level in dB relative to 1 dyne/cm^2 in a 1 Hz band at a frequency of fKHz . is given by

$$N_o = -115 + 20 \log f$$

When measured with a directional hydrophone the above expression becomes:

$$N_o = -115 + 20 \log f + DI$$

DI = directivity index of hydrophone.

If the Input bandwidth of the Receiver hydrophone combination is W then the noise output of the receiver is:

$$N = N_o . W$$

therefore $10 \log N = 10 \log N_o + 10 \log W$

i.e.

$$10 \log N = -115 + 20 \log f + 10 \log W + DI \qquad (34)$$

2.10.1. Surface Noise

Surface Noise predominates in the frequency range 1 KHz to 50 KHz. The major sources of ambient noise appears to be wind speed and wave height. Extensive measurements have been summarised in [13]. At all sea states the spectrum level decreases about 5 dB/octave and the intensity varies approximately as the 1.8 power of wind speed.

2.10.2. Biological noise

Biological noise is appreciable only in shallow coastal waters. The sources of this noise is thought to be snapping shrimp and croakers. Fig.19 shows typical ambient noise levels produced by these sources.

2.10.3. Sonar platform noise

Platform noise is the name given to noise caused by the platform on which the Sonar system is mounted. Sources of platform noise are:-

1) Propeller noise

2) Machinery noise

3) Turbulence

4) Water movement within the transducer dome.

For speeds less than 10 knots the predominant noise component is due to machinery. From 10 to 20 knots the noise is primarily flow noise. Above 20 knots screw noise and local cavitation at surface irregularities predominate. See Fig 20.

2.11. General comments on Rigid Model for Signal Dependant Interference

When the transmitter radiates energy into the water, some fraction of this energy is scattered from the medium boundaries and from the many inhomogenities that are always present in the volume of the medium itself. The portion of the scattered energy which returns to the transducer can be regarded as interference which is dependant upon the transmitted signal energy. This signal dependant interference is known as "reverberation".

According to Naval tradition reverberation is identifiable in three forms according to the portion of the medium from which the scattering takes place.

Thus,

a) Surface reverberation is identified as arising from scattering by the irregular medium surface and from bubbles near the surface.

b) Bottom reverberation is due to energy returned from bottom topography.

c) Volume reverberation occurs when the transmitted energy is reflected from marine organisms, turbulence and temperature gradients distributed throughout the medium's volume.

The fundamental unit upon which reverberation depends is called scattering strength. Scattering strength is the ratio, expressed in dB's of the scattered intensity at unit distance from unit volume (or unit area) to the incident intensity i.e.

$$S_s = 10 \log_{10}\left(\frac{I_s}{I_i}\right)$$

I_s = scattered intensity

I_i = incident intensity.

A vast amount of the earlier measurements on reverberation was done in terms of a unit known as scattering coefficient. The scattering properties of the body of the ocean were traditionally [75, chapter 12] described in terms of a scattering coefficient M = 10 log m.

The quantity m was defined to be the total power that would be scattered by unit area or volume, per unit intensity of an incident plane wave. The assumption is made that scattering is equal in all directions.

For volume reverberation this definition may be illustrated with reference to Fig. 2. A plane wave of intensity I_i is incident upon a small volume Δv centred at Q. If I is the intensity of the scattered sound at P, at distance 1 yard from Q then the total power scattered by the volume Δv is $4\pi \cdot I_s$ and m_v is defined by:-

$$10 \cdot \log m_v = 10 \cdot \log \left(\frac{4\pi \cdot I_s}{\Delta v \cdot I_i} \right) \qquad (35)$$

Similarly for surface and bottom reverberation we have

$$10 \log m_{s,b} = 10 \log \left(\frac{2\pi I_s}{\Delta_{s,b} I_i} \right) \qquad (36)$$

The relationship between S and M is obviously given by:-

$$S_v = 10 \log_{10} \left(m_v / 4\pi \right) \qquad (37)$$

$$S_{s,b} = 10 \log_{10} \left(m_{s,b} / 2\pi \right) \qquad (38)$$

and the apparent scattering strength is stabilized. In [83] it was found that:

$$S_{s,b} = 10 \log \mu_n \cdot \sin^2 \theta \qquad (39)$$

provides a reasonable fit to most experimental data. In the above equation μ_n is the bottom scattering strength at normal incidence. Table 2 shows a range of values of S_b for mud, sand and rock bottoms.

2.12. Model for Surface reverberation

In this derivation of a model for surface reverberation we follow [34] and [7].

The surface reverberation level is defined as the level of the axially incident plane wave which produces the same voltage at the transducer output terminals as the received surface reverberation. [7] derives the formula:-

RL = (Source level) - 40 log r + S_s + 10 log A

RL_s = Surface reverberation level

S_s = Surface reverberation scattering strength

A = the area of surface of scattering strength S_s lying within the ideal beamwidth which produces the same reverberation as that actually observed.

It can be shown that

$$A = C \cdot \frac{\tau}{2} \cdot r \cdot \phi \qquad (40)$$

ϕ = the plane angle of the equivalent beamwidth of the transducer

τ = duration of transmitted signal.

Table 3 gives expressions for ϕ for the usual sonar case when the axis of the transducer beam is only slightly inclined towards the scattering surface. Table 3 is based on [7].

The scattering strength S_s has been measured by many researchers. It has been shown that the scattering strength is a function of the angle of incidence, θ. In low sea states and for small grazing angles

$$S_s = -36 + 40 \log (\tan \theta) \qquad (41)$$

At grazing angles of the order to 40 degrees.

$$S_s = 3.3 \log(\frac{\theta}{30}) - 4.24 \log \beta + 2.6 \qquad (42)$$

where

β = 158 (wind velocity in knots) $\sqrt[3]{f}$ - 0.58

θ = grazing angle in degrees

f = frequency in Hz.

2.13. Volume Reverberation Model

Following [3] once more the Volume Reverberation level RL_v is given by:

$$RL_v = (\text{Source level}) - 40 \log r + S_v + 10 \log V$$

where V = the reverberation volume

$$= c \cdot \frac{\tau}{2} \cdot \psi \cdot r^2$$

ψ = solid angle beamwidth of the transducer.

Expressions for ϕ for simple transducers are given in Table 3. In the absence of a deep scattering layer the value of S_v diminishes at the rate of 0.5 dB per 100 feet and has a value of -77 dB at 300 feet and a value of - 91 dB at 3,000 feet. See also Figs.3, 4 and 5.

2.14. Bottom Reverberation Model

Bottom reverberation is given by:-

$$RL = (\text{Source level}) - 40 \log r + S_b + 10 \log A \quad \cdots (43)$$

A = the bottom area os scattering strength lying within the ideal beamwidth which produces the same reverberation as that actually observed.

$$= c \cdot \frac{\tau}{2} \cdot \phi \cdot r$$

The nature of the bottom has an effect on the scattering coefficient S_b. In [83] ocean bottoms have been divided into the following groups:

1) Silt and mud
2) Sand
3) Rock and gravel.

Table 2 shows typical values for the scattering coefficient for the types of bottom listed above. Within any one of the groups no evidence has been found

between scattering coefficient and particle size.

For grazing angles up to the critical angle, scattering increases with grazing angle. For grazing angles greater than the critical angle attenuation within the bottom decreases the available energy.

2.15. General comments on Rigid Model for Array Gain

In all practical Sonar systems use is made of an additive array the elements of which are so combined that the noise background is uncorrelated from element to element of the array while the signal has perfect correlation along some direction.

The simplest way to form a beam is by a plane array with all its elements correctly in phase. About 25 dB is a usual value for directivity index for shipbourne sonar and a designer rarely attempts to achieve a directivity index greater than 30 dB because this would involve great difficulty in the construction of the transducer to the precise measurements required. 30 dB is also round about the point at which an increase in detection range may be more easily gained by reducing the operating frequency than by increasing the directivity index.

Planar arrays are commonly used in 'searchlight' sonar in which electrical beam steering is performed by switching of delay networks. Beams for transmitting or receiving can be steered vertically and horizontally but unless operation in the convergence zone is specifically required the advantages offered by vertical steering do not outweigh the attendant complexity of equipment.

In general a shipborne transducer is built as a cylindrical assembly of vertical line arrays. Each line of 'stave' is sharply directional in the vertical plane and broad in the horizontal. The combination of a group of lines with suitable time delays allows the formation of a number of beams in the horizontal plane. In general all the staves are driven in parallel to radiate omnidirectionally. For receiving [75] the staves are connected individually to the beam forming networks and the electrically steered receiving beam is rotated rapidly to scan in azimuth. Most such arrays are split into right and left halves and used with phase comparison circuits that determine the left or right sense of the target echo.

It is desirable to concentrate the transmitted power into as small a region as possible. For two harmonic point sources of equal amplitude and phase,

lying on a straight line, the pressure P at great distances from the point array is:

$$P = \rho \cdot \frac{\sin\left(\left(\pi/\lambda\right) \cdot d \sin\theta\right)}{\pi/2\lambda \cdot d \sin\theta}$$

where θ = the angle between the field point and the array axis

ρ = the source strength

d = the separation of the sources

λ = the wavelength of the transmitted energy.

If the two points are replaced by a line source of length each point of which has equal amplitude and phase the far field pressure is:

$$P = S_T \cdot \int_{-\frac{L}{2}}^{\frac{L}{2}} \exp\left(-i \cdot \frac{2\pi}{\lambda} \cdot x \sin\theta\right) dx$$

$$= S_T \cdot \sin\left(\left(kL/2\right) \sin\theta\right) \Big/ \left(kL/2\right) \sin\theta$$

where $k = \frac{2\pi}{\lambda}$ = wave number

S_T = source strength of a point on the line.

Consider an array of small elements in the shape of an arc of a circle. Common element sizes range from $\frac{3\lambda}{8}$ to $\frac{\lambda}{2}$. The spacing between elements is such that the edges of the elements are much less than a wavelength apart. If the elements oscillate in phase with equal

amplitude the array will have a pattern approximated by:

$$P(\theta) = \frac{1}{2m+1}\left[\sum \cos\left[\frac{2\pi r'}{\lambda}\cos(\theta+k\alpha)\right]\cdot\sin\left(\frac{\pi D/\lambda\cdot\sin(\theta+k\alpha)}{\pi D/\lambda\cdot\sin(\theta+k\alpha)}\right)\right.$$

$$\left. i\cdot\sin\left[\frac{2\pi r'}{\lambda},\cos(\theta+k\alpha)\right]\cdot\sin\left(\frac{\pi D/\lambda\cdot\sin(\theta+k\alpha)}{\pi D/\lambda\cdot\sin(\theta+k\alpha)}\right)\right]$$

where

$P(\theta)$ = the ratio of the pressure amplitude at angle to the pressure of amplituce at 0°

r' = radius of curvature of the array

α = angular spacing of the elements.

$2m + 1$ = total number of elements.

It is assumed that one element is positioned at $\theta = 0^\circ$ and that the remaining elements (2m in number) are positioned symmetrically about $\theta = 0^\circ$ i.e.m elements on either side.

The arc source can be reduced to an equivalent line source if the i th element is advanced by so that it is in phase with the zero th element. If all the elements are adjusted in this fashion the cylindrical array will produce a far field pattern equivalent to a straight line array.

The elements of a cylindrical array are in the form of a cylindrical matrix the rows of which are called

layers and the columns are called staves. Beam forming is done by summing the signals of the elements in each stave, properly phased; then the stave signals are summed with appropriate phasing. It is customary to define the directivity of an array in terms of the point at which the response is 3 dB below the peak and of the maximum relative height of the sidelobes. In [7] a more general term which applies equally well to both line or two dimensional arrays shown to be directivity factor. For an array in the 'TRANSMIT' mode directivity factor is defined [7] as the ratio:

$$DF = \frac{\text{Max. transmitted intensity in the direction of max. response}}{\text{Intensity from the same transmitted power distributed uniformly in all directions}} \quad (44)$$

For an array in the 'RECEIVE' mode:

$$DF = \frac{\text{Output power developed by a signal in the direction of max. response}}{\text{Output power developed by the same signal if it were uniformly distributed over all directions}} \quad (45)$$

Directivity Index is defined as 10 log $\{D F\}$

For simple arrays [7] has given the data shown in Table 3 in terms of the dimensions of the array. For more complex array forms the directivity index can be found by integration of the beam patterns.

2.16. Noise due to beam forming

The signal to noise ratio at the output of the transducer is affected by the size and the taper function of the array. For continous transducer arrays [6] defined the noise figure as

$$NF = \frac{\int_{-\infty}^{\infty} [T(r)]^2 dr}{\left(\int_{-\infty}^{\infty} T(r)\, dr \right)^2} \qquad (46)$$

Table 4 is taken from [76]. This measurement was more or less confirmed in [64].

At a frequency of 10 KHz rain can raise the underwater noise level 15 dB to 24 dB above the level indicated by Knudsen's curves [84] for a given sea state. The Knudsen curves are reproduced in Fig.6.

The Statistical Model

3.0. General comments on the Statistical Model

The objective of this section is to develop a Time variant statistical model, for underwater echo ranging, which can be easily set up in a digital computer. A physically oriented channel model which incorporates a delay line with taps spaced according to the observed multipath will be developed.

The model is based on the work done by T. Kailath [2] in which it is shown that a multipath channel can be represented by the sum of n transfer functions, each with different time varying amplitude and phase. For the sake of simplicity we will assume that a simulation can be done at an intermediate frequency which is selected to reduce the complexity of the model.

3.1. The Linear Time varying stochastic model

A simple but adequate model of an underwater acoustic channel is a linear time varying stochastic filter [2][3], [85]. The assumption of linearity permits the use of the superposition theorem and the time varying stochastic features allow a multipath structure to change with time in an unpredictable way.

It is convenient to use a single tapped delay line to represent a single path, and for separate paths

the taps on the delay line are made coincident with the individual paths. Thus, given a bathythermograph of the ocean, one can use the ray path tracing method outlined in [86] to determine the number of paths between source and target and set up a delay line model with taps which represent each of the paths. Such a model can also be used to simulate a possible continium of paths, a discrete multipath with random modulation delays, and arbitrary variations of path characteristics.

3.1.1. Transfer function

The time varying transfer function used in this analysis is

$$H(f,t) = \begin{cases} \sum A_k(t) \exp i\phi_k(f,t) & f_o - W_s \leq |f| \leq f_o + W_s \\ 0 & \text{elsewhere} \end{cases} \quad (47)$$

In the above equation f_o is the centre frequency of the chosen IF bandwidth and $2W_s$ is the IF bandwidth. $H(f,t)$ can be physically interpreted in terms of $H(f_o,t)$ which gives the ratio of output to input at time t when the input is:

$$S(t) = \exp(i.2\pi f_o, t)$$

$S(t)$ is a low frequency function.

Thus $H(f,t)$ at fixed t gives the instantaneous amplitude gain and phase shift for each component of the input

spectrum.

The time varying phase is given by

$$\phi_k(f,t) = \begin{cases} \theta_k(t) - 2\pi \cdot f \cdot T_k & f > 0 \\ \theta_k(t) - 2\pi \cdot f \cdot T_k & f < 0 \end{cases} \qquad (48)$$

The K th transfer function therefore contains a random, time varying phase component which we will call $\theta_k(t)$ and which is proportional to the time dealy Tk. The amplitude functions $A_k(t)$ are non negative and real. The Doppler spread of the channel due to it's time varying aspect is assumed to be W_cHz.

3.1.2. Impulse response

To obtain the time varying response we take the Fourier transform of equation(47) with respect to f while holding t constant

$$\begin{aligned} h(\tau,t) &= \int_{-\infty}^{\infty} H(f\,t)\, \exp j(2\pi \cdot f\,\tau)\, df \\ &= 2 \sum_{k}^{n} A_k(t) \cdot \int_{f_0 - W_s}^{f_0 + W_s} \cos\left\{\phi_k(f,t) + 2\pi \cdot f \cdot \tau\right\} \cdot df \\ &= 4W_s \cdot \sum_{k=1}^{n} A_k(t) \left\{ \frac{\sin 2\pi \cdot W_s(\tau - T_k)}{2\pi \cdot W_s(\tau - T_k)} \cdot \right. \\ &\qquad \left. \cos\left[2\pi \cdot f_0(\tau - T_k) - \theta_k(t)\right] \right) \end{aligned} \qquad (49)$$

For a given location and geometry, and given values of τ and t, $h(\tau, t)$ is a member of an ensemble. For fixed t, the extent of $h(\tau, t)$ on the τ scale measures the amount of time delay spreading caused by the channel.

For a fixed value of τ the behaviour of $h(\tau,t)$ with t indicated how rapidly the filter characteristics are changing with time and hence is a measure of the frequency shift spreading caused by the medium. Typically, fluctuating multipath might well be characterized by:

$$h(\tau,t) = g_k \delta(\tau - T_k)$$

where

$g_k(t)$ = the time varying gain

T_k = the stable delay of the Kth path.

Separating the effects of pure delay in eqn.(49)

$$h(\tau,t) = 4W_s\left(\frac{\sin 2\pi W_s \tau}{2\pi W_s}\right)\sum A_k(t)\cdot\cos\left|2\pi f_o\tau - \theta_k(t)\right| \cdot\delta(t - T_k) \quad (50)$$

Equation(50) can be expressed in terms of its quadrature components viz.

$$h(\tau,t) = 4W_s \frac{\sin 2\pi W_s\tau}{2\ W_s}\cos 2\pi f_o\tau * \sum A_k(t)\cos\theta_k(t)\delta(\tau - T_k) + 4W_s\frac{\sin 2\pi\cdot W_s\tau}{2\ W_s} \sin 2\pi f_o\tau * \sum A_k(t)\sin\theta_k(t)\delta(\tau - T_k) \quad (51)$$

Hancock and Winz [86] have shown that for $f_o \gg W_s$ it is possible to separate out the bandlimiting effect expressed in equation(47) by writing:

$$\frac{\sin 2\pi\cdot W_s\tau}{2\ W_s}\cos(2\pi f_o\tau) = \frac{\sin 2\pi W_s\tau}{2\ W_s}\sin 2\pi f_o\tau = \frac{\sin 2\pi W_s\tau}{2\ W_s}\cos 2\pi f_o\tau * g(\tau) \quad (52)$$

where $\widehat{\ }$ denotes the Hilbert transform and $g(\tau)$ is given by

$$g(\tau) = \frac{1}{\pi\tau} \qquad -\infty < \tau < \infty \qquad (53)$$

i.e. $g(\tau)$ is the impulse response of a non reliazable Hilbert transforming filter. Expressing equation(51) in terms of equation(52)

$$h(\tau,t) = \frac{\sin 2\pi W_s \tau}{2 W_s} \cos 2\pi f_o \tau * 4W_s \sum A_k(t) \cos\theta_k(t) + \sin\theta_k(t) \cdot g(\tau) * \delta(\tau - T_k) \quad \ldots\ldots\ldots \qquad (54)$$

In order to simplify equation(54) we make the assumption that the input signal is bandlimited to $2W_s$ so that the terms denoting the effect of the ideal bandpass filter in equation(54) can be dropped

$$h_{BL}(\tau,t) = 4W_s \sum A_k(t) \cos\theta_k(t) + \sin\theta_k(t) \cdot g(\tau) * \delta(\tau - T_k) \qquad (55)$$

In Eqn.(55) let us choose

$$4W_s A_k(t) \cos\theta_k(t) = h(\tau_{k-1}, t) \qquad (56)$$

$$4W_s A_k(t) \sin\theta_k(t) = h(\tau_{k-1}, t) \qquad (57)$$

and

$$T_k = \frac{k-1}{2W_s} \qquad (58)$$

where $h(\tau_{k-1},t)$ and $h(\tau_{k-1},t)$ are sampled on τ at a rate of $2W_s$Hz. As $n \to \infty$ Eqn.(51) thus is identical to the causal channel model of [2] and proper choice of $A_k(t)$ and $\tau_k(f,t)$ will permit any bandlimited time varying channel to be successfully modelled.

The frequency domain model of Eqn.(47) can be easily adapted to cover the situation of a few distinct multipaths by letting N be equal to the number of multipaths and characterizing the amplitude and phase functions by CW signals. Such a model is suitable for describing bottom and surface reverberation. When, however, it comes to modelling volume reverberation the uniformly spaced tapped delay time model depicted in Eqns.(51), (56), (57) and (58) is more useful and a large number of multipaths (over 100) can be simulated successfully by as few as 10 taps.

3.1.3. The spreading function

A more convenient description [85] of the filter is given by the Fourier transform of $h(\tau,t)$ on t. This transformed impulse is called the spreading function $a(\tau,\eta)$ where $a(\tau,\eta)$, for specific values of τ and η, measures how much simultaneous time delay τ and frequency shift η is suffered by the signal s(t). By substitution of

$$h(\tau,t) = \int d\eta \exp(2\pi\eta t)\, a(\tau,\eta)$$

into equation, z(t) becomes

$$z(t) = \int\int d\tau\, d\eta \left\{ s(t-\tau)\exp(i\,2\pi\eta\cdot t)\right\} a(\tau,\eta)$$

The last equation can be interpreted as saying that the output waveform is obtained by summing time delayed

and frequency shifted versions of the signal weighted by the spreading function at each value of delay and shift. Obviously $a(\tau,\eta)$ is also a random variable. The total extent of $a(\tau,\eta)$ on the (τ,η) plane measures the amount of spreading any signal will incur on passage through the filter. The time delay spread on the τ axis will be called L and the extent on η (frequency spread) will be denoted by B. Since $a(\tau,\eta)$ is random we must determine L and B as ensemble average parameters. The product B.L measures the area of spread in the delay shift plane. L and B represent the distance between extremities of a multimodal function.

3.1.4. Channel output

The channel output z(t) of a time varying channel and input s(t) has neen expressed

$$z(t) = \int_{o}^{\infty} h(\tau,t) \cdot s(t-\tau)\,d\tau \qquad (59)$$

The impulse response given by equation(51) is in a convenient form for digital simulation. Substituting Eqn.(51) into Eqn.(59)

$$z(t) = 4W_s \sum_{K=1}^{n} A_k(t) \frac{\sin 2\pi W_s \tau}{2\pi W_s} \left\{ \left| \cos\theta_k(t) \cdot \cos 2\pi f_o \tau \right| + \left| \sin\theta_k(t) \sin 2\pi f_o \tau \right| \right\} \cdot S(t-\tau-T_k) \qquad (60)$$

3.2. Average descriptors of the Linear Model

The autocorrelation of the impulse response of the filter is sufficient knowledge to evaluate the output correlation function. Since the spreading function, transfer function, and bi-frequency function are all Fourier transforms of each other, knowledge of the correlation function of any one of them enable the others to also be known. The autocorrelation function of the filter can be expressed as:

$$z(t_1)\ z(t_2) = \int\int d\tau_1\ d\tau_2\ \underline{h}(\tau,\ t_1)\ \ h^*(\tau_2,\ t_2)\ x(t_1 - \tau_1)\ x^*(t_2 - \tau_2)$$

where the $\underline{h}$ implies an ensemble average and * the complex conjugate.

3.2.1. The spreading function

Let us make the following assumption regarding the value of the spreading function [85]:-

The spreading function at each time delay and frequency shift is uncorrelated with the value at any other delay and/or frequency shift. This assumption can be expressed as

$$\underline{a}(\tau_1,\eta_1)\ \ a(\tau_2,\eta_2) = \sigma(\tau_1,\ \eta_1)\ \delta(\tau_1 - \tau_2)\delta(\eta_1 - \eta_2)$$

$\sigma(\tau, \eta)$ is called the scattering function and is a measure of the average amount of signal power undergoing

delay τ and shift η. This assumption leads to the following conclusions:-

$$|H(f,t)|^2 = \int d\tau \, d\eta \; \sigma(\tau,\eta)$$

i.e. the ensemble average power transmission through the medium is independant of frequency and time. Also since

$$\underline{H}(f_1,t_1)\cdot H^*(f_2,t_2) = \Gamma(f_1 - f_2,\ t_1 - t_2)$$

where

$$\Gamma(f_1 - f_2,\ t_1 - t_2) = \iint d\tau\, d\eta \cdot \exp\left\{ i.2\pi(f\tau - \eta t)\right\}\cdot\sigma(\tau,\eta)$$

it follows that the ensemble average of the product of the transfer function at different frequencies and times depends only upon the difference of the two frequencies and times. This implies that this ensemble average of the product of the transfer function at different frequencies is decorrelated for frequency separations as small as $\frac{1}{L}$ and time separation as small as $\frac{1}{B}$.

Both of the above limitations are not physically applicable to the real life situation.

We know that

$$z(t) = \iint d\tau\, d\eta \cdot \exp(i\,2\pi\eta\cdot t)\ \underline{a}(\tau,\eta)\ X^*(t - \tau,\ f_s - \eta)$$

and

$$a(\tau_1,\eta_1)\ a^*(\tau_1,\ \eta_1) = \sigma(\tau_1,\eta_1)\cdot\delta(\tau_1 - \tau_2)\delta(\eta_1 - \eta_2)$$

combining these two equations

$$\overline{|z(t)|^2} = \int\int d\tau\, d\eta \cdot \sigma(\tau, \eta) \cdot |X(t - \tau\ f_s - \eta)|^2$$

In order to make the model more realistic we now examine the consequences of the assumption that the spreading function is locally stationary [85].

This assumption implies that the values of the spreading function at different delays and shifts are partially correlated but can become uncorrelated for delay and/or shift separations small compared to the total delay spread L and frequency shift spread B. Mathematically:

$$\underline{a}(\tau, \eta)\ \underline{a}^*(\tau_2, \eta_2) = \sigma\left(\frac{\tau_1 + \tau_2}{2}, \frac{\eta_1 + \eta_2}{2}\right) g(\tau_1 - \tau_2, \eta_1 - \eta_2)$$

$g(\tau, \eta)$ is called the interaction function. The peaks of $g(\tau, \eta)$ are a measure of the interdependance of different delays and shifts on one another.

In the low frequency equivalent of the transfer function domain the assumption of a locally stationary spreading function gives:

$$\overline{|H(f_1,t_1)\ H^*(f_2,t_2)|^2} = \Gamma(f_1 - f_2,\ t_1 - t_2)\ C\left(\frac{f_1 + f_2}{2}, \frac{t_1 + t_2}{2}\right)$$

Here $\Gamma(f,t)$ is as previously defined and $C(f,t,)$ is the double Fourier transform of $g(\tau, \eta)$. The last equation indicates that filter transmissions at frequencies and times separated by $\frac{1}{L}$ and $\frac{1}{B}$ can be uncorrelated. For closer spacings the amount of filter transmission

depends upon the exact frequency ensemble average power transmission and is given by:-

$$\overline{|H(f,t)|^2} = \iint d\tau\, d\eta\, \sigma(\tau,\eta) C(f,t)$$

Therefore the extent of C(f,t) on f measures the filter bandwidth and the extent of C(f,t) on t measures the time duration D of the filter.

The correlated spreading assumption gives a filter model whose average transmission depends upon frequency and time. For limited observation times of wideband signals C(f,t) can be assumed to be independant of t but dependant upon f. This gives uncorrelated spreading at different shifts but correlated spreading in delay with peaks of $g(\tau,\eta)$ as narrow as $\frac{1}{f}$ in τ.

3.3. General comments on a statistical target model

It is necessary to adapt the linear filter model in order to describe the echo from a moving target having several strong highlights.

From what has been said before it follows that a moving target with highlights can adequately be described by a linear filter model having a transformed spreading function $\underline{a}(\tau,\eta)$ where

$$\underline{a}(\tau,\eta) = \delta(\eta - \eta_d) \sum_{k=1}^{n} A_k \delta(\tau - T_k)$$

In the above equation

η_d = doppler shift

A_k = relative strength of the k th highlight

T_k = relative delay of the k th highlight

In order for this model to be realistic the $\{A_k\}$ must be chosen from realistic distributions.

3.3.1. Distributions for target fluctuation

For a target which can be represented as several independantly fluctuating reflectors of approximately equal echoing area, the density function should be close to exponential [87] when the number of reflectors is greater than four or five. For this situation it would seem reasonable to assume that the returned signal power per pulse is constant for the time on target during a single scan but that this returned signal power will fluctuate independantly from scan to scan. A reasonable probability density function for this situation [4] is

$$p(x, \bar{x}) = \frac{1}{\bar{x}} \exp\left(-\frac{x}{\bar{x}}\right) \text{ for } x$$

x = input snr

$\bar{x}$ = average x over all target fluctuations.

Another representation of the target is obtained by regarding it as one large reflector together with

other small reflectors. Such a target will exhibit fluctuations that are independant from pulse to pulse. A suitable probability density function for this case is [4].

$$p(x, \bar{x}) = \frac{4}{\bar{x}^2} \exp(-2x/\bar{x}) \text{ for } x \geq 0$$

The pulse to pulse fluctuation model should apply to stern aspect submarines and also to cases when reasonably small changes in orientation give rise to large changes in echoing area.

The design of a Sonar System

4. General comments on the Design of a Sonar Detection System

The equations developed in Sections 2 and 3 show the relationship that exists between the factors that determine how a sonar signal returned from a target is related to the signal originally radiated by the source. These equations will now be used to design a shipborne Sonar Detection System.

The parameters which define a Sonar Detection System are:-

1. Frequency of operation
2. Acoustic Power radiated
3. Signal transmitted
4. Signal processing in the Receiver
5. The Sonar Transducer.

4.1. General comments on optimum carrier frequency

It has been suggested [79 , pp.317-324] that there should be a distinct maximum in the relationship between maximum detection range and carrier frequency for the case when the echo is masked only by ambient sea noise. One approach that has been taken [88] is to compute the echo to ambient noise ratio and equate the first derivative of this ratio with respect to frequency

equal to zero.

It has been shown [90], [91] that there is very little (if any) dependancy of frequency for reverberation intensity. The backscattering cross section of the target appears to be independant of frequency. It is evident therefore that no optimum carrier frequency exists in the case where the echo is masked by reverberation alone. It is therefore only feasible to attempt to solve the problem for a background of reverberation plus noise, and an attempt will be made to obtain a solution for the optimum frequency for backgrounds of different Reverberation to Noise ratios.

It should also pointed out at this stage that some interesting targets are fast moving. If this movement is sufficient to allow the Doppler effect to separate the target echo from the reverberation then the background against which targets are to be detected is essentially stationary Gaussian noise and not reverberation. A solution for the optimum frequency under Gaussian noise limited conditions is therefore also very relevant to the design of an active Sonar System. On the other hand the ambiguity function of the signal determines directly the target speed at which the echo is sufficiently Doppler shifted to be

separable by Doppler filtering. Peak power limitations placed upon the Transmitter may dictate the use of long duration pulses which imply wide Doppler Tolerance. Under these conditions most interesting targets will not be separable from the reverberation spectrum by Doppler filtering and an optimum carrier frequency must be sought for different reverberation to noise backgrounds. If a family of curves of optimum frequency against maximum range can be drawn for various reverberation to noise ratios then the other parameters of the System can be designed to achieve a selected reverberation to noise ratio at maximum range.

In order to simplify the computations it is possible to rearrange the equations of Section 2 so that terms like Directivity Index and Receiver Signal Processing Gain are included in the individual terms for Ambient Noise and Reverberation Interference.

<u>For the echo we have</u>:-

$$10 \log E = 10 \log P - 40 \cdot \log(r) - 10 \log e + 10 \log(2 \alpha . r) + \text{target strength}$$

<u>For the Ambient Sea Noise at the Receiver Output we have</u>:-

$$10 \log N = \text{Noise Spectrum level} + 10 \log W + \text{Directivity Index}$$

For Boundary Reverberation at the Receiver output:-

$$10 \log R = 10 \log P - 10 \log e + 10 \log(2.\alpha.r) - 30 \log(r) + \text{Boundary Scattering strength} + 10 \log \frac{c}{2W_o} + \text{Directivity Index.}$$

For Volume Reverberation at the output:-

$$10 \log R = 10 \log P - 10 \log e + 20 \log(2.\alpha.r) - 20 \log(r) + \text{volume scattering strength} + 10 \log \frac{c}{2W_o} + \text{Directivity Index.}$$

The terms Target Strength, Noise spectral level Boundary and Volume Scattering Strength and Directivity Index have been defined in Section 2.

c = the velocity of sound in sea water

W_o = the output bandwidth of the Receiver

P = Power output of the Transmitter

r = Range of target.

4.1.1. Effect of Practical System Parameters

In order to study the effect of frequency from the rigid model it is necessary to take into account some of the limitations imposed upon system parameters by practical considerations.

In practice active Sonars are used to search an area for interesting targets. In general [86] each element in the search area must be inspected at a constant

rate which is fixed by the minimum allowable time between inspections. Usually only a single source with a finite horizontal beamwidth is available to search a given area of water. The source can be steered to direct a pulse down each sector of width in sequence. We assume that the receiving array will be able to receive independantly and simultaneously from each of the sectors of width so that the search in range will be conducted continiously. If the total sector to be searched is 360° and the minimum allowable period between searched is T' then the search rate is obviously $B = \frac{2\pi}{T'}$ The maximum pulse length t can now be determined from the beamwidth ϕ for it is obvious that

$$B = \frac{2\pi}{T'} = \frac{\phi}{t}$$

i.e. the pulse length is directly proportional to beamwidth.

The minimum receiver output filter bandwidth is now automatically defined by t to be:

$$W_o = \frac{1}{t}$$

so that the minmum receiver bandwidth is inversely proportional to the pulse duration which is in turn directly proportional tothe beamwidth.

We have seen in Section 2 that beamwidth is inversely proportional to frequency. We can therefore write

Directivity Index is α to f^{-2}

i.e. $$D.I. = \phi_o \cdot \psi_o \cdot f_o^{-2}$$

Receiver bandwidth is $\frac{1}{\alpha}$ to beamwidth,

i.e. $$W = W_o \cdot f.$$

We have seen [84] that the Ambient Sea Noise power decreases at a rate of 6 dB per octave. This means that the noise power N can be written from equation

$$N = \frac{N_o}{f^2} \cdot W_o f \cdot \frac{\phi_o \psi_o}{f^2} = C_1 \cdot f^{-3}$$

In a similar fashion Volume and Boundary Reverberation Power can be written as:-

$$R_B = \frac{P}{r^3} \exp(-2\alpha_o \cdot r) \cdot S_B \cdot r \cdot \frac{\phi}{f} \cdot \frac{c}{2W_o} \cdot \frac{1}{f}$$
$$= C_2 \exp(-2\alpha_o \cdot r)$$

The echo power is given by:-

$$E = \frac{P}{r^2} \cdot TS \cdot f^2 \cdot \exp(-2\alpha_o \cdot r)$$
$$= C_3 \cdot f^2 \cdot \exp(-2\alpha_o \cdot r)$$
$$\frac{N+R}{E} = \frac{C_1}{C_3} \cdot f^{-5} \exp(2\alpha_o \cdot r) + \frac{C_2}{C_3} \cdot f^{-2}$$

At the optimum frequency $\frac{d}{df} \frac{(N + R)}{E} = 0$. This gives

$$2 \frac{R}{N} = \left(-5 + 2 f \cdot r \cdot d\alpha_o/df\right)$$
$$f_{opt} = \frac{5 + 2 R/N}{2 r \, d\alpha_o/df}$$

From Section 2 we have $\alpha_o = 0.2f$ when f is in KHz

and in dB/K yd.

i.e. $$d\alpha_o/df = 0.2$$

Fig.22 is a family of curves for optimum frequency vs maximum range for different ratios of $\frac{R}{N}$.

4.1.2. Optimum frequency for Ambient Noise background

Using the equations already developed for the case where the background interference is only Ambient Sea Noise

$$E/N = (C_3/C_2)\, f^5 \exp(-0.2f.r)$$

$$C_2 \frac{d}{df}(E/N) = C_3 \cdot f^5 \exp(-0.2\, f.r)\left(\frac{5}{f} - 0.2r\right)$$

$$\frac{d}{df}\left(\frac{E}{N}\right) \equiv \left(\frac{5}{f} - 0.2\, r\right)\frac{E}{N}$$

At $f = f_{opt}$ we have $\frac{d}{df}\left(\frac{E}{N}\right) = 0$

which gives

$$f_{opt} = 5/0.2\, r$$

Stuart and Westerfield have shown [86] that the width of the $\frac{E}{N}$ maxima is several octaves.

4.2. The Transmitted Signal

There is no exact criterion to apply to the design of the transmitted signal waveform. The system designer may desire to

a) Maximize snr at the receiver output

b) Minimize Receiver complixity

c) Maximize system range resolution.

Each one of the above objectives will place a bound on the duration and bandwidth of the optimum signal. We will consider all three objectives in turn. The one feature which will be common to all three designs will be the general form of the receiver. It has been shown [88] that the optimum receiver for a Gaussian noise background is a matched filter or cross correlator. We will therefore assume that the receiver will always consist of a filter matched to the transmitted signal. Because the only interesting targets are moving target we must assume that the receiver has stored all possible doppler shifted versions of the transmitted signal so that its performance is independant of target speed.

4.2.1. Maximization of Receiver output snr

The received echo which has been distorted by reflection and passage through the medium has to be filtered to maximize the snr. It has been shown [88] that the optimum receiver is a matched filter. We can represent the matched filter operation by its impulse response according to:

$$h(\tau) = \mathrm{Re}\ \underline{S}^{*}(-\tau)\exp\ -i\left[2(f_o+f_s)\right]$$

where

$\underline{S}$ = a low frequency time function

fs = local frequency shift to compensate for any unknown doppler shift caused by moving platforms and/or the passage of the signal through the medium.

The complex envelope of the matched filter output is

$$z(t) = \iint d\tau \cdot d\eta \cdot \exp(i \cdot 2\pi\eta \cdot t)\, \underline{a}(\tau,\eta) \cdot \chi^{*}(t-\tau, f_s-\eta)$$

where $\chi(t,\eta)$ is the cross ambiguity function of the transmitted signal and the matched filter i.e.

$$\chi(t,\eta) = \int du \cdot \exp(i \cdot 2\pi\eta u) \cdot \underline{S}(u) \cdot \underline{S}^{*}(u+\tau)$$

To study the effect of a correlated spreading channel on the output of a matched filter receiver we take as in Section 3

$$a(\tau_1,\eta_1) \cdot a^{*}(\tau_2,\eta_2) = \sigma\left(\frac{\tau_1+\tau_2}{2}, \frac{\eta_1+\eta_2}{2}\right) \cdot g(\tau_1-\tau_2, \eta_1-\eta_2)$$

and the receiver output $\underline{Z}(t)$ is given by

$$\underline{Z}(t) = \iint d\tau \cdot d\eta \, \exp(i \cdot 2\pi \cdot \eta t) \cdot a(\tau,\eta)\, \chi^{*}(t-\tau, f_s-\eta)$$

where $\chi(t,\eta)$ is the cross ambiguity function of the transmitted signal and the receiving filter i.e.

$$\chi(t,\eta) = \iint d\tau \cdot d\eta \, \exp(i\,2\pi\eta t)\, a(\tau,\eta) \cdot \chi^{*}(t-\tau, f_s-\eta)$$

combining this equation with

$$z(t) = \iint d\tau \cdot d\eta \, \exp(i\,2\pi \cdot \eta t) \cdot \underline{a}(\tau,\eta)\, \chi^{*}(t-\tau, f_s-\eta)$$

we obtain

$$z(t)^2 = \iint d\tau \cdot d\eta \, \sigma(\tau,\eta) \cdot A(t-\tau, f_s-\eta; t)$$

where

$$A(\tau,\eta;t) = \iint du \cdot dv \cdot \exp\{i \cdot 2\pi \cdot vt\} \cdot g(u,v) \; \chi^*\left(\tau - \frac{u}{2}, \eta - \frac{v}{2}\right) \cdot \left(\tau + \frac{u}{2}, \eta + \frac{v}{2}\right)$$

Thus the average envelope squared value of the matched filter receiver output is the double convolution of the spreading function with a local average of the cross ambiguity function.

The average power output of the filter model is therefore the double convolution of the scattering function with the square of the magnitude of the cross ambiguity function. Thus for a fixed average power gain in the receiver and small values of Time and Frequency spreading in the medium the value of $|z(t)|^2$ will not be degraded because the scattering function will only sample the peak of the cross ambiguity function and hence a smaller value of $|z(t)|^2$ will result.

For a signal of durationT and bandwidth W, the widths of the cross ambiguity function in the τ and η direction are $\frac{1}{W}$ and $\frac{1}{T}$ if matched filtering is employed. Therefore if T is the time spreading in the medium and B is the frequency spreading in the medium we must have:-

$$L \leq \frac{1}{W}$$
$$B \leq \frac{1}{T}$$

in order to ensure very little loss due to spreading. For any signal with $TW > 1$ therefore, for negligible spreading losses, i.e. to maximize the output of the matched filter, we must choose a signal whose ambiguity function is contained within the scattering function so that total overlap occurs.

Let us now consider some of the implications of choosing

$$z(t)^2 = \int\int d\tau\, d\eta\, \sigma(\tau, \eta) \cdot A(t-\tau, f_s - \eta; t)$$

when the average transmission in the medium varies across the bandwidth but is constant with time.

In Section 2 we have defined the interaction function $g(\tau, \eta)$ and its double Fourier transform $C(f,t)$. Because no experimental data is available, and in order to reduce the mathematical manipulations required, let us take $C(f,t)$ to be given by [85]

$$C(f,t) = 1 + \zeta \cos(\pi \cdot f \cdot \tau_c + \theta)$$

where $\frac{1}{\tau_c}$ is the distance between a peak and a valley of $C(f,t)$.

ζ is the amount of variation of the transmission function

θ places the peak of the frequency variations at an arbitary frequency with respect to the input signal bandwidth. This gives

$$g(\tau,\eta)=\delta(\eta)\cdot\left[d(\tau)+\frac{\zeta}{2}\exp(-i\theta)\cdot\delta(\tau-\frac{\tau_c}{2})+\frac{\zeta}{2}\exp(i\theta)\cdot\delta(\tau+\frac{\tau_c}{2})\right]$$

Substituting this equation for $g(\tau,\eta)$ into $A(\tau,\eta;t)$ where

$$=\iint du\cdot dv\ \exp(i\,2\pi v\,t)\cdot g(u,v)\cdot \chi^*(\tau-\frac{u}{2},\eta-\frac{v}{2})\cdot(\tau+\frac{u}{2},\eta+\frac{v}{2})$$

we get

$$A(\tau,\eta;t)=|\chi(\tau,\eta)|^2+\frac{\zeta}{2}\exp(-i\theta)\cdot\chi^*(\tau-\frac{\tau_c}{4},\eta)\cdot\chi(\tau+\frac{\tau}{4},\eta)+\frac{\zeta}{2}\exp(i\theta)\cdot\chi^*(\tau+\frac{\tau_c}{4},\eta)\cdot\chi(\tau-\frac{\tau_c}{4},\eta)$$

where $\chi(\tau,\eta)$ is Woodward's cross ambiguity function and $A(\tau,\eta;t)$ is the spreading function.

Thus there are two components in addition to the contribution usually present for uncorrelated scattering.

In order to prevent the output of the matched filter being degraded by these extra terms we select the width of the ambiguity function so that the peaks of the new components do not overlap the peak of the first term. This is accomplished when

$$\frac{1}{W}<\frac{\tau_c}{4}$$

i.e. $$W > \frac{4}{T_c}$$

Although the interaction function performs a local averaging of the ambiguity function, it does not destroy the volume beneath it. The uncertainty relation for A is [85]

$$\omega = \iint d\tau \cdot d\eta \cdot A(\tau, \eta, t)$$

which can be shown to be:- $\iint df \cdot du \cdot |S_x(f)|^2 \cdot |S(u)|^2 \cdot C(f, t+u)$

Now C(f,t) is unity for uncorrelated scattering. For correlated scattering since C(f,t) is a weak function of f and t its average value is still small and there is but little change in the volume of the uncertainty relation for A.

When, however the signal bandwidth is smaller than and lies in a deep valley of the transmission function. If the filter variation with time is also constant over the signal duration the uncertainty relation becomes:-

$$\omega \approx C(0,t) \cdot \int df \cdot |S_x(f)|^2 \cdot \int du \cdot |S(u)|^2$$

which gives very little output from the matched filter. Therefore we must have $\frac{4}{T_c} > W > \frac{1}{T_c}$

Measurements on the medium [85] indicate that

$$T_c \approx 10 \times 10^{-3} \text{ sec}$$

i.e. $$400 \text{ Hz} > W > 10 \text{ Hz}$$

4.3. Minimization of receiver complexity

Relative motion between the target and the Receiver will cause a Doppler shift in the echo frequency. For simplification we can make the assumption that all frequencies are shifted by approximately the same amount. There is a maximum relative velocity that can exist between a surface vessel and a submarine. This relative velocity is approximately $\pm$ 10 knots. Using the usual Doppler relationship

$$\nu = \frac{2\dot{r}}{c}$$

where ν = doppler shift

$\dot{r}$ = relative velocity

c = speed of sound in water

we can calculate the maximum doppler shift to be approximately $\pm$ 100 Hz.

In order to prevent deterioration in the snr at the output we must have a sufficient number of matched filters to cover the entire doppler band of $\pm$ 100 Hz.

4.3.1. Pulse duration

For a simple CW pulse of duration t seconds the bandwidth of the transmitted pulse is $\frac{1}{t}$ Hz. The number of 'matched' filters required to cover the Doppler band is:-

$$N = \frac{200}{1/t} = 200\ t$$

Since it is necessary to search in azimuth as well as in doppler the Rx must have a complete set of doppler filters for each receiver beam. In general the directivity index obtainable is about 25 dB which means that there are 20 separate beams. The total number of doppler filters required is therefore

$$N = 200 \times 20 \times t.$$

If we wish to restrict the equipment to the order of 200 doppler filters

$$t_{max} = \frac{1}{2 \times 20} = 50\text{m sec}$$

Thus we see that the required range and doppler resolution gives rise to equipment costs which prove to be the determining factor for the lower bound of pulse length.

4.3.2. Maximization of Range discrimination

It is necessary to consider the optimum spatial discrimination required from a pulsed Sonar. According to the statistical target model of Section 3, when the discrimination of the pulse is increased a stage will be reached when the target is resolved into a number of individual reflecting highlights. These

sources will give a more reliable indication of the targets, size, shape and echoing area. The statistical target model also indicates that the apparent centroid of the target will wander erratically over the body of the target with changes in propagation path length and target motion.

The individual scatterers giving rise to reverberation are much smaller and closer together than the individual target highlights. As the sonar pulse length is reduced the number of reverberating elements contributing to the interference at any one instant will also be reduced. At the point where a small number of individual target highlights are just resolvable the individual scatterers will not be resolved and the pulse volume will contain a large number of reverberating elements. For this reason the interference will still exhibit a random phase distribution. The reverberation power will therefore be only a function of pulse energy and not pulse duration up to the point where individual scatterers are resolved. An increase in signal to reverberation ratio can be obtained by increasing the range resolution of the system to the point where the pulse length just fails to resolve the individual reverberators.

Experimentation with high resolution Sonars [92] indicate that highlight structures become visible at about 25 m.secs. According to [85] 1 m.second pulses definitely resolve individual scatterers whereas 10 m.second pulses positively do not. An upper bound for pulse resolution of 10 m.seconds would therefore appear to be reasonable.

4.4. General comments on the Sonar Transducer

There is a great variety of electroacoustic transducers currently used in Sonar. The current trend however is towards the use of the piezoelectric or magnetostrictive principle even though this means transducers of large size at the lower frequencies are employed. Originally quartz crystals were widely used for piezoelectric transducers but the advent of artificially grown crystals such as Rochelle salt and Ammonium di-hydrogen phosphate (ADP) led to these being more generally used after about 1940. In about 1950 piezoelectric ceramics such as barium titanate, lead zirconate titanate and many others became popular because of their low cost. A drawback of these ceramics is that they must be artificially polarized and tend to loose this polarization if driven too hard.

Magnetostrictive transducers usually consist of a stack of laminations or of a scroll formed by winding one long ribbon tightly on itself. The alloys of iron, nickel and cobalt all have good magneto-strictive properties but pure nickel is most commonly used. Magnetostrictive ferrites are also used to some extent.

In the design of a projector for underwater sound the most important consideration is high efficiency. This is so because the power available in the case of shipborne sonar can be expensive and limited and also because an excessive loss of power can result in destructive heating. To attain a high efficiency the transducer must be matched to the radiation impedance presented by the water. The transducer has a vibrating mass and there is also a mass reactive component of the radiating impedance. The compliance of the conjugate impedance will match the mass only at resonance. This feature limits the efficient use of the projector transducer to approximately one octave centered about the resonant frequency.

Shipborne transducer elements are usually used in large arrays of elements which are packed in a common watertight housing. The acoustic window of the housing is usually rubber. Rubber has a specific impedance

very close to that of water and makes a very efficient acoustic window even when it is several centimeters thick. The rubber usually specified for use is known as 'ρc' rubber. This rubber has a specific impedance which matches water almost perfectly. The acoustic coupling liquid within the housing is traditionally castor oil.

Because a transducer projects outside the hull of a moving ship it is surrounded by a streamlined sonar dome which acts like a wind screen to reduce flow noise. The space within the dome is usually filled with sea water. The dome must have an acoustically transparent window all around it which is usually thin metal whose mass reactance per unit area is small compared with the specific acoustic impedance of water. This window usually requires structural support and consequently sonar domes introduce transmission loss and also distort the beam width.

The onset of cavitation [93] determines the maximum power that can be transmitted by a transducer of a given surface area. Cavitation occurs [93] when the instantaneous acoustic pressure becomes greater than the sum of the static pressure and the cohesive pressure of the liquid. If we assume that sea water does not exhibit a cohesive force the relationship [93] between

acoustic intensity to produce cavitation and the depth of the projector in feet is:-

$$I = 0.3\left(\frac{H}{32} + 1.8\right)^2$$

I = acoustic intensity in W/cm^2

H = depth of the projector in feet.

Although cavitation is the ultimate factor limiting the power output, a limiting factor which may prove to be of a higher order is the voltage at which breakdown occurs across the surface of the crystals. For barium titanate this breakdown occurs at about $6W/cm^2$.

4.4.1. Beam forming

If we consider an array in which small elements are arranged in the shape of an arc of a circle it is possible to reduce the arc source to an equivalent line source by phase delaying the individual elements to improve the radiation pattern. If the ith element is phase advanced by $\frac{2\pi d_s}{\lambda}$, where d_s is the diameter of the circle, then it will be in phase with the zero i th element. If all elements are adjusted in this fashion the array will produce a far field pattern in a manner equivalent to a straight line array. A cylindrical array of elements in which the elements are arranged

in horizontal rows and columns is a usual transducer configuration. Generally element sizes range from $\frac{3\lambda}{8}$ to $\frac{\lambda}{2}$ and the spacing between elements is quite small, the edges of the elements being much less than a wavelength apart. A 60° arc source having a radius 16 feet will have a projected length of 8 feet. From Table 3 the directivity of such a transducer is 10 log $\left(\frac{2L}{\lambda}\right)$. When a D.I. of 25 dB is required we have

$$= 314.0$$

Now $$L = \frac{2\pi d_s}{\lambda}$$

which gives f = 14 KHz for the operating frequency if d_s is to be 2 feet.

4.5. Acoustic Energy radiated

We wish to specify the acoustic power required to produce a 50% probability of detection at a False Alarm rate of 1×10^{-3}. It is obvious from what has gone before that the Sonar System will be limited by Ambient Sea Noise and Self Noise at far ranges (since reverberation decays as a function of range), that Boundary reverberation will limit the detection probability at short ranges while Volume reverberation is the limiting factor at intermediate ranges.

The parameters of the rigid models for Echo strength and Background Interference have so far been defined in Section 2 in terms of intensity or time rate of change of energy density. We have seen, however in Section 3 that the medium and target both distort the shape of the transmitted pulse and that, in general, the echo from an interesting target is shaped very differently from the pulse originally transmitted. Under these conditions it is more meaningful to compute the signal to noise ratio at the receiver output in terms of its average over the duration of the echo. Under these circumstances the rigid model would be more meaningful if expressed as an equality between the energy density of echo and background interference.

Basing the equality on energy density we have:-

(Echo energy level) = (Average energy of source taken over the echo duration) -2 (Transmission Loss) + (Target strength) (61)

For the noise limited case:-

(Background Noise level) = (Spectral density of Background) +(Recognition differential)+ (Directivity Index) (62)

For the reverberation limited case:-

(Background Reverberation Energy) = (Source intensity level)
-2(Transmission Loss)
+(Scattering strength)
+10 log(Factor) (63)

where

$$(\text{Factor}) = \frac{\psi \cdot r^2 \; c \; t}{2}$$

for volume reverberation and

$$(\text{Factor}) = \frac{\phi \cdot r \cdot c \cdot t}{2}$$

for Boundary reverberation.

ϕ = plane angle beamwidth

ψ = solid angle beamwidth.

Up to now the term target strength has been defined as the ratio of intensity of the scattered wave to the intensity of the incident wave i.e.

$$(TS)_i = 10 \log_{10} \frac{I_s}{I_i}$$

Following [5] we now define a similar quantity in terms of energy density

$$(TS)_E = 10 \log \frac{E_R}{E_i}$$

where E_R and E_i are the scattered and incident energy densities. It can be easily shown [5] that

$$(TS)_E = (TS)_i - 10 \log \frac{to}{te}$$

where to and te are the durations of the incident pulse

and echo respectively. For long pulses, te = to and hence

$$(TS)_i = (TS)_E$$

4.5.1. Recognition differential

Some investigation is necessary to determine the signal to noise ratio required at the receiver output to achieve a 50% probability of detection at a specified False Alarm rate. Woodward [94, pp.114] has shown that the occurence of noise peaks large enough to be confused with the peak echo depends on K, the number of independant samples at the Receiver output, and the output signal to noise ratio ρ. For the case where the receiver is a matched filter in the Doppler sense, the ambiguity due to noise is given by

$$\rho = \frac{\Omega \exp(\rho/2)}{k(1-\Omega)}$$

For a 50% probability of detection we have

$$\Omega = \tfrac{1}{2}$$

i.e.
$$\frac{\Omega}{k} = \rho/2 \cdot \exp(-\rho/2)$$

K can be calculated from

K = No. of Range bins X No. of Doppler bins X No. of bearing intervals

i.e. $K = \frac{7.5 \times 10^3}{20} \times 100 \times 36 = 4.6 \times 10^6$

which gives $\rho = 15$ dB.

4.5.2. Acoustic energy required under Gaussian Noise limited conditions

Let us make the assumption that the temperature structure of the water permits long range acoustic propagation and that the echo is masked at Maximum Range by Noise which is independant of Signal energy i.e. Ships Noise plus Ambient Sea Noise. Under these conditions, if matched filtering employed in the Receiver, the Principle of Conservation of Energy states that the signal to noise ratio at the Receiver output is the ratio of the total energy in the echo to the spectral density of the noise at the Receiver input i.e.

$$\left(\frac{S}{N}\right)_{out} = \frac{E}{N_o}$$

where

E = echo energy

N_o = noise power spectrum density in a 1 Hz bandwidth at the receiver input.

If we can assume that the Background Noise has a uniform spectral density over the Receiver bandwidth then we can conclude that at maximum range the choice of signal waveform and bandwidth is unimportant and that a pulse of long duration and low peak power provides the same

signal to noise ratio at the receiver output as a short duration pulse of high peak power but identical energy.

The only factor which modifies the above condition is that as the pulse length decreases below half the effective length of the target, the entire target is not insonified and the target strength diminishes according to the equations in Section 4.1.

Consider now the case when a 50% probability of detection is required at a maximum range of 7.5 K yds. We take a value of N_o from Fig.20 i.e.

N_o = -30 dB

(Required Echo energy) = 2(Transmission Loss)
-(Target Strength) +(Spectral Energy of Background Noise)
+ (Transmission Anomaly)
- (Directivity Index)

Taking the value of Directivity Index as 25 dB and a carrier frequency of 14 KHz we have, at a maximum range of 7.5 K yds, with a target strength of 18 dB,:-

2(Transmission loss) = 40 log(7,500) = 155 dB
Spectral Energy of Noise= -17 dB for a 200 Hz bandwidth
Transmission anomaly = 28 dB
Directivity Index = 25 dB

Therefore Echo energy density required to give a 15 dB signal-to-noise ratio at 7.5 K yds is 155 dB.

Energy density is the product of the average intensity and pulse length so that

$$155 \text{ dB} = I + 10 \log \frac{c.t_o}{2}$$

where I = source intensity level at one yard

t_o = pulse length in seconds.

From the foregoing discussion on pulse length a reasonable pulse length is 50 m.seconds. This gives

$$I = 138 \text{ dB}$$

4.6. Summary of Design Parameters

The design objectives which must be achieved for a shipborne Sonar System are defined to be:-

1) Maximum operating range of 7,500 yards
2) Transducer diameter 2 feet
3) Minimum receiver complexity.

The System designed in Section 4 has the following parameters:-

Source level 138 dB

Pulse length 50 m.sec.

Frequency 14 KHz

Transducer size - 2 feet diameter

Beamwidth 20°

No. of Doppler filters 200

Range predictions for the designed System

5. Range predictions for the designed System

Since the System has not been constructed the range predictions will be done on paper by making use of 'real life' oceanographic measurements and the mathematical model developed in Sections 2 and 3.

Three temperature profiles of randomly selected deep water locations in the Atlantic Ocean are shown in Figs.24, 25 and 26. These measurements were made using a conventional bathythermograph. The computer program of Appendix I was used to produce data for ray path plots under these ocean conditions. The transducer was assumed to be at a depth of thirty feet. The ray path plots are shown in Figs. 27, 28 and 29.

5.1. Range predictions for location A

According to Fig.27 the top 100 foot layer of the ocean receives nearly all of the energy radiated by the transducer. This surface layer acts like a cylindrical channel for all the radiated energy. The target echo in this region will decay according to the model of Section 2 and hence we can write an equation for echo power in this region according to Section 4 and equation 61 i.e.

Echo power at range r = Source level + Target strength
$- 20 \log(r) - 2\alpha r$ = R.D.

From the ray path plot it can be seen that surface reverberation will be the limiting factor for target detectability at close ranges. Using the model developed in Section 4.5 the surface reverberation energy can be calculated from equation .

S_s can be calculated from equation 40 i.e.

$$S_s = -36 + 40 \log (\tan \theta)$$

From the ray path plot we can see that θ lies between 4° and 14° which give $m_s = 2\pi \cdot S_s = -50$ dB

The first bottom reverberation return will appear at about 3.7 K yds. and its power can be calculated from the model of Section 4.5, equation 63. S_B is obtained from Table 1 for a muddy bottom.

Assuming a ships' speed of 20 knots and a Sea State 2 we can use Figs.16 and 20 to obtain values for the background noise energy. It is now possible to plot a graph of the mean echo energy as a function of range.

The noise energy and the reverberation energy can also be plotted on the same graph. The graph with all three quantities is shown in Fig.30.

Assuming that a snr of 15 dB is required for adequate performance, the detection range for location A is in excess of 10 K yds.

5.2. Range prediction for location B

The ray path plot for location B is shown in Fig.28. From Fig.28 we see that rays emerging at an angle greater than 4° are refracted to the bottom. The effective power radiated into the main volume of the ocean is reduced to 84% of the total power radiated by the transducer. The target echo now decays as twice $20 \log(r) + 2\alpha r$. Fig.31 is drawn under the same conditions as Fig.30 and we obtain 5 K yds. as the maximum operating range at location B.

5.3. Range prediction for location C

The ray path plot for location C is shown in Fig.29. The situation is very similar to that at location A. Fig.32 enables the maximum detection range at location C to be estimated as 8 K yds.

Conclusions

6. Conclusions

A Mathematical Model has been developed for acoustic propagation in the Ocean. This Model consists essentially of a rigid model in series with a stochastic model. The combination can be used to predict both the mean value and the variations to be expected in echo and interference energy for any given oceanographic situation.

A detailed literature search has shown that the parameters for the rigid portion of the model have been extensively measured and that the connection between these parameters and physical properties of the Ocean is well documented. An extensive search of the unclassified literature has failed to yeild measurements of parameters which are required for the stochastic model. An educated guess, based on personal experience, has been made for two important parameters required in the stochastic model.

The combined mathematical model has been used to design a shipborne Sonar System. It is quite obvious that no unique design for a Sonar system exists. The model, however, enables an orderly step by step approach to be adopted for any given set of constraints. Let us assume that one makes certain assumptions, follows

the step by step approach outlined later in this Section, and obtains trial values for transducer size, pulse length and operating frequency. It is always assumed that a maximum operating range will be specified. Using the trial values of the parameters one determines, by the model of Section whether the system is reverberation limited at maximum range. Since reverberation is not a stationary random process any matched filtering in the Receiver is not optimum for the reverberation limited while still ensuring that a sufficiently high detection performance is maintained at the maximum range. The model next enables a choice of optimum frequency in terms of a given reverberation limited at range r_{max} K yds. the model developed in Section shows that a doubling of the transducer dimensions will give an increase of 12 dB in two way directivity index. This increase in transducer size will also permit a further increase of 6 dB in transmitted power. The signal to noise ratio at range r max. therefore increases by 18 dB each time the transducer size is doubled. The model of Section 2 indicates that a 6 dB increase in transmitter power only increases the reverberation power by 6 dB if the system was Volume

reverberation limited and by 3 dB if the system was Boundary Reverberation limited.

If the input and output bandwidths can be increased by 21 dB by shortening the pulse length the model of Section shows an improvement of echo to reverberation ratio of 27 dB for the Volume reverberation limited case and 24 dB for the Boundary reverberation limited case. Of this improvement the stochastic target model indicates that 3 dB will be lost in target strength which reduces the gains in echo to reverberation ratio to 24 dB and 21 dB respectively. The echo to noise ratio at r max. has now returned to the original value it had before the transducer dimensions were doubled.

The stochastic medium model of Section 3 indicates that a limit exists to the bandwidths that can be used. Beyond this limiting point, time and frequency spreading in the medium nulify any expected gains in echo to reverberation ratio.

In general practical considerations such as available electrical power, transducer size and receiver complexity will halt the bandwidth widening proceedure before medium spreading considerations.

In cases where only a very small peak transmitter power is available and detection is required for ranges

the stochastic model indicates that signals with time bandwidth product > 1 can be used to increase signal to reverberation ratios. Such signals can be produced by modulating the carrier with linear FM(slide) signals or pseudo random codes.

The combined mathematical model has been used to design Sonar system parameters for a hypothetical Sonar System.

Oceanographic measurements have been made at three separate locations in the Atlantic Ocean. The performance of the Sonar system has been evaluated and compared against the desired performance at these three locations. The System performs according to the specifications.

A step by step Design Proceedure

Step 1

Parameters required

(a) Maximum peak power of Transmitter. This will wither be determined by considerations of cavitation (see Section) or maximum available electrical power in the ship.

(b) Maximum size of Sonar dome for mounting transducers.

Estimate

If the peak power is limited by the maximum available electrical power on the ship make a guess at transducer dimensions.

Compute

a) The maximum acoustic power radiated from equation 8.

Step 2

Parameters required

(a) The maximum Doppler over which a search is to be maintained

(b) The maximum number of parallel Doppler filters which are economically possible.

Estimate

Transducer beamwidth

Compute

Minimum pulse length which can be used

Step 3

Parameters required

(a) Maximum range of operation in a specified Sea State.

Estimate

Target strength

Compute

(a) The signal to noise ratio required at maximum range from equation

(b) The signal energy required to obtain the required echo to interference ratio

Step 4

Compute the value of at maximum range

Go through the optimization proceedure outlined above to obtain the minimum value of

Use Fig.22 to check for the optimum value of

Use Fig.22 to obtain carrier frequency.

LIST OF REFERENCES

1. Kailath, T., "Sampling models for Linear Time Variant Filters", MIT Res. Lab. Electron., Cambridge, Mass., Tech Report No.352, (May 1959)

2. Kailath, T., Channel characterization:- Time variant dispersive channels, Chap.6, Lectures in Communication System Theory, McGraw Hill Book Co., 1961.

3. Kailath, T., Sampling Models for Linear Time Variant Filters, MIT Cambridge, Mass.,Tech Report 1959.

4. Swerling, P., Probability of detection of fluctuating targets, Rand Research Memo ORM 1217, March 17, 1954.

5. "The descrimination of transducers against reverberation", Univ. of Calif., War research Memo. UT5, File 01-40, NDRC Div. 6.1-5530-968, May 1943.

6. Schofield, D., "Transducers", Lecture 1 presented at the Institute of Underwater Acoustics, Dept. of Physics, Imperial College of Science & Technology, Univ. of London, July31-Aug.11,1961.

7. Urick, R. J., "Principles of underwater Sound for Engineers", McGraw Hill Book Co.1967.

8. Cron, B.F. & Schumacher, W.R., "Theoretical and Experimental Study of Underwater Sound Reverberation", JASA 33, 1961, pp.881.

9. Hersey, J.B., & Backus, R. H., & Hellwig, Jessica., "Sound scattering spectra of deep scattering layers in the Western North Atlantic Ocean", Deep Sea Research 8, 1961, pp.196-210.

10. Chapman, R. P., & Harris, J. W., "surface backscattering strengths measured with explosive sound sources", JASA 34, 1962, pp.1952.

11. Hersey, J. B., Johnson, H.R., & Davis, L.C., "Recent findings about the Deep Scattering layer", J. Marine Res: 11, 1952, pp.1.

12. Marshall, J.R. & Chapman, J. P., "Reverberation from a deep scattering layer measured with explosive sound sources", JASA 36, 1964, pp.164.

13. Garrison, G.R. & Murphy, S.R., & Potter, D.S., "Measurements of the backscattering of Underwater Sound from the Sea Surface", JASA 32, 1960, pp.104.

14. Gulin, E. P., "Amplitude and Phase fluctuations of a Sound wave reflected from a Sinusoidal surface", Soviet Physics-Acoustics 8, No.3, Jan/March 1963, pp.223-227.

15. Gulin, E.P. "Amplitude and Phase fluctuations of a sound wave reflected from the undulating sea surface", Soviet Physics-Acoustics 8, No.3, Jan/March 1963, pp.228-234

16. Gulin, E.P. & Malyshev, K. I., "Statistical characteristics of Sound Signals reflected from the Undualting Sea surface", Soviet Physics-Acoustics 8, No.3 Jan/March 1963, pp.228-234.

17. Chapman, R.P. & Scott, H.D., "Surface backscattering strengths measured over an extended range of frequencies and grazing angles", JASA 36, 1964, pp.1735.

18. Clay, C.S. & Medwin, H., "High frequency acoustical reverberation from a rough sea surface", JASA 36, 1064. pp.2131

19. Marsh, H. W., "Comments on Generalized form of the Sonar equation", JASA 34, 1962, pp.1789.

20. Marsh, H.W. & Schulkin & Neale, S. "Scattering of Underwater sound by the sea surface", JASA 33, 1961, pp.334.

21. Marsh, W., "Non specular scattering of underwater sound by the sea surface", Lecture #11 in Underwater Acoustics, published by Penn.State Univ. editor V. Albers.

22. Andreev, J. B., "Scattering of Sound by Air bladders of fish in Deep Sound scattering Ocean Layers", Sov.Physics-Acoustics 10 No.1, Jly/Sept 1964, pp.17-24.

23. Richter, R. M., "Measurement of backscattering from the Sea surface", JASA 36 1964, pp.864.

24. Schulkin, M. & Shaffer, R.L., "Backscattering of Sound from the Sea surface", JASA 36 1964, pp.1699-1703.

25. Clay, C. S., "Fluctuations of Sound reflected from the Sea surface", JASA 32, 1960, pp.1547.

26. Batzler, W. E. & Westerfield, E. C., "Sonar studies of the Deep scattering layer in the North Pacific", U.S. N.E.L. Report #334, Jan.1953.

27. Machlup, S. & Hersey, J. B., "Analysis of sound scattering observations from non uniform distributions of scatterers in the Ocean", Deep Sea Res. 3, 1955, pp.1-22.

28. Hersey, J. B. & Backus, R. H., "Sound scattering by marine organisms", Chap.13 in "The Sea", Vol.1, Physical Oceanography, M.N.Hill, editor:Interscience(Wiley) New York, 1962.

29. McKinney, C. M. & Anderson, C.D., "Measurement of Backscattering of sound from the Ocean bottom" JASA 36, 1964, pp.158.

30. Mackenzie, K. V., "Bottom reverberation for 530 and 1030 c/s sound in deep water", JASA 33, 1961, pp.1498 -1504.

31. Mackenzie, K. V., "Long range shallow water reverberation", JASA 34, 1962, pp.62.

32. Mackenzie, K. V., "Possible effects of sea surface or volume reverberations on low frequency deep water bottom reverberation measurements",JASA 38, 1965,pp.368.

33. Urick, R. J., "The backscattering of sound from a harbour bottom", JASA 26 1954, pp.231-235.

34. Urick, R. J. & Hoover, R. M., "The backscattering of sound from the sea surface:-its measurement, causes and application to the prediction of reverberation levels", JASA 28 1956, pp.1038-1042.

35. Eckart, C., "The scattering of sound from the sea surface", JASA 25, 1953, pp.566.

36. Kuo, E.Y.T., "Wave scattering and transmission at irregular surfaces", JASA 36, 1964, pp.2135.

37. LaCase, E. O., Note on the backscattering from the Sea surface, JASA 30, 1958, pp.578.

38. Mellen, R. H., "Doppler shift of Sonar backscatter from the sea surface", JASA 36, 1964, pp.1395.

39. Patterson, R. B., "Backscatter of sound from a rough Boundary", JASA 35, 1963, pp.2010.

40. Patterson, R. B., "Model of a rough boundary as a backscatterer ofWave Radiation", JASA 36, 1964, pp.1150.

41. Ol'Shevskii, V.V., "Statistical spectra of Sea Reverberation", Sov. Phys./ Acoust. 10 No.2 Oct/Dec 1964, pp.183-186.

42. Ol'Shevskii, V.V., "Probability distribution of Sea reverberation levels", Sov. Phys.-Acoust. 9 No.4 Apr/Jun 1964, pp.378.

43. Ol'Shevskii, V.V., "Correlation characteristics of Sea reverberation", Sov. Phys.-Acoust. 10 No.1 Jly/Sept 1964, pp.81-85.

44. "Physics of Sound in the Sea", Part II Reverberation NDRC Summary Tech.Rep. of Div.6 Vol.8, 1946.

45. Mintzer, D., "Wave Propagation in a Randomly Inhomogeneous Medium I", JASA 25, No.5, 1953.

46. Mintzer, D., "Wave Propagation in a Randomly Inhomogeneous Medium II", JASA 25, No.6 1953.

47. Mintzer, D., "Wave Propagation in a Randomly Inhomogeneous Medium III", JASA Feb. 1954.

48. Urick, R. J., "Attenuation over RSR paths in the deep sea", JASA 36 1964, pp.786.

49. Urick, R. J. & Lund, G. R., "Vertical coherence of explosive reverberation", JASA 36 1964, pp.2164.

50. Toulis, W. J., "Acoustic Wave theory interpretation of surface and bottom reverberation", JASA 35 1963, pp.656.

51. Northrop, J.; Tyson, L.E. & Ransome, M. A., "Long range multiple arrivals received at deep hydrophones from shots in the Gulf of Maine", JASA 36 1964, pp.215.

52. Marsh, H. W., "Doppler of boundary reverberation", JASA 35 1963, pp.1836.

53. Mellen, R. H. & Marsh, H. W., "Underwater reverberation in the Arctic Ocean", JASA 35 1963, pp.1645.

54. Milne, A. R., "Underwater backscattering strengths of Arctic pack ice" JASA 36 1964, pp.1551.

55. Vakhitov, N.G., "Influence of the surrounding fluid on the propagation of flexural waves along an elastic strip of finite width", Sov. Phys.-Acoust.10 No.4 Apr/Jun 1965, pp.350-353

56. Zavadskii, V.Yu., "Longtitudinal and transverse waves in elastic layered inhomogeneous media", Sov. Phys.-Acoust. 10 No.4 Apr/Jun 1965, pp.407-409.

57. Zavadskii, V. Yu., "Concerning wave motion in an Elastic layerwise inhomogeneous medium with power law variations in density and Lame' parameters", Sov. Phys.-Acoust.10 No.1 Jly/Sept 1964 pp.94-96.

58. Zavadskii, V. Yu., "Critical frequencies associated with sound propagation in a layerwise inhomogeneous fluid half space bounded by a thin elastic plate", Sov. Phys.-Acoust. 10 No.4 Oct/Dec 1964, pp.137-142.

59. Becken, B. A., "Directional distribution of Ambient Noise in the Ocean", Scripps Inst. Oceanographic Rep.,1961, pp.61-64.

60. Ezrow, D. H., Measurement of thermal noise spectrum of water, JASA 34, 1962, pp.550.

61. Fish, M. D., Marine Mammals of the Pacific with particular reference to the production of underwater sounds, Woods Hole Oceanographic Inst. Rep.49-30. 1949.

62. Fish, M. D., "An outline of sounds produced by fishes in Atlantic Coastal Waters", Narrangansett Marine Lab. Special Rep.#1, 1953, pp.53-1.

63. Calderon, M. A., "Probability density analysis of Ocean ambient and ship noise", NEL Rep.Nov.1964, pp.1248.

64. Heindsmann, T. E., Smith, R. H. & Arneson, A. D., "Effects of rain on underwater noise levels", JASA 27, 1955, pp.378-379.

65. Mellen, R. H., "Thermal noise limit in the detection of Underwater Acoustic Signals", JASA 24, 1952, pp.278.

66. Wenz, G. M., Acoustic Ambient Noise in the Ocean Spectra and Sources, JASA 34, 1962, pp.1936.

67. Wenz, G. M., Some periodic variations in low frequency ambient noise levels in the Ocean, JASA 36 1961, pp.64.

68.		Survey of Underwater Sound: NDRC Div.6 Rep.#3.
69.	Arase, E.M. & Arase, T.,	"Correlation of Ambient Sea Noise", JASA 40, 1966, pp.205
70.	Urick, R. J.,	"Some directional properties of deep water ambient noise", Naval Res. Lab.Rep.3796, 1951.
71	Urick, R. J.,	"Prediction methods for Sonar Systems", Journal Brit.IRE, June 1963.
72.	Bennet, G. S.,	"The Sonar Equation", JASA 35 1963, pp.408.
73.	Urick, R. J.,	"Generalized form of the Sonar equation", JASA 34, 1962, pp.547.
74.	Grindall, E. L.,	"Introduction to Underwater Sound", Lecture#1 of Seminar on Underwater Acoustics July 21-Aug.2, 1963.
75.		NDRC Summary Tech. Rep. Div. 6, Vol.8 (Part I).
76.	Tucker, D.A. & Gazey, B.K.,	"Applied Underwater Acoustics" Commonwealth & International Library, 1966.
77.	Pedersen, Melvin,A.	"Acoustic Intensity Anomalies introduced by constant velocity gradients", JASA 33, No.4, April 1961.
78.	Fox, G.R.,	Ambient Noise Directivity Measurements, JASA 36, 1964, pp.1537.
79.	Horton, J. W.,	"Fundamentals of Sonar", U.S.Naval Inst., 2nd edition (1954).
80.	Fisher, R. H.,	"Effect of High Pressure on Sound absorbtions and chemical equilibrium", JASA 30, 1958, pp.442.

81.	Schulkin, & Marsh,	"Absorbtion of Sound in Sea water", J.Brit.IRE., 25, 1963, pp.493.
82.	Wilson, O.B. & Leonard, R. W.,	"Measurement of sound absorbtion in aqueous salt solutions by a Resonator method", JASA 26, 1954, pp.223.
83.	Mackenzie, K. V.,	"Bottom reverberation for 530 and 1030 c/s sound in deep water", JASA 33, 1961 pp.1498-1504.
84.	Knudsen, V.O., Alford, R.S. & Emling, J.W.,	"Underwater ambient noise", J. Marine Research 7, 1948, pp.410.
85.	Ellinthorpe, A.W.& Nuttal, A.H.,	Theoretical and Empirical Results on the characterization of Under Sea Acoustic channels, Convention paper, First IEEE Annual Communication Convention, Boulder, Colorado, June 1965.
86.	Hancock, J.C. & Winz, P.A.,	"Channels and Models", Signal Detection Theory, Chap.2, McGraw Hill. 1966.
87.	Walker, W.F.,	Linear modelling of long underwater acoustic paths, JASA 37, No.6, June 1965.
88.	Stewart, J.L. Westerfield, E.C.& Brandon, M.K.	"Optimum frequencies for Active Sonar Detection", JASA 33, No.9, Sept 1961.
89.	Elspas, B.	"A Radar System based on statistical estimation considerations", Tech.Rep. NO.361-1, Applied Electronics Lab., Stanfork Univ.Aug.1 1955
90.	Albers, V.M.,	"Underwater Acoustics", Penn.State Univ.Press, 1962.

91.	Albers, V.M.,	"Underwater Acoustics Handbook", Penn.State Univ. Press, 1960.
92.		"Principles and Applications of Underwater Sound", NDRC Summary Tech.Rep. Div.6, Vol.8, 1946.
93.	Schofield, D.	Lecture One "Transducers" presented at the Inst. of Underwater Acoustics, held at the Dept. of Physics of The Imperial College of Science & Technology, Univ. of London, Jly31-Aug11,1961.
94.	Woodward, P. M.,	Probability and Information Theory with applications to Radar. McGraw Hill Inc.1955.
95	Reynolds, C.	Private communication, September 1966.
96	Kuwahara, S.	"Velocity of Sound in Sea water", Hydrographic Review 16, pp.123, 1969.

BIBLIOGRAPHY

1 Horton, J.W. Fundamentals of Sonar, Annapolis Md., U.S.Naval Institute, 2nd edition, 1959

2 Officer, C.B. Introduction to the Theory of Sound Transmission, McGraw Hill, 1958

3 Albers, V.M. Underwater Acoustics Handbook, The Pennsylvania State University Press, 1960

4 Morse, P.M. Vibration & Sound, McGraw Hill Inc., 1948

5 Brekhovskikh, L.M. Waves in a Layered Media, Academic Press Inc., New York, 1960

6 Chernov, I.A. Wave propagation in a Random Medium, McGraw Hill Book Co., 1960

7 Lee, Y.W. Statistical Theory of Communication John Wiley & Sons Inc., 1964

8 Woodward, P.M. Probability and Information Theory, with application to Radar, McGraw Hill Inc., 1955

9 Goldman, Stanford. Information Theory, Prentice Hall Inc., Englewood Cliffs, New Jersey, 1953

10 Fry, T.C. Probability and its Engineering Uses, D. Van Nostrand Co. Inc., New York, 1928

11 Introduction to Sonar Technology, Bureau of Ships-Navy Dept., Washington, D.C. 1965

APPENDIX I

A Computer Program for Ray Path Tracing

1. INTRODUCTION

A coordinate system is set up in which the xy plane is parallel to the Ocean surface and the z axis is taken positive downwards. The temperature profile along the z axis can be obtained from a bathythermograph record which gives temperature in °F against depth. In order to facilitate the entering of the bathythermograph record into the computer, the temperature - depth profile is approximated by a series of straight lines whose end points are termed 'break points'. See figures 25 , 26 and 27 .

2. Mathematical basis

The assumption is made that there is little change in the temperature structure of the ocean along the xy plane as compared to the temperatures change in the xz plane.

The process of ray path plotting is made iterative by starting at the transducer and computing the ray position at successive increments of time Δ t. By using the

equations developed in Section 2.5.2 of this Thesis the increments Δx and Δz for a ray currently at angle θ to the horizontal is

$$\Delta x = c_z \cos\theta \cdot \Delta t$$

$$\Delta z = c_z \sin\theta \cdot \Delta t$$

The velocity c_z at depth Z is obtained from the temperature depth profile and $\cos\theta$ is obtained from

$$\cos\theta = \frac{c_z}{c_o} \cos\theta_o$$

when c_o is the ray velocity at the source and the ray emerges at angle θ_o to the horizontal. With some manipulation it can be shown [95] that

$$\Delta(\sin\theta) = -(\frac{c}{c_o}\cos\theta)^2 \; g(z) \cdot \Delta t$$

where $\Delta(\sin\theta)$ is the increment in $\sin\theta$ for the interval Δt and $g(z)$ is the velocity gradient along the z axis.

The total distance travelled by the ray can be computed from

$$(\Delta S)^2 = (\Delta x)^2 + (\Delta y)^2$$

3. Program Execution

The data is read into the computer as a series of punched cards which carry the coordinates of the

end points of the straight lines which approximate the temperature-depth profile. The temperature depth profile is converted into a velocity profile by using the Kuwahara formula [96].

$$C = 1.445.5 + 4.664T-(0.0554)T^2 + 1.307(S-35)$$

where

C = sound velocity in metres/sec

T = temperature in degrees C

The program interpolates in this profile for successive time increments and computes

a) the velocity gradient g(z) at the depth being considered

b) the velocity C at the depth being considered

It uses the values of g(z) and C to produce

i) an updated range x

ii) a value at sin θ at the new location

ii) the depth z of the new location.

The total distance travelled is accumulated and the program stops automatically if

1) the maximum horizontal range of interest (preset) is exceeded

2) more than a certain (pre set) number of reflections has taken place.

3) The range covered by the temperature depth profile is exceeded.

The above proceedure is then repeated for rays at pre set angular increments at the transducer.

```
C      THIS PROGRAM ACCEPTS A BATHYTHERMOGRAPH
C      RECORDING OF DEPTH VS TEMPERATURE
C
       DIMENSION DEPTH (50),TEMP(50),VEL(50),RAYZ(200)
C      ZDEP   IS DEPTH AT WHICH COMPUTATION IS MADE
C      ZLAST IS DEPTH AT WHICH COMPUTATION STOPS
C      XLAST IS HORIZONTAL RANGE AT WHICH COMPUTATION STOPS
C      DELFI IS THE ANGULAR INCREMENT AT WHICH RAYS ARE
       PLOTTED
C      FIMAX IS THE MAXIMUM RAY ANGLE OUT OF THE SOURCE
C      ZDEL IS THE INCREMENT IN THE Z DIRECTION
C      IPLOT = 0  GIVES A NUMERICAL OUTPUT
C      FIZ  IS RAY ANGLE AT DEPTH ZDEP
C      SAL IS SALINITY IN PPT
       READ(105,5) ZSRC,ZLAST,FIZ,DELFI,FIMAX,XLAST,
      1ZDEL,INC,MXTRY
       WRITE(108,6)
     6 FORMAT (1HI,20H,OUTPUT OF RAY TRACER,//)
     5 FORMAT (2F6.0/3F6.2/F7.0/I3/F7.2/I4)
       WRITE (108,5)ZDEP,ZLAST,FIZ,DELFI,FIMAX,XLAST,
      1ZDEL,INC
       READ (105,10) K, (DEPTH(I),TEMP(I),I=1,K)
       WRITE(108,10) K, (DEPTH(I),TEMP(I),I=1,K)
    10 FORMAT (I3/(F6.0,F6.1))
       SAL = 33.0
       DO 150 I=1,L
       TEMP(I) =1TEMP(I)-32.0)*(5/9)
   150 VEL(I) =(1445.5+4.664*(TEMP(I))-0.0554*(TEMP(I))**2
      1+1.307*(SAL-35.))*1.094 +0.01815  * DEPTH(I)*3.0
       LSTEP =XLAST/120.0 +0.5
     8 IF(IPLOT .EQ.0 ) GO TO 55
       WRITE (108,20)
    20 FORMAT (1HO,    ' TIME     RANGE    DEPTH   DISTANCE ')
    55 Z =ZDEP
       X=0.0
       DIST =0.0
       ICNT1 =0
       ICNT2 =0
       ICNT3 =0
       LCOMP = LSTEP
       KUP = 2
```

```
      XPREV =0.0
      ZDEP =ZSRC
      ZPREV=ZDEP
      PHI = FIZO *3.1416/180.0
      COSPHI = COS(PHI)
      SINPHI = SIN(PHI)
      RAYZ(1) = -ZDEP
      IUPCNT =1
  330 IF(Z .GE. 0.0 )GO TO 44
      Z=-Z
      SINPHI = -SINPHI
      ICNT3 = ICNT3 +1
      ICNT = 1
   44 IF(Z.GE.ZMAX) GO TO 77
      Z1 = DEPTH(K)
      IF (Z.LE.Z1) GO TO 88
      Z =DEPTH(K) *2.0 -Z
      SINPHI = -SINPHI
      ICNT3 = ICNT3 +1
      ICNT2 = 1
   88 DO 99 I=2,K
      INC =I
      ZI = DEPTH(I)
      IF (Z.LE.Z1) GO TO 15
   99 CONTINUE
   15 GRADZ = (VEL(INC)-VEL(INC-1))/(DEPTH(INC)-DEPTH
     1(INC-1))
      CRAY  = VEL(INC-1)+(Z-DEPTH(INC-1)) * GRADZ
      IF (ICNT1.NE.0) GO TO 9
      CO =CRAY
    9 NEWX =COSPHI * C * * 2 * ZDEL /(1000.0 * CO)
      NEWZ =CRAY * SINPHI * ZDEL /1000.0
      X =X+NEWX
      Z =Z+NEWZ
      DIST =DIST+ SQRT ((NEWX**2) +(NEWZ**2))
      SINPHI = SINPHI -((COSPHI* CRAY/CO)**2)*(GRADZ*
     1(0.001*ZDEL))
      ICNT1 =ICNT1+1
      IF(IVPDAT.EQ.0) GO TO 35
      IF(ICNT.EQ.1)GO TO 93
      IF( IUPCNT.NE.IPLOT) GO TO 19
      TIME = FLOAT(ICNT1)*0.001*ZDEL
      WRITE (108,44) TIME ,X,Z,DIST
```

```
44 FORMAT (1HO,F7.3,3F10.2)
   IUPCNT =0
19 IUPCNT =IUPCNT +1
   GO TO 35
93 TIME =FLOAT(ICNT1) * 0.001 * ZDEL
   WRITE(108,57) TIME ,X,Z,DIST
57 FORMAT (1HO F7.3,3F10.2,' REFLECTION ')
   ICNT =0
   IUPCNT =IUPCNT+1
   IF(X.LT.FLOAT(LCOMP)) GO TO 86
   RAYZ(KUP)=((Z-ZPREV)*(X-FLOAT(LCOMP))/(X-XPREV))-Z
   JUPCNT = JUPCNT +1
   LCOMP = LCOMP +LSTEP
   ZPREV =Z
   IF(X.GT.XMAX)GO TO 77
   IF(ICNT3.EQ.MXTRY)
   GO TO 330
77 KUP = KUP-1
   D =-MAXZ
   RAYCNT =KUP
   CALL PLOT 1(RAYZ,0.0,D,RAYCNT,0.0,51,KUP,10)
   WRITE (108,42) FIZO
42 FORMAT (' SOURCE ANGLE = ',F6.2,' DEGREES ',//)
   FIZO =FIZO +DELFI
   IF(FIZO.LE.FIMAX)GO TO 8
   STOP
   END
```

LOCATION A

Bathythermograph Breakpoints

DEPTH	TEMPERATURE
0	36.4
27	35.2
31	34.5
50	34.5
80	36.7
90	42.5
103	50.0
120	50.0
130	47.5
150	49.0
163	49.0
167	46.0
173	46.0
206	43.0
233	42.5
240	43.3
256	42.4
320	42.0
343	42.6
380	41.5
416	41.3
450	41.0

RESULTS FOR LOCATION A

TIME	RANGE	DEPTH	DISTANCE	
0.100	158.	22.	159.	
0.200	316.	42.	318.	
0.300	473.	61.	477.	
0.400	632.	78.	636.	
0.500	791.	85.	796.	
0.600	950.	72.	955.	
0.700	1108.	54.	1115.	
0.800	1266.	33.	1273.	
0.900	1424.	14.	1432.	
0.982	1554.	0.	1563.	(REFLECTION)
1.000	1582.	3.	1592.	
1.100	1740.	22.	1751.	
1.200	1898.	42.	1910.	
1.300	2055.	61.	2069.	
1.400	2214.	78.	2228.	
1.500	2373.	85.	2388.	
1.600	2533.	72.	2547.	
1.700	2691.	53.	2707.	
1.800	2848.	32.	2866.	
1.900	3006.	13.	3025.	
1.973	3121.	0.	3141.	(REFLECTION)
2.000	3164.	5.	3184.	
2.100	3322.	24.	3343.	
2.200	3480.	44.	3502.	
2.300	3638.	64.	3661.	
2.400	3796.	81.	3820.	
2.500	3956.	84.	3980.	
2.600	4115.	69.	4140.	
2.700	4273.	50.	4299.	
2.800	4430.	29.	4458.	
2.900	4588.	9.	4617.	
2.951	4669.	0.	4698.	(REFLECTION)
3.000	4747.	9.	4776.	
3.100	4904.	29.	4936.	
3.200	5062.	50.	5095.	
3.300	5220.	69.	5254.	
3.400	5379.	84.	5413.	
3.500	5539.	82.	5573.	
3.600	5697.	64.	5733.	
3.700	5855.	43.	5892.	
3.800	6013.	22.	6051.	
3.900	6171.	3.	6210.	
3.917	6198.	0.	6237.	(REFLECTION)

Tabular output. Initial angle= 6.0° Initial depth= 4yds.

APPENDIX II

Simulation of a Stochastic channel model

1. General

The Stochastic Model of Section 3 can be simulated in a digital computer. The simulation is based on equation(60) in Section 3.

Equation(60) can be computed by straightforward digital techniques of sampled values of the input signal are available. Channel parameters $A_k(t)$ and $\theta_k(t)$ can be derived from probability density functions characterizing the channel.

We have shown in Section 3 that the channel output $z(t)$ for an input $s(t)$ can be expressed as

$$z(t) = 4W_s \sum_{k=1}^{N} A_k(t) \frac{\sin 2\pi \cdot (W_s \tau)}{2\pi W_s \tau} \Big(\cos\theta_k(t) \cos 2\pi f_o \tau + \sin\theta_k(t) \sin 2\pi f_o \tau \Big) s(t - \tau - T_k) d\tau \quad \text{(II.1)}$$

This can be rearranged in a more useful form by writing

$$h^k(\tau) = 4W_s A_k(t) \frac{\sin 2\pi (W_s \tau)}{2\pi W_s} \Big(\cos\theta_k(t) \cos 2 \ f_o \tau + \sin\theta_k(t) \sin 2\pi f_o \tau \Big) \quad \text{(II.2)}$$

This gives the expression

$$z(t) = \sum_{k=1}^{N} \int_0^{\infty} h^k(\tau, t) \, s(t - \tau - T_k) d\tau \quad \text{(II.3)}$$

2. Implementation

Since the channel output is centered about the

intermediate frequency f_o with the bandwidth $2W_s$ then the highest frequency component is located at

$$f_h = f_o + (W_s + W_c) \qquad (II.4)$$

Equation(II.2) can be numerically integrated as a means of simplifying the problem of sampling the channel at bandpass frequencies in order to obtain in phase and quadrature components. f_o can be chosen so that h is integer valued. Under these circumstances Hancock 26 has shown that equation(II.2) can be represented by uniform time samples taken at a rate

$$f_s = 4(W_s + W_c) \qquad (II.5)$$

We can now replace $h^k(\tau, t)$ and $s(t - \tau_j - T_k)$ in equation(II.2) with generalised Fourier series where the coefficients are uniform time samples taken on τ. Hence we can express the discrete channel output at t_i as:

$$z(t_i) = \frac{1}{2W} \sum_{k=1}^{N} \sum_{j=1}^{M} h^k(\tau_j, t_i)\, s(t_i - \tau_j - T_k) \qquad i = 1.2.....n \qquad (II.6)$$

where $\frac{1}{2W}$ is the norm squared of the basis functions. For practical situations, the impulse response will have a finite duration and it follows that m will also

be finite. For any finite duration of channel output N will also be finite.

Equation(II.6) can be expressed in vector form as:

$$z(t_i) = \frac{1}{2W} \sum_{k=1}^{N} H_i^{k^T} \cdot S_i^k \qquad \text{(II.7)}$$

by letting

$$H_i^{k^T} = \left[h^k(\tau_j, t_i) \right] \qquad \text{(II.8)}$$

and

$$S_i^k = \left[s(t_i - \tau_j - T_k) \right] \qquad \text{(II.9)}$$

The transmitted signal is first lowered to an optional IF and then A - D converted. The stored samples of the signal are then convolved digitally with each of the N multipaths which represent the channel. The path delays are mechanized by shifting to a different set of stored values of the incoming signal. The computed output of each of these paths is then summed and weighted by the normalizing factor $\frac{1}{2W}$ to form the channel output. The $H_i^{k^T}$ are formed by equation(II.2) and (II.8) from deterministic or statistical data representing the channel. Fig.21 shows a block diagram of the digital computation.

From equations(III) and (II7) we see that for each time instant t_i and each path k we need to

compute the column vector H_i^k where its entries are values of the m sample instants of τ_j in

$$h^k(\tau_j, t_i) = 4W_s A_k(t_i) \frac{\sin 2\pi(W_s \cdot \tau_j)}{2 W_s \cdot \tau_j} \cdot \left(\left\{ \cos\theta_k(t_i)\cos 2\pi f_o \cdot \tau_j \right\} + \left\{ \sin\theta_k(t_i)\sin 2\pi f_o \tau_j \right\} \right) \qquad \text{(II.8)}$$

Then each of these entries is multiplied by the sample of delayed signal in:

$$S_i^k \quad s(t_i - \tau_j - T_k)$$

and summed according to the matrix operation in Eqn(II7). This proceedure is repeated for each path k, the results being summed and multiplied by the sampling constant to obtain one sample instant of the channel output.

The quantities indexed on j can be tabulated before simulation. Then each time $\sin 2\pi f_o \cdot \tau_j$, $\cos 2\pi f_o \cdot \tau_j$ or $\frac{\sin 2\pi(W_s \tau_j)}{2\pi W_s \tau_j}$ are called for, the computer refers to the tabulated values corresponding to the relevant index. The parameters $A_k(t)$ and $\theta_k(t)$ are generated separately. It was not found to be practical to compute and store the $\sin\theta_k(t_i)$ and $\cos\theta_k(t_i)$ before simulation. Use however was made of the periodic nature of the sine and cosine functions to compute tables of their values corresponding to values

of $\theta_k(t_i)$ lying in the interval $(0, 2\pi)$. During simulation the closest value in the table to $\theta_k(t_i)$ (mod 2π) was found.

The components of the signal vector were obtained by first subtracting indices to form (i - j + k). The sample value of the signal corresponding to this index was then extracted from memory.

3. Comments

The Stochastic Model described here was set up in a Packard Bell 250 Digital computer using CINCH. A FORTRAN version of the CINCH program is included here but since no measurements could be found in the unclassified leterature to provide distribution values for $A_k(t)$ and $_k(t)$ the simulation results are of no more than passing interest.

```
C       II = COUNTER FOR SIGNAL TIME INCREMENTS
C       JJ = COUNTER FOR NO  OF TAPS ON  DELAY LINE
C       KK = COUNTER FOR NO  OF PATHS IN THE OCEAN
C       M  IS TOTAL  NO  OF TAPS ON  DELAY LINE
C       N  IS MAXIMUM  NO  OF MULTIPATHS
C       S  IS THE ARRAY CONTAINING STORED SAMPLES OF THE SIGNAL
C       SIG  IS THE  OUTPUT SIGNAL
C       A( ) IS THE ARRAY CONTAINING SAMPLES OF THE
C       DISTRIBUTION
C       WHICH CHARACTERIZES THE TAP GAINS
C       THETA( )  IS  THE  SAMPLES OF TIME VARYING PHASE
C       VALUES FOR S,A,AND THETA ARE READ IN ON CARDS

      DIMENSION  SIG(100), H(1,100),A(10,10),THETA
     1(10,10),S(100)
      READ (105,21) SIG(100),H(1,100),A(10,10),THETA
     1(10,10),S(100),FO,M,N,W,IMAX
   21 FORMAT (10F10.0)
      II =1
   77 KK =1
      JJ =1
      DO 20 KK=1,N
      DO 20 JJ=1,M
      PHI =2.0 *3.14 * W *JJ
      PHIZ = SIN (PHI)
      FACT1 = PHIZ/PHI
      FACT2 = (6.28*FO *JJ
      FED=COS(THETA(KK,II)) COS(FACT2)
      TED=SIN(THETA(KK,II)) SIN(FACT2)
      H(KK,JJ) =4.0* W *A(KK,II) *FACT1 *(FED + TED)
   20 CONTINUE
      DO 30   KK=1,N
      DO 30   JJ=1,M
      KOUNT  =II-(JJ+KK)
      SIG(II) = H(KK,JJ) * S(KOUNT)
   30 CONTINUE
      II=II+1
      IF(II.LE.IMAX)GO TO 77
      WRITE (108,51)(SIG(II),I=1,100)
   51 FORMAT (1HO ,F10.4)
```

TABLE 1

SEA STATE VS WAVE HEIGHT

SEA STATE NUMBER	DESCRIPTION	WAVE HEIGHT IN FEET
0	Calm	0 - 1
1	Smooth	1 - 2
2	Slight waves	2 - 3
3	Moderate sea	3 - 5
4	Rough sea	5 - 8
5	Very rough sea	8 - 12
6	High sea	12 - 20
7	Very high sea	20 - 40
8	Precipitous sea	40+
9	Confused sea	---

TABLE 2

BOTTOM REVERBERATION COEFFICIENTS

TYPE OF BOTTOM	GRAZING ANGLE IN DEGREES	BOTTOM REVERBERATION COEFFICIENT dB (TYPICAL VALUES)
SOFT MUD	5	-42
	10	-18
	15	-27
	20	-22
SAND	5	-30
	10	-21
	15	-15
	20	-10
ROCK	5	-21
	10	-35
	15	-8
	20	-5

TAKEN FROM REFERENCES [7] [5] and [44]

TABLE No.3

DIRECTIVITY OF SIMPLE TRANSDUCERS

TRANSDUCER TYPE	PATTERN FUNCTION	D.I. = 10 $\log_{10}$ ( )
CONTINIOUS LINE OF LENGTH L, $L > \lambda$	$\left(\frac{\sin \frac{\pi L}{\lambda} \cdot \sin\theta}{\frac{\pi L}{\lambda} \sin\theta} \right)^2$	$\left(\frac{2L}{\lambda}\right)$
PISTON OF DIAMETER D IN AN INFINITE BAFFLE, $D > \lambda$	$\left(\frac{2J_1\left(\frac{\pi D}{\lambda} \sin\theta\right)}{\frac{\pi D}{\lambda} \sin\theta} \right)^2$	$\left(\frac{\pi D}{\lambda}\right)^2$
LINE OF n ELEMENTS OF EQUAL SPACING d	$\left(\frac{\sin\left(n\pi d \cdot \sin\frac{\theta}{\lambda}\right)}{\sin\left(\left(\frac{\pi d}{\lambda}\right)\sin\theta\right) \cdot n} \right)^2$	$\left(\frac{n}{1 + \frac{2}{n}\sum_{\rho=1}^{n-1} \frac{(n-\rho)\sin\left(\frac{2\rho \cdot \pi d}{\lambda}\right)}{2\rho \frac{\pi d}{\lambda}}} \right)$
TWO ELEMENT ARRAY AS ABOVE BUT WITH n = 2	$\left(\frac{\sin\left(2\pi d \cdot \sin\frac{\theta}{\lambda}\right)}{2\sin\left(\frac{\pi d}{\lambda}\sin\theta\right)} \right)^2$	$\left(\frac{2}{1 + \frac{\sin(2\pi d/\lambda)}{2\pi d/\lambda}} \right)$

TABLE TAKEN FROM REF. [7]

TABLE No.4

NOISE FIGURES OF ARRAYS

NAME OF ARRANGEMENT	TAPER FUNCTION T(r)	N.F.	
COSINE TAPER	$\cos\left(\frac{\pi r}{l}\right)$	0.92 dB	
LINEAR TAPER	$1 - 2\lvert r\rvert / l$	1.26 dB	N.B. T(r) extends over distance r from $-\frac{\ell}{2}$ to $\frac{\ell}{2}$
CIRCULAR TAPER	$1 - \frac{4r^2}{l^2}$	0.34 dB	
FLAT TOPPED BEAM	$1 + 2\cos\left(\frac{2\pi r}{l}\right)$	4.28 dB	

TABLE TAKEN FROM REF. [76]

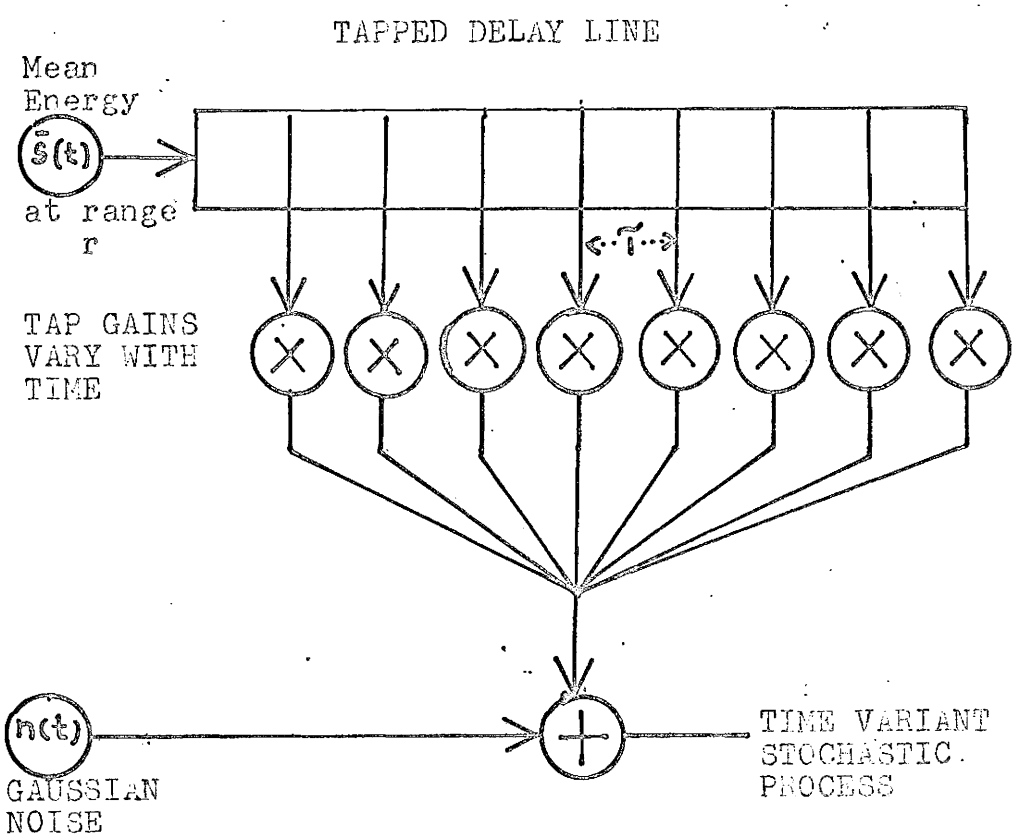

FIGURE 1 GENERALISED TIME VARIANT STATISTICAL MODEL

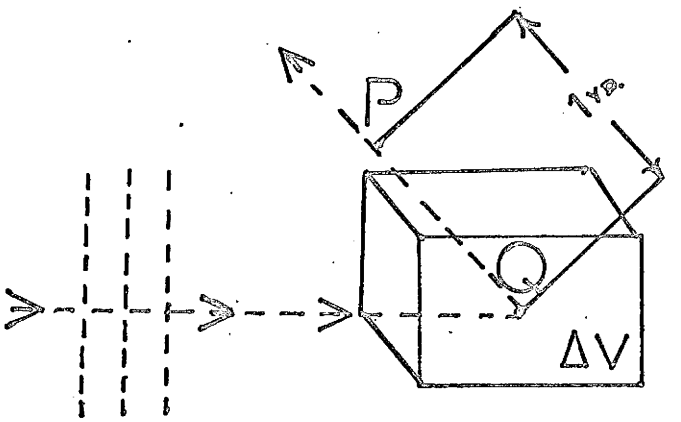

INCIDENT
PLANE
WAVE

Total Power Scattered
by Volume ΔV is $4\pi I_s$

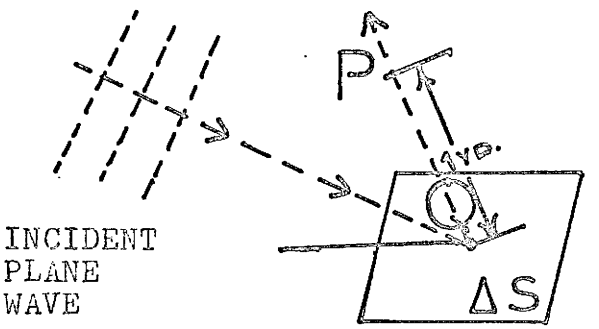

INCIDENT
PLANE
WAVE

Total Power Scattered
by Area ΔS is $2\pi I_s$

FIGURE 2 SCATTERING COEFFICIENTS

FIGURE 4.

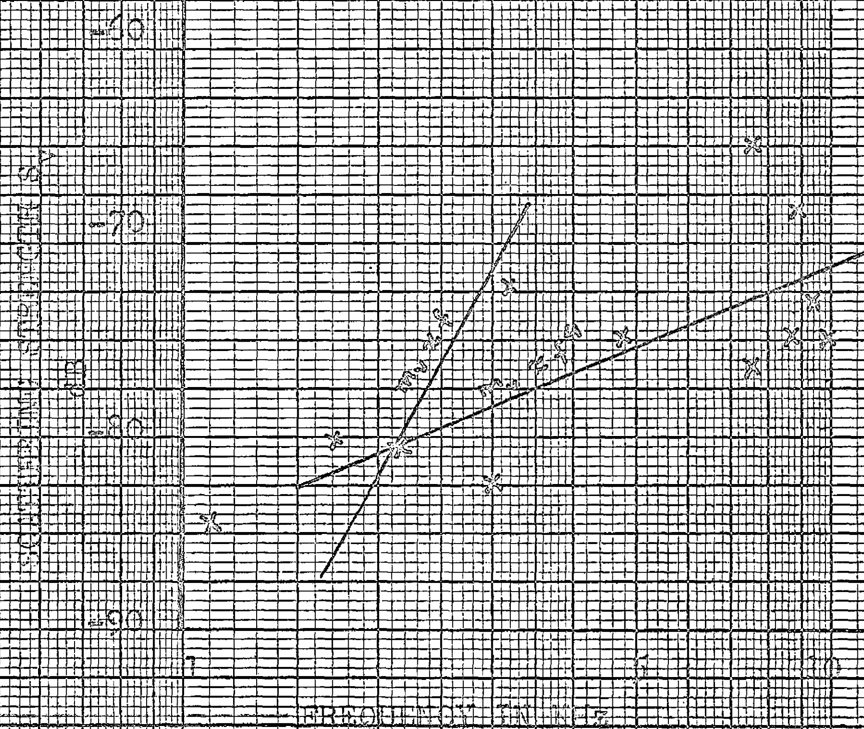

FIGURE 5

SCATTERING STRENGTH
VS
FREQUENCY
(Deep Scattering Layer)

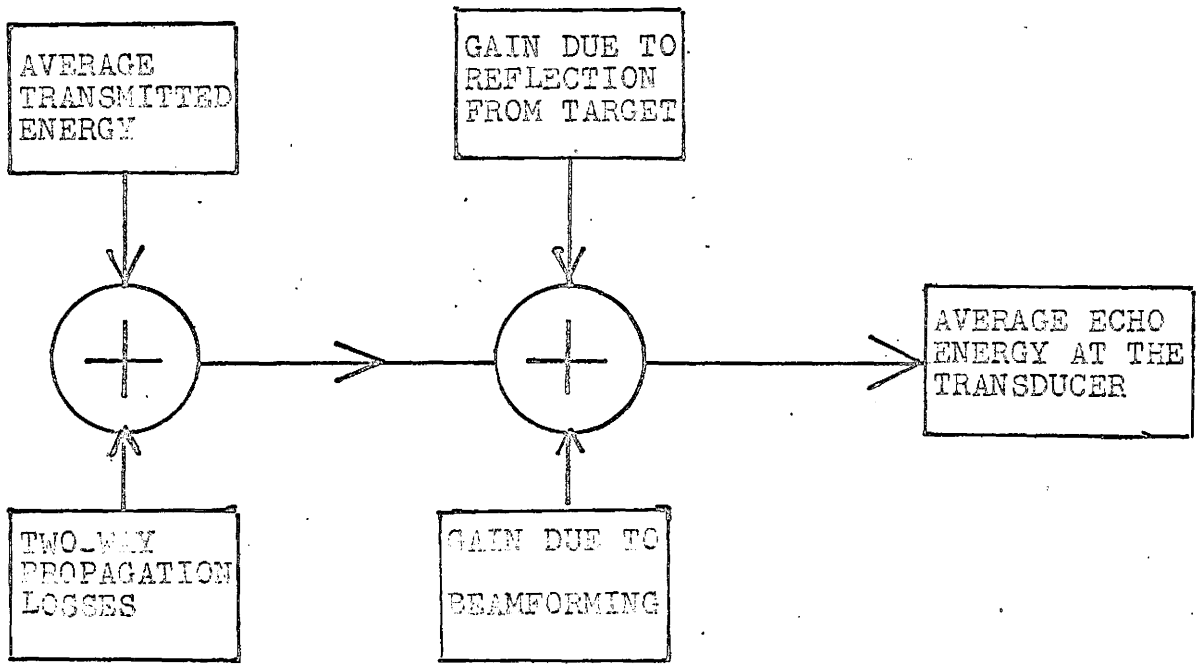

FIGURE 7 RIGID MODEL FOR ECHO ENERGY

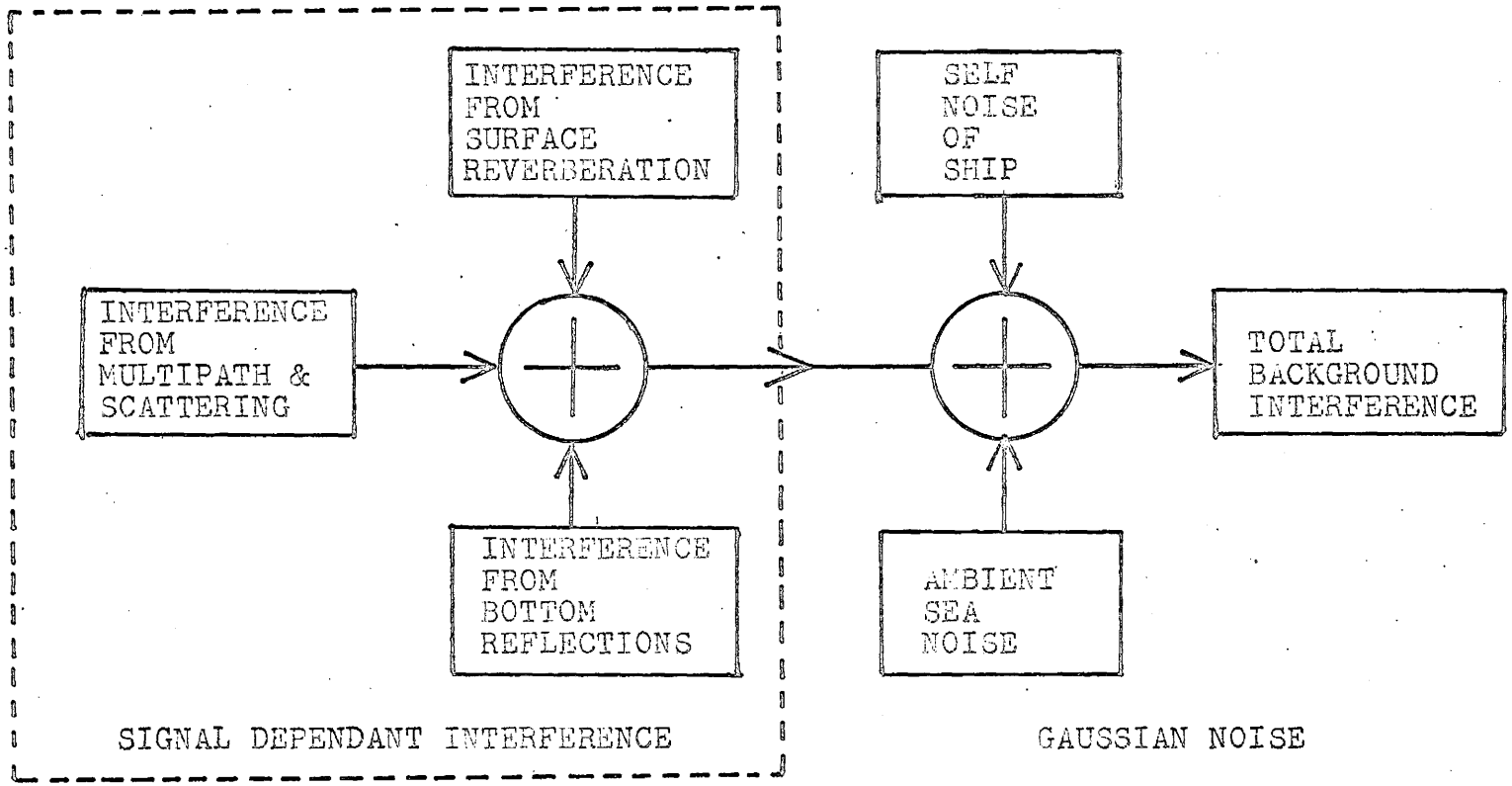

FIGURE 8

RIGID MODEL FOR INTERFERENCE ENERGY

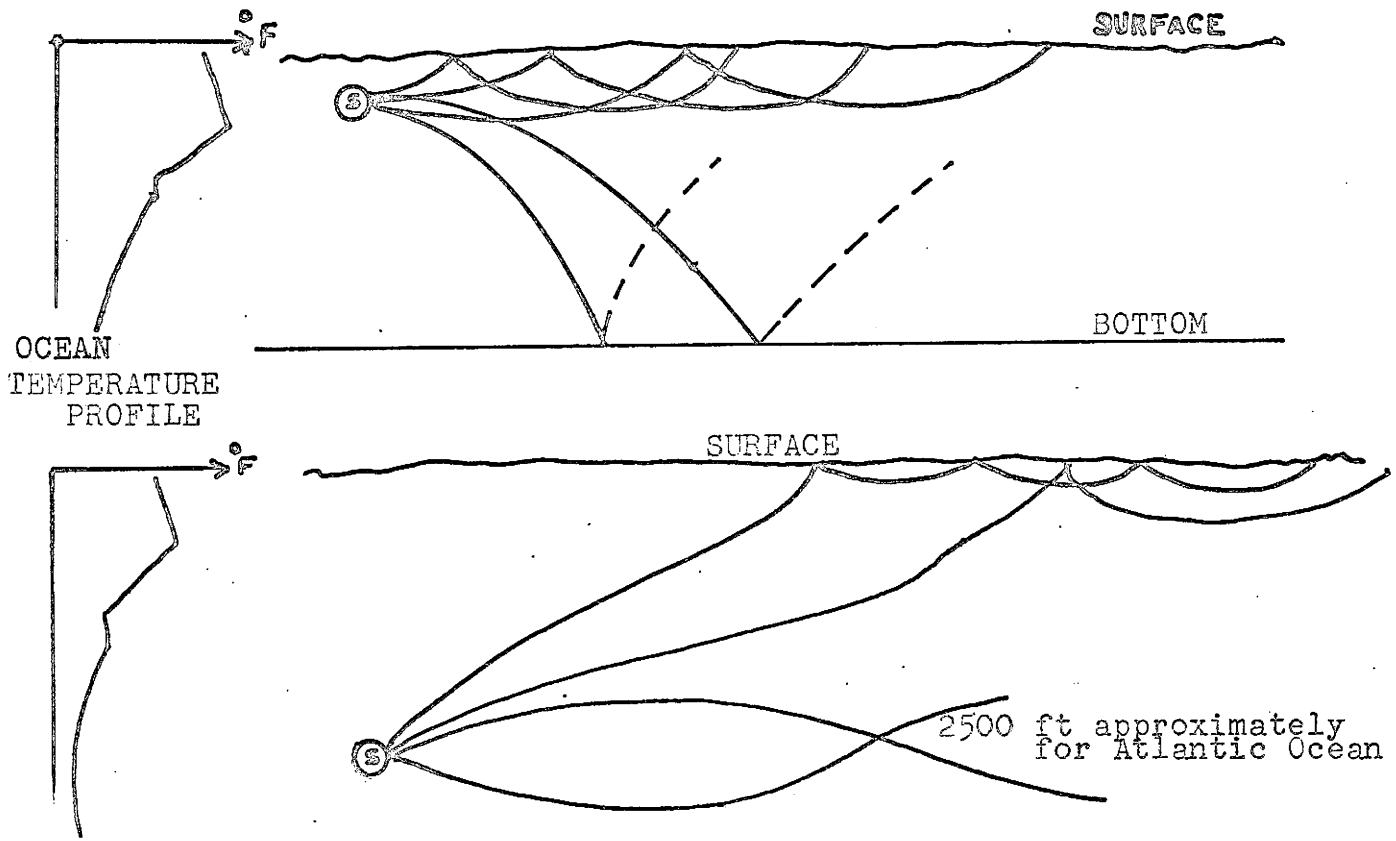

FIG 9. RAY PATHS IN A TEMPERATURE STRUCTURED OCEAN

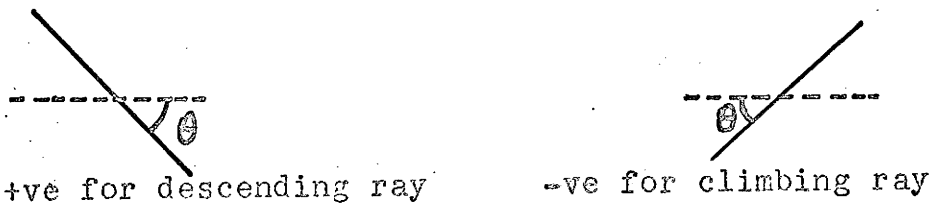

(a) SIGN CONVENTIONS

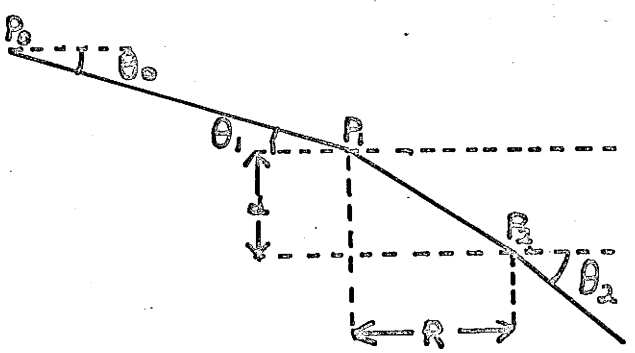

(b) REFRACTION IN A LAYER

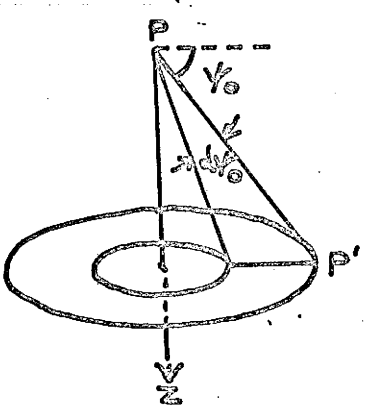

(c) INTENSITY ALONG A RAY PATH

FIG 10 CONVENTIONS USED IN RAY PATH TRACING

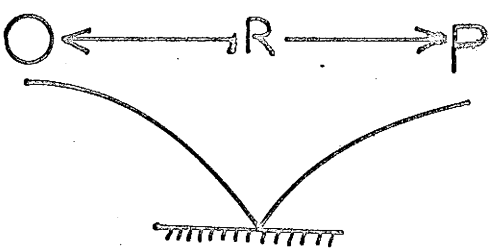

A SINGLE BOTTOM REFLECTION

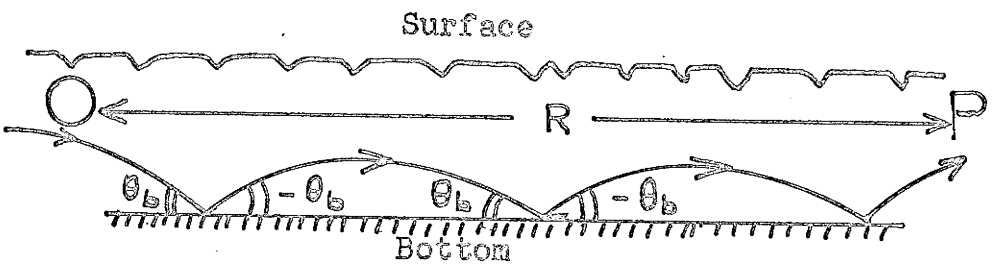

MULTIPLE BOTTOM REFLECTIONS

FIG 11 SOUND RAYS SHOWING BOTTOM REFLECTIONS

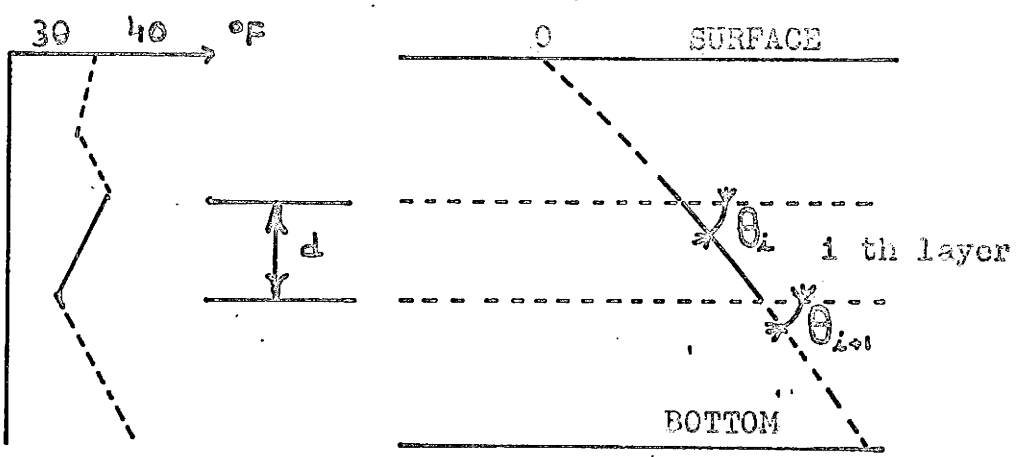

FIGURE 12 RAY PATH in the i th LAYER

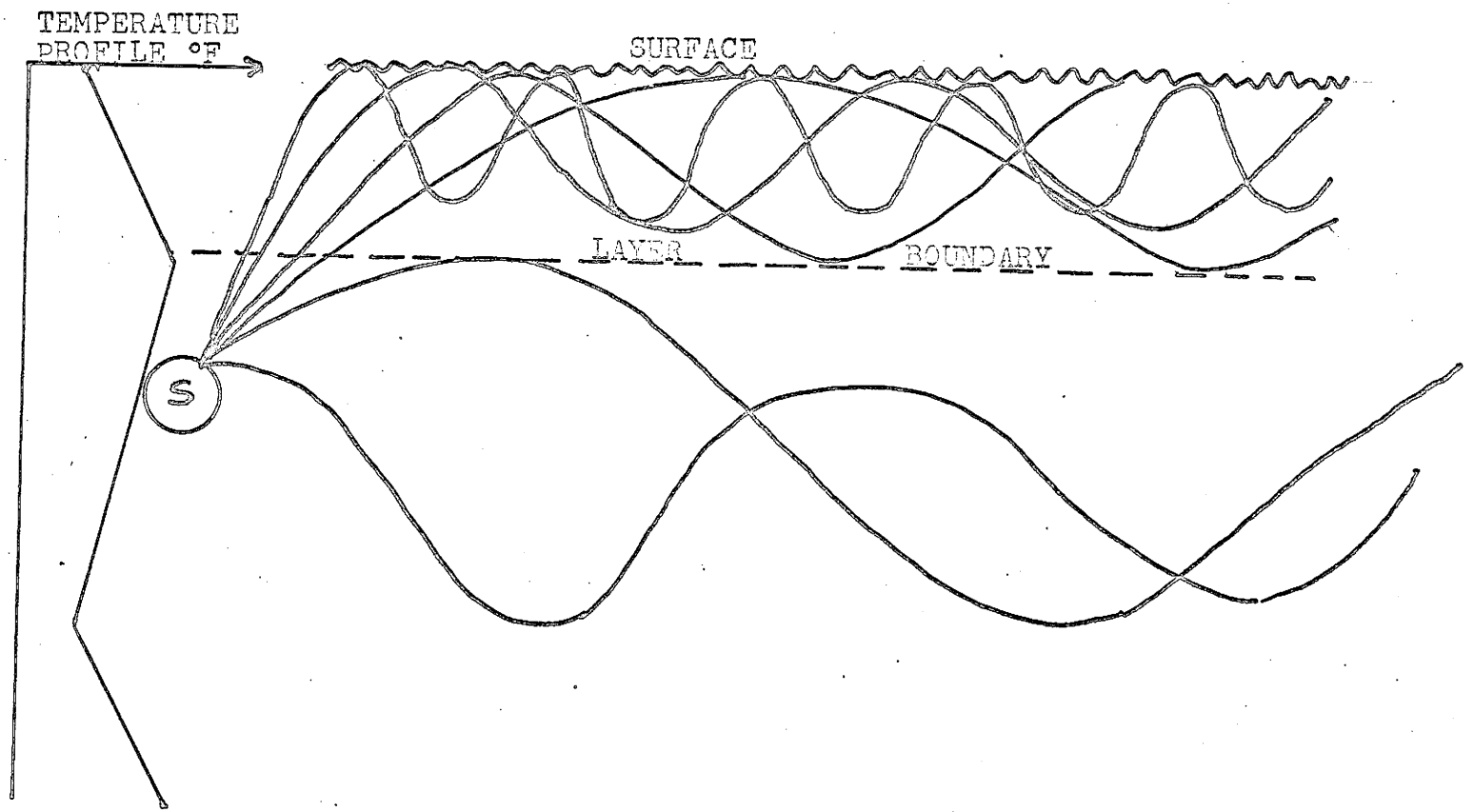

FIGURE 13

CYLINDRICAL SPREADING

FIGURE 14. ABSORPTION COEFFICIENT VS. FREQUENCY

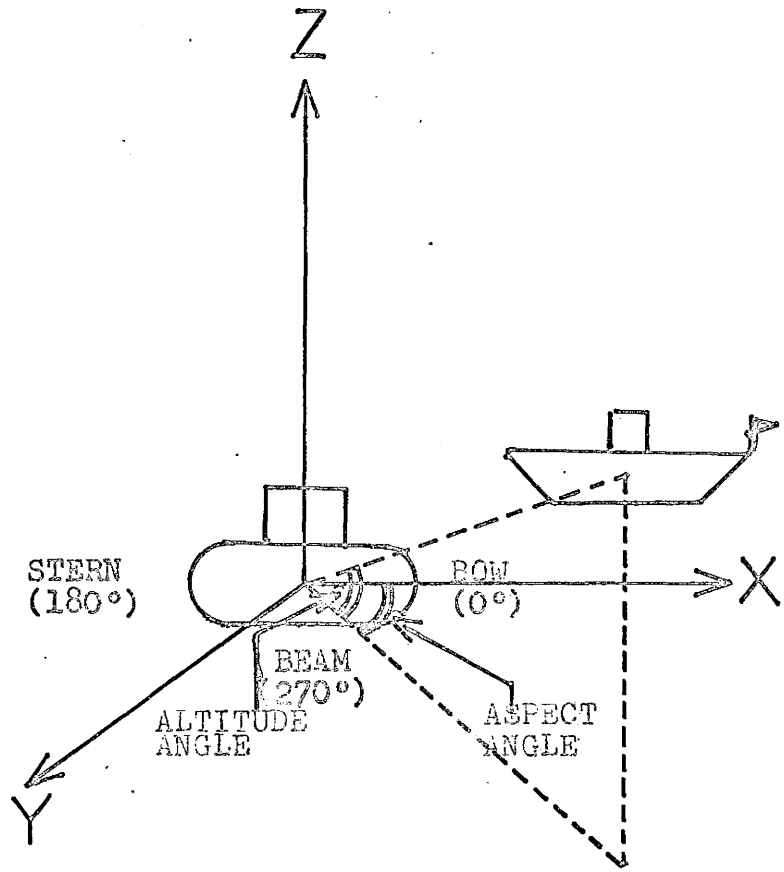

FIGURE 15 TARGET COORDINATE SYSTEM

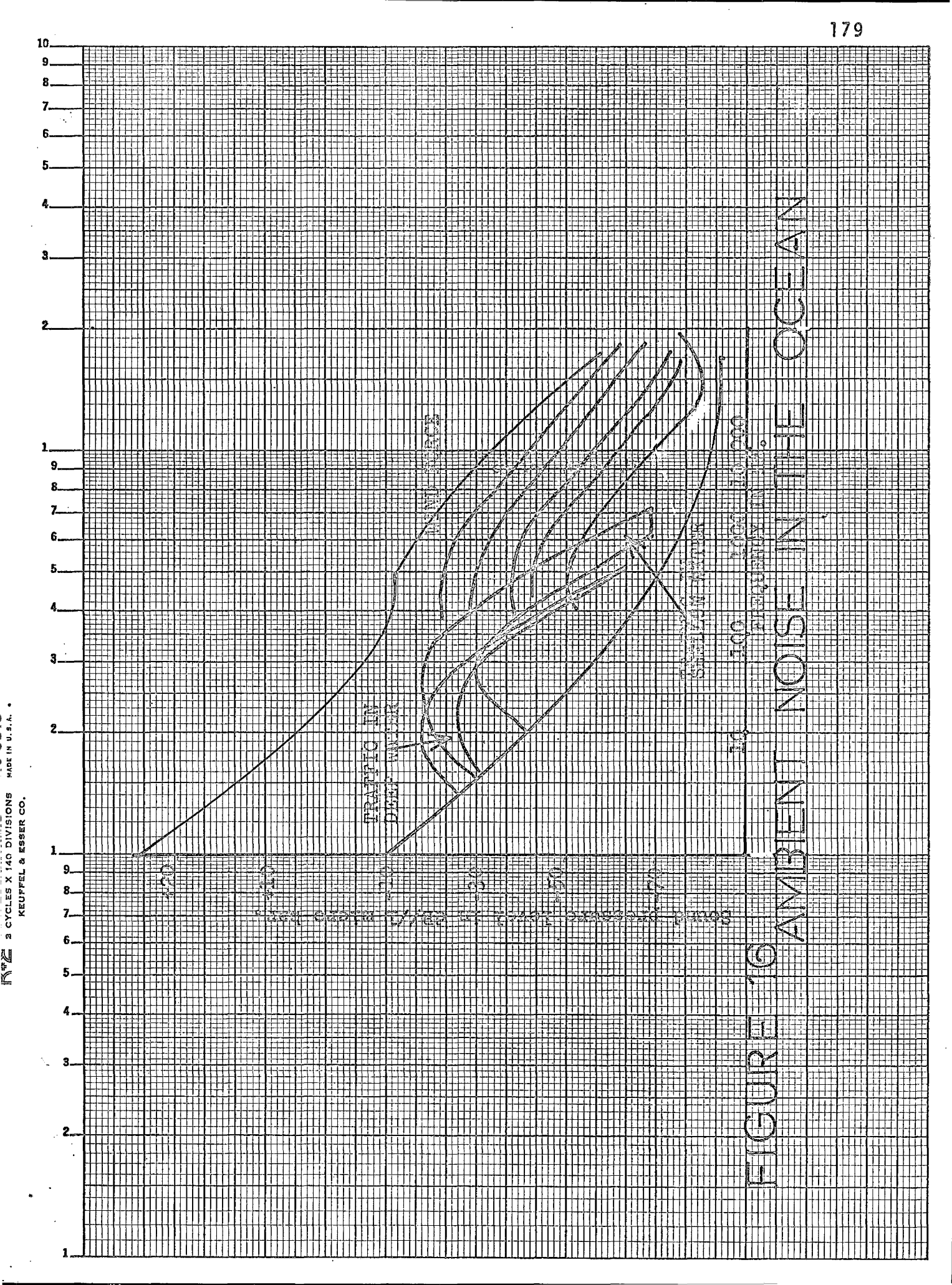

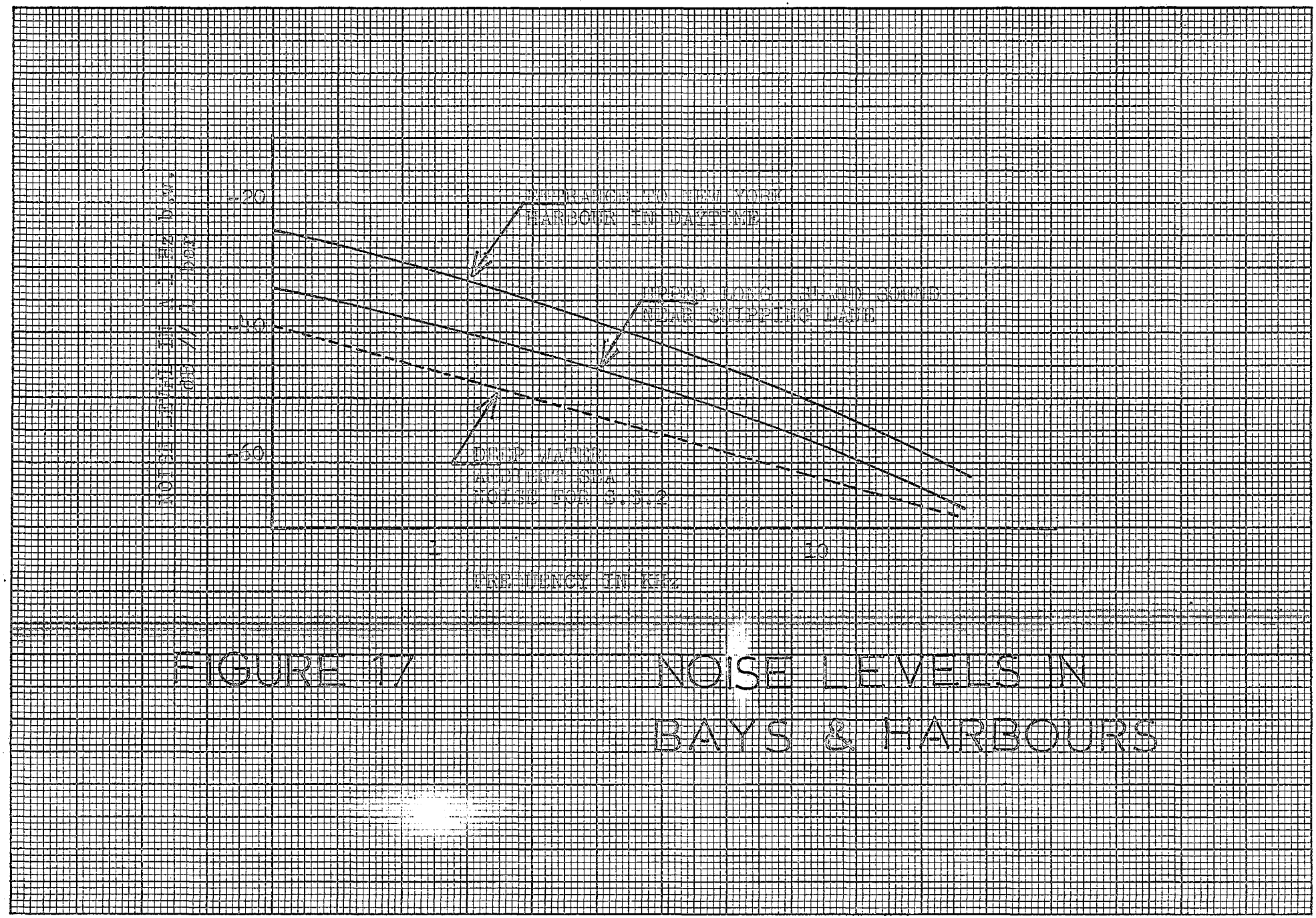

FIGURE 17 NOISE LEVELS IN BAYS & HARBOURS

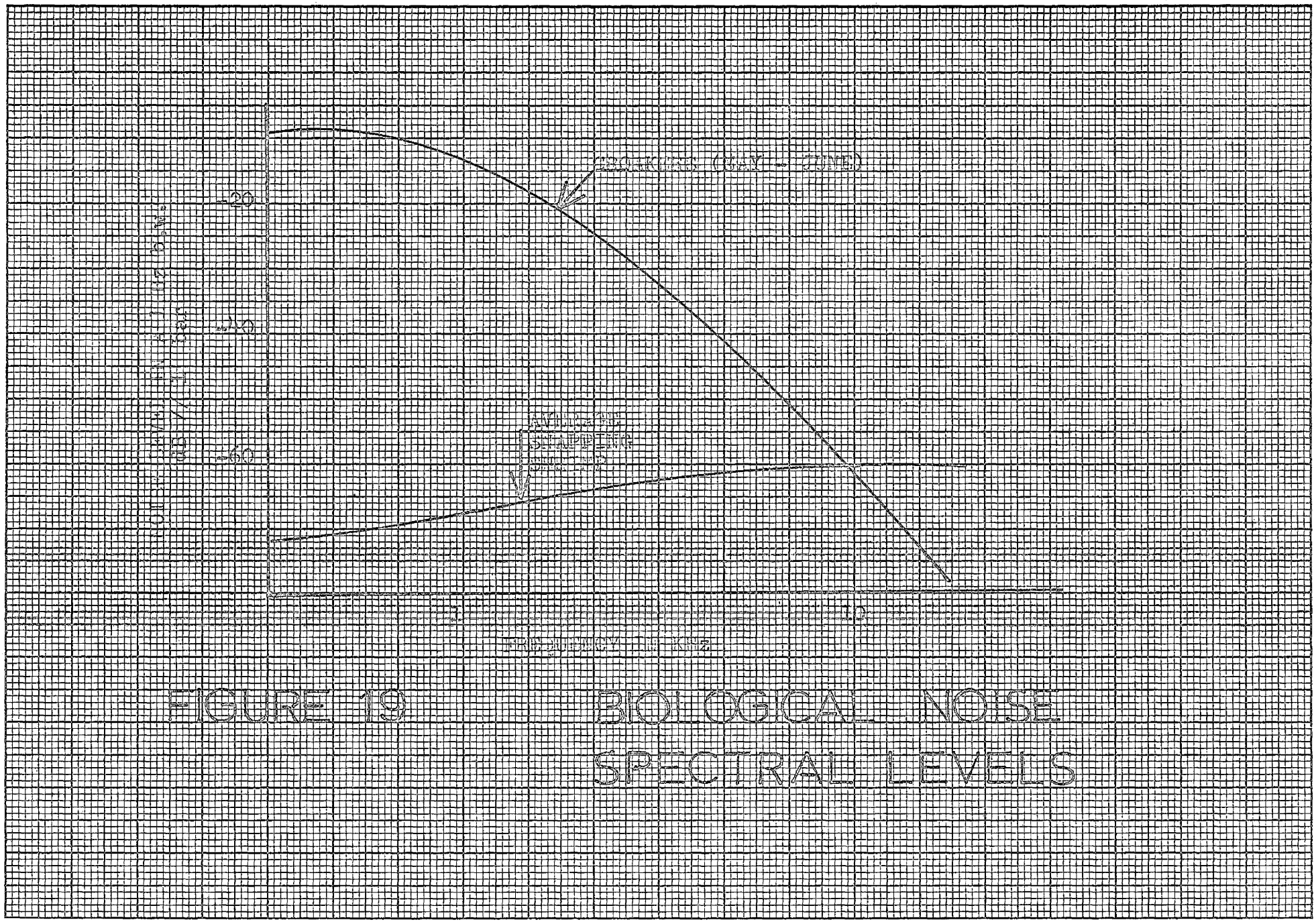

FIGURE 19 BIOLOGICAL NOISE SPECTRAL LEVELS

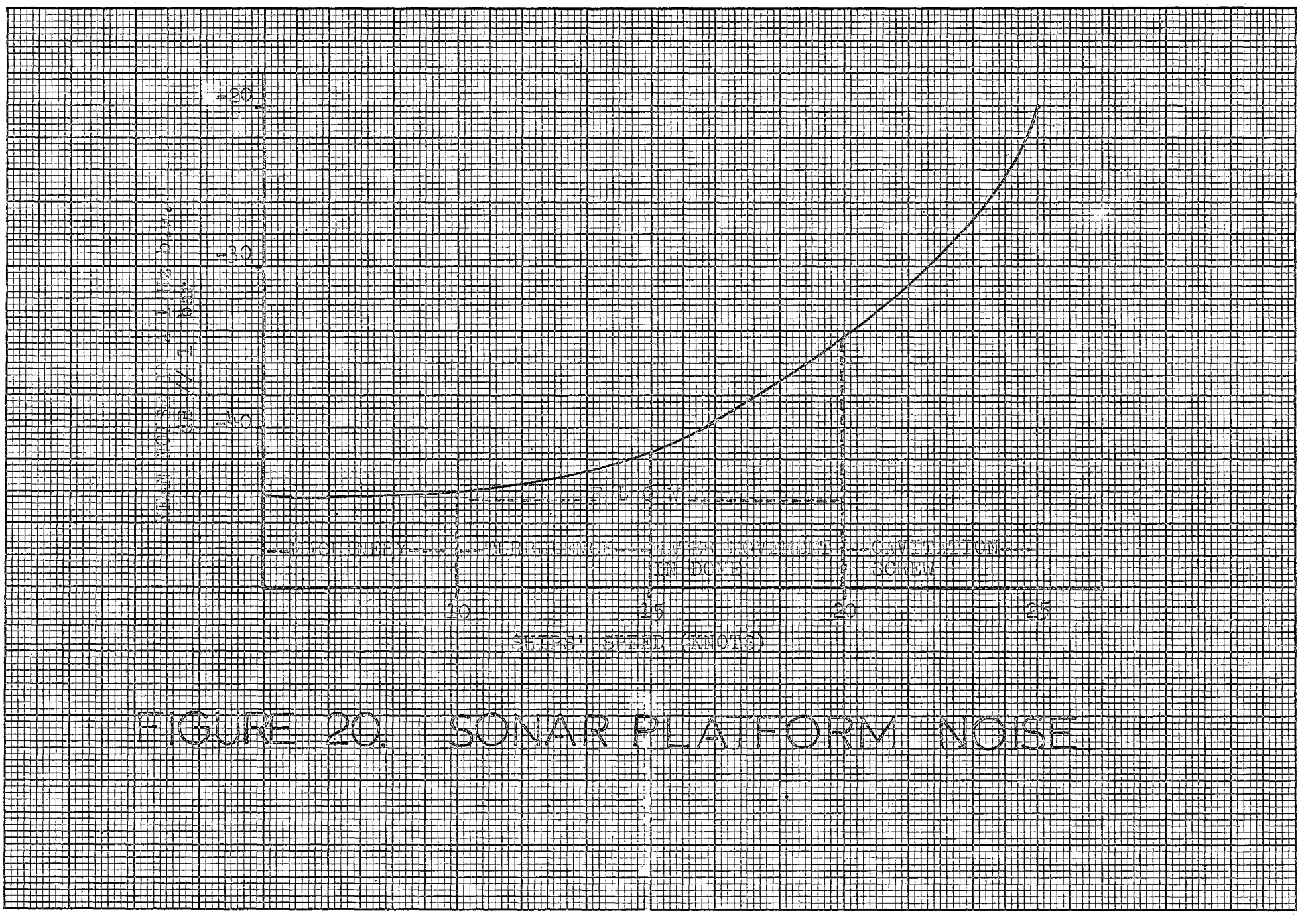

FIGURE 20. SONAR PLATFORM NOISE

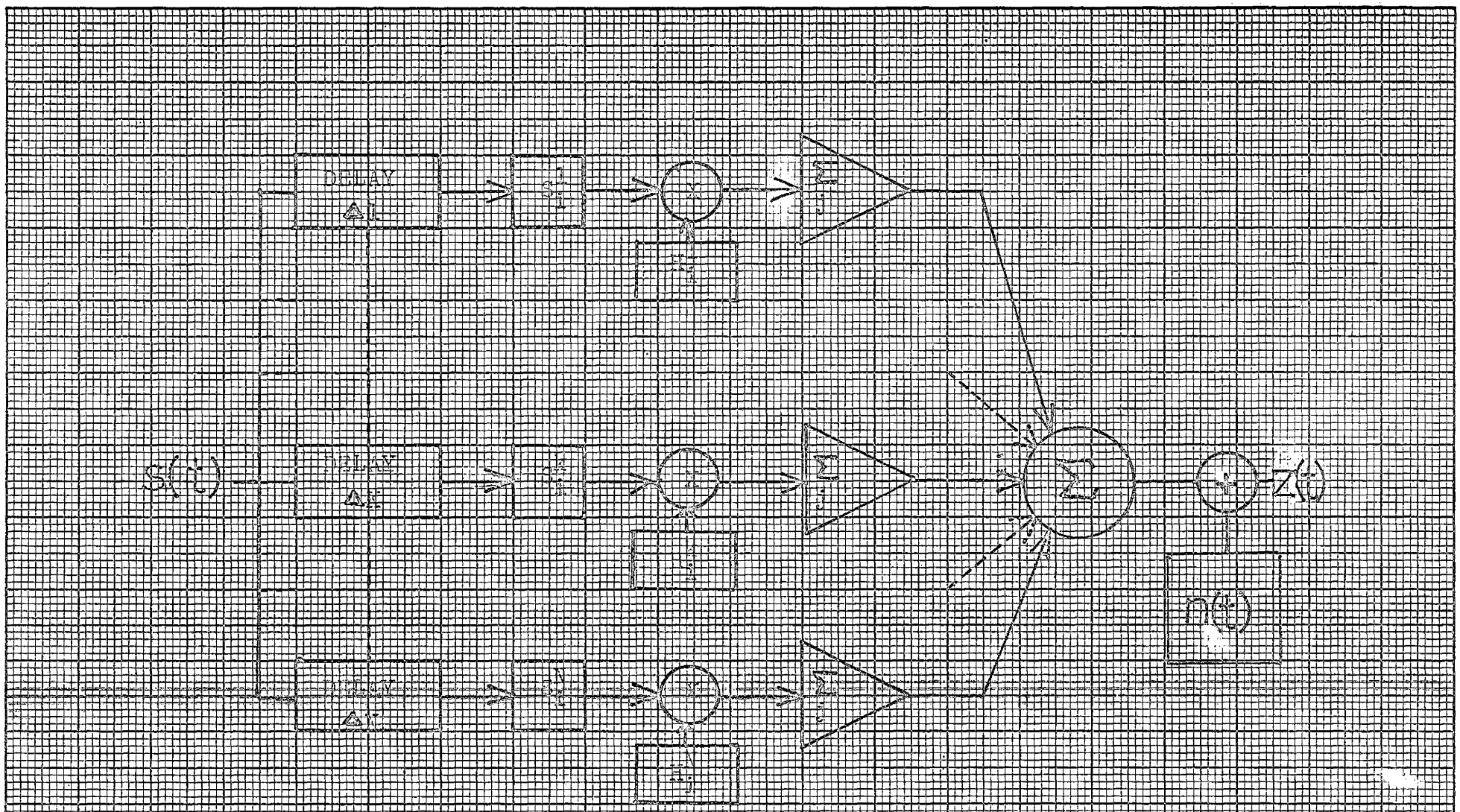

FIGURE 21 TIME VARIANT DIGITAL MODEL

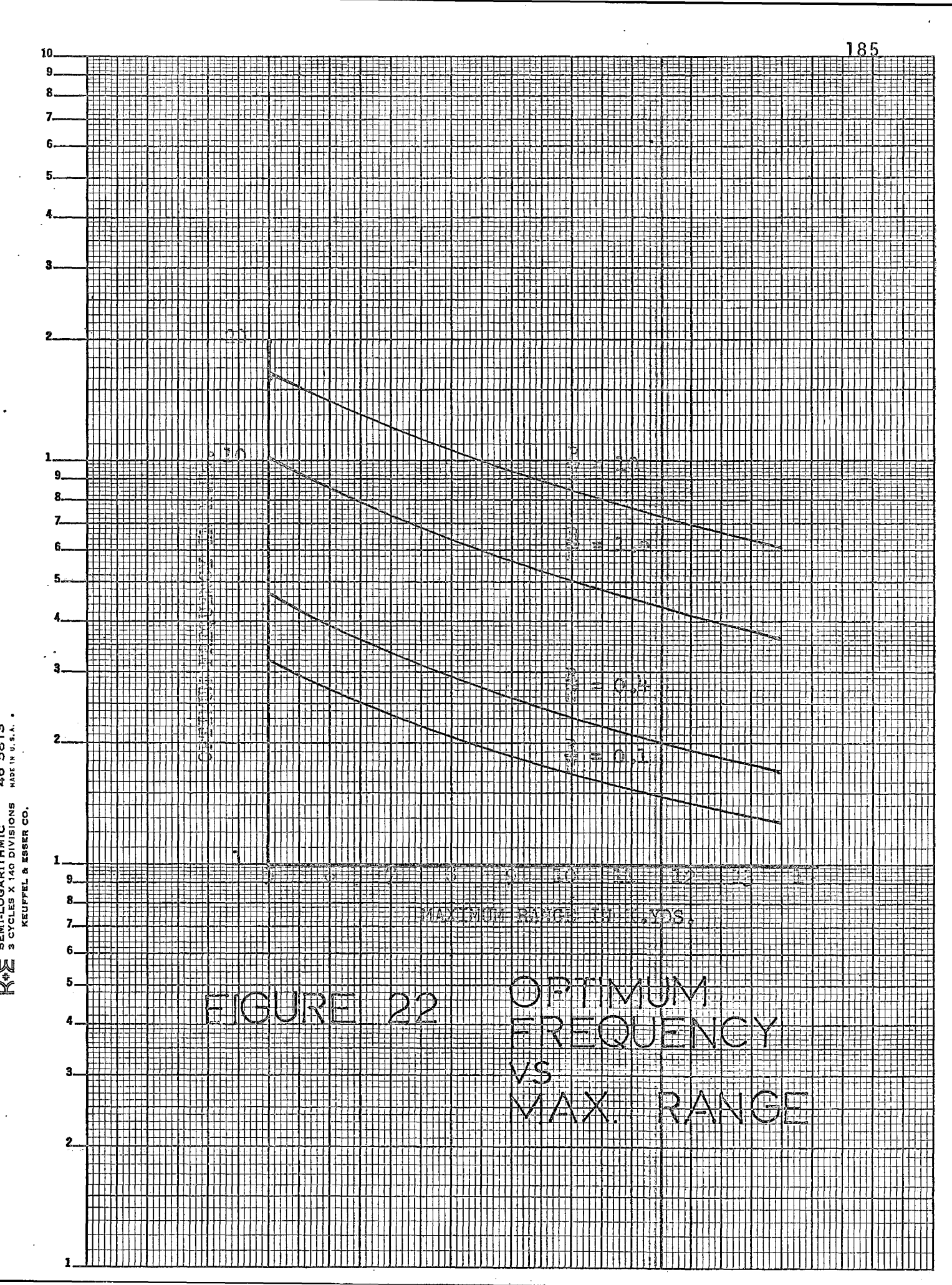

FIGURE 22 OPTIMUM FREQUENCY VS MAX. RANGE

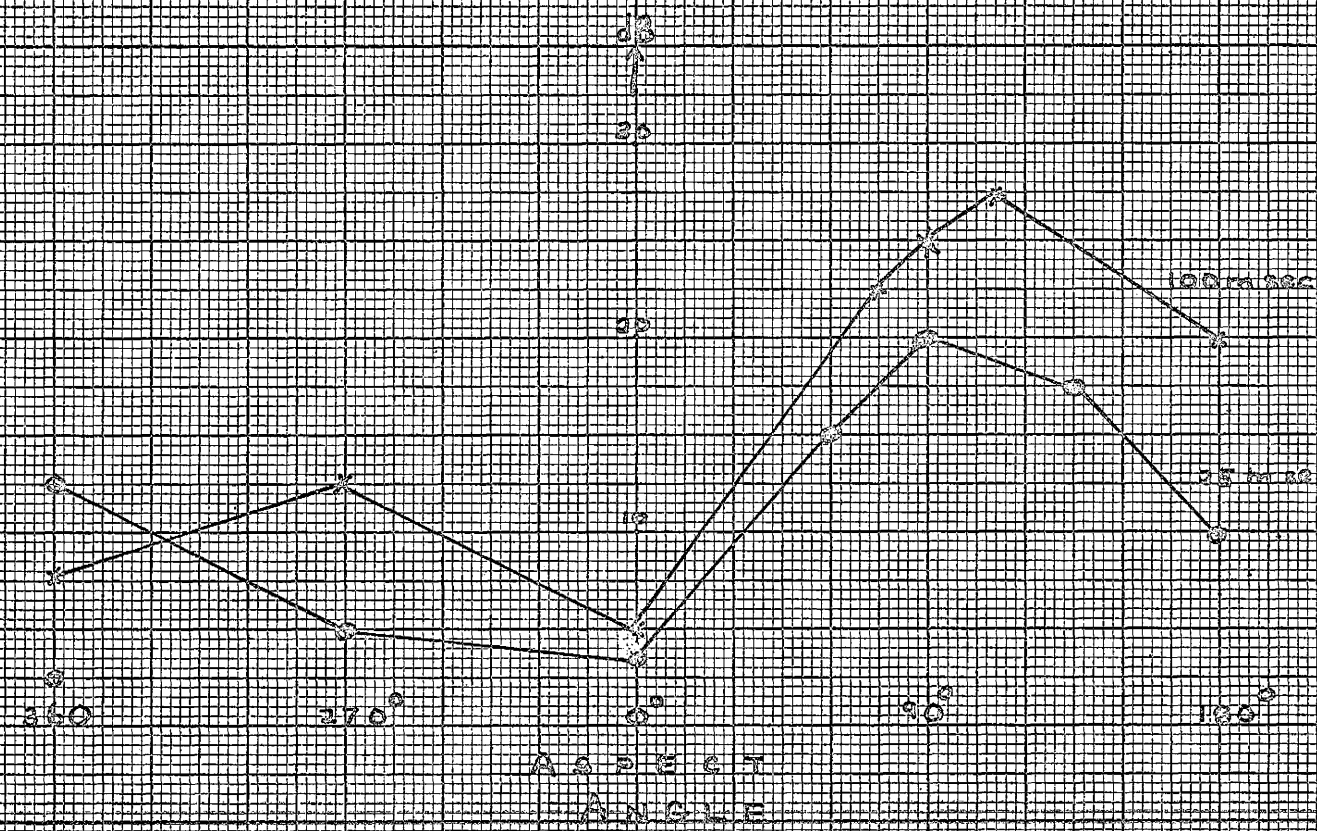

FIGURE 23 TYPICAL TARGET STRENGTHS VS ASPECT ANGLE

FIGURE 24 LOCATION 'A' DEPTH VS TEMPERATURE

FIGURE 25 LOCATION 'B' DEPTH VS TEMPERATURE

FIGURE 26 LOCATION 'C'
DEPTH-
VS
TEMPERATURE

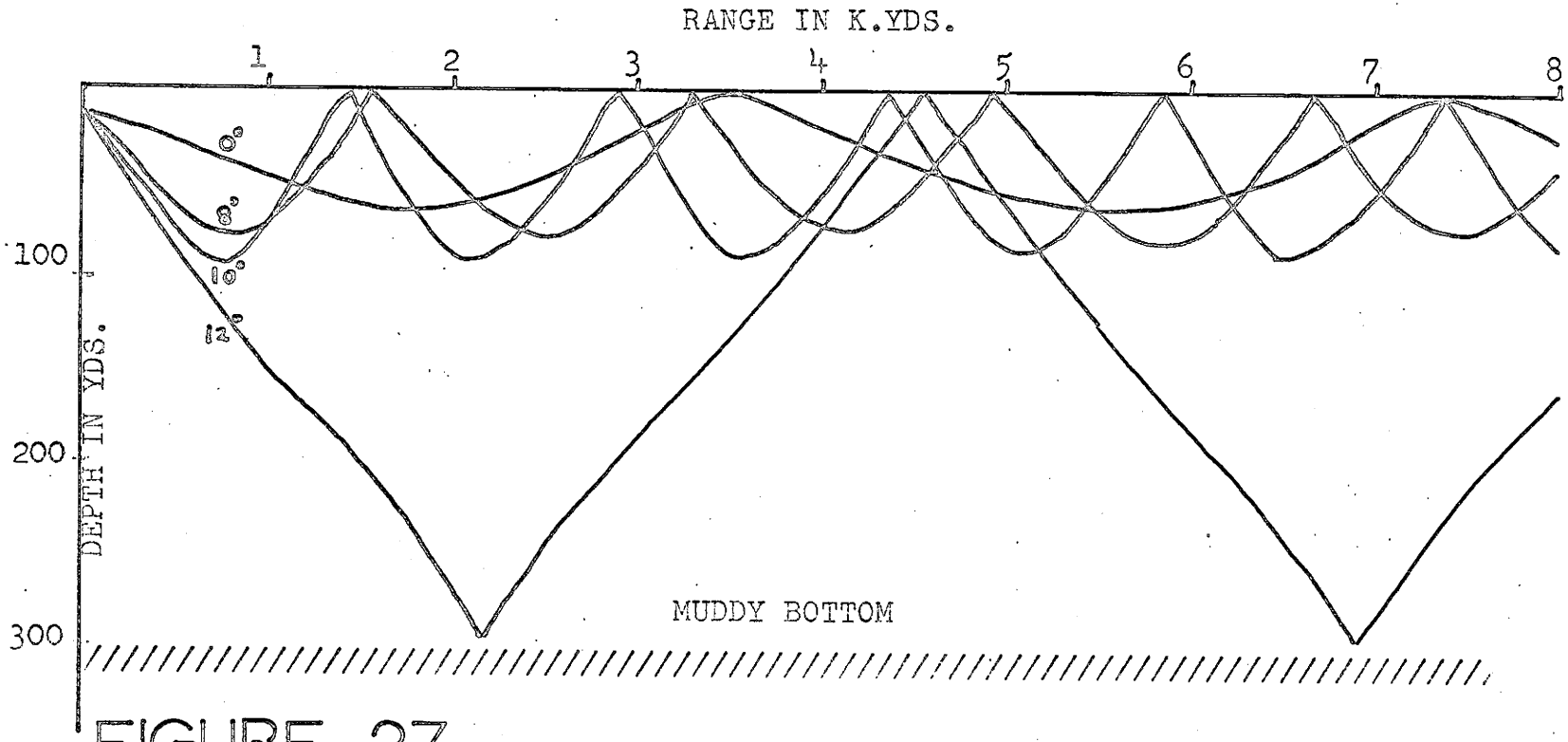

FIGURE 27 RAY PATHS FOR LOCATION 'A'

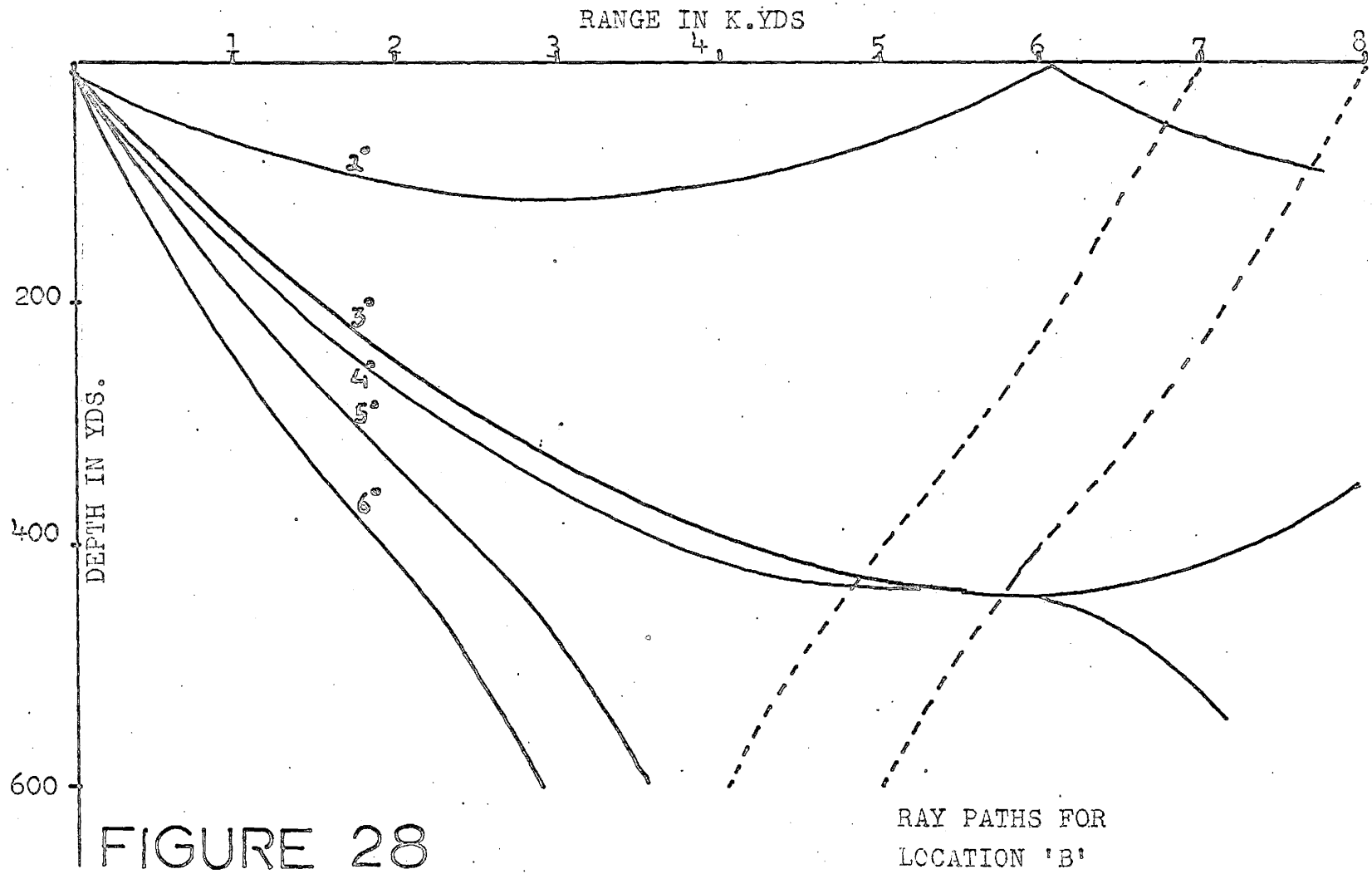

FIGURE 28

RAY PATHS FOR
LOCATION 'B'

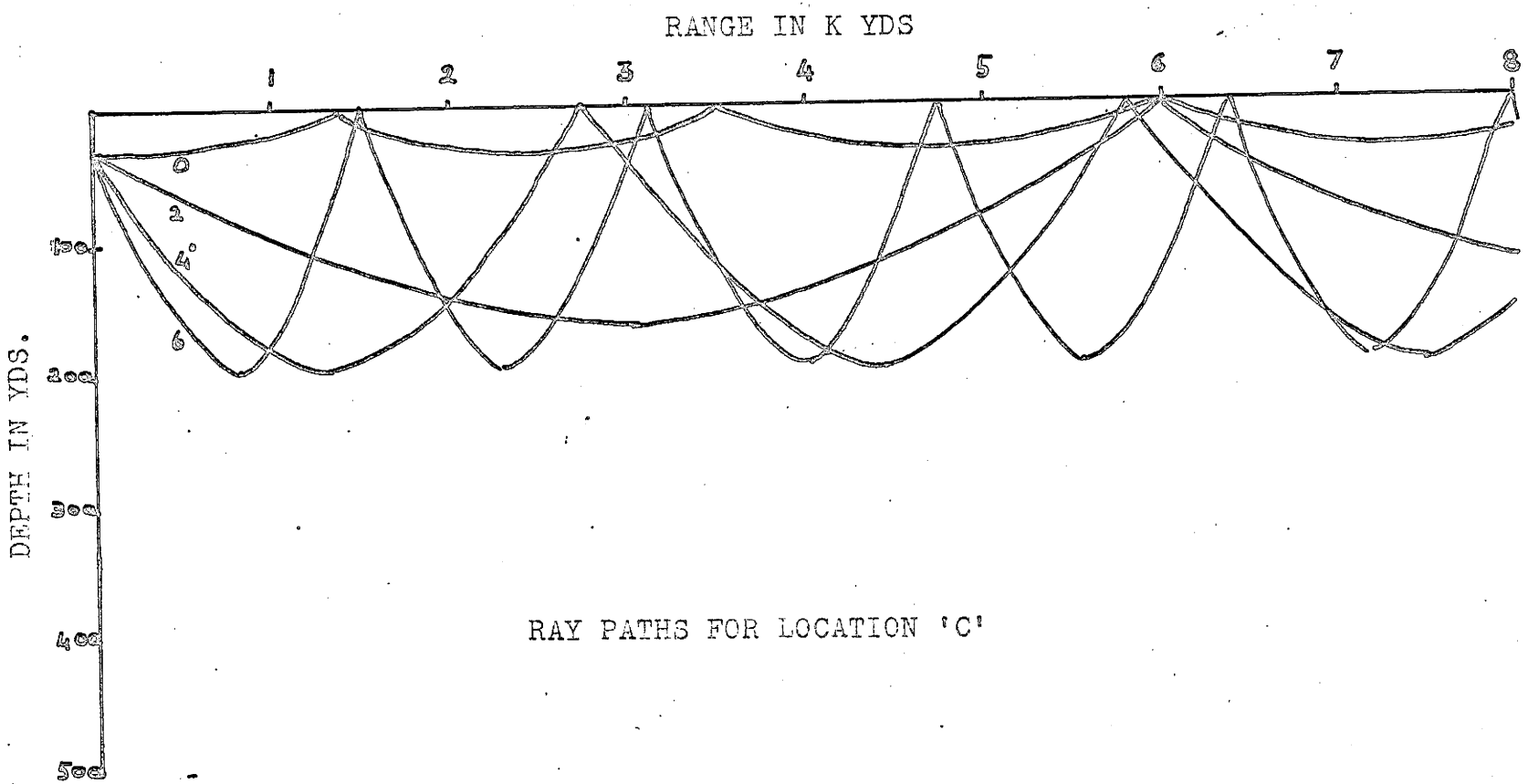

RAY PATHS FOR LOCATION 'C'

FIGURE 29

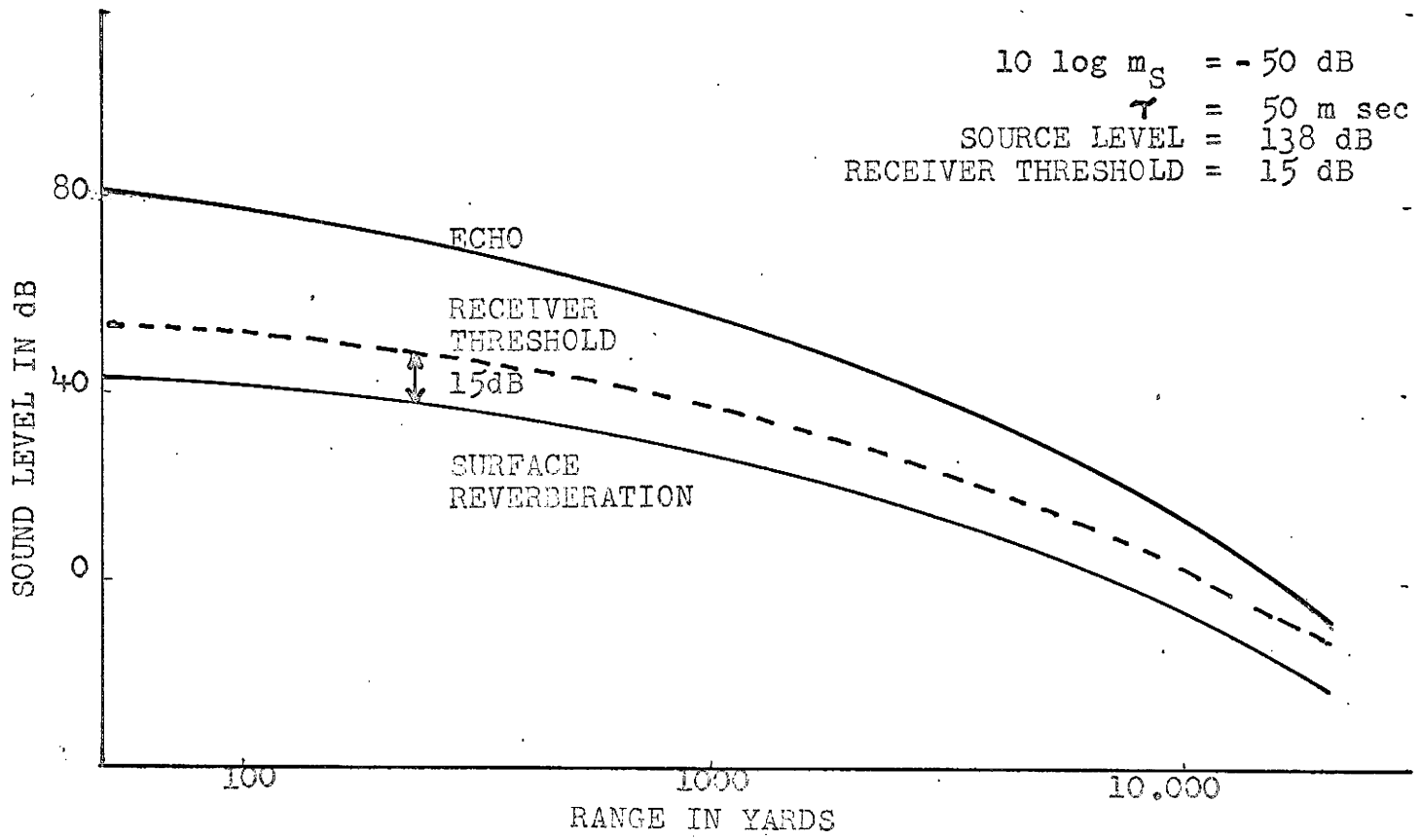

FIGURE 30 ECHO and INTERFERENCE at LOCATION 'A'

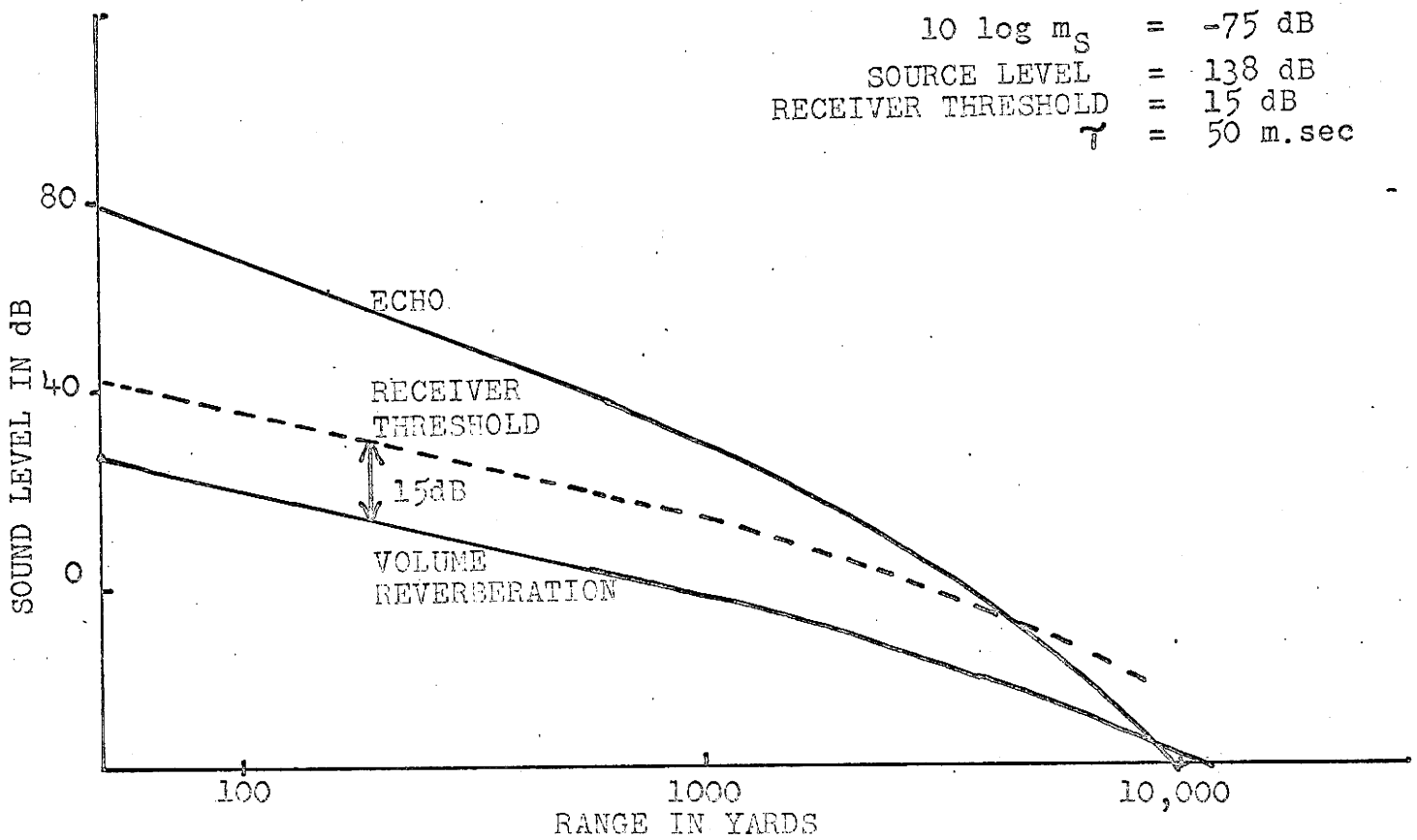

FIGURE 31 ECHO and INTERFERENCE at LOCATION 'B'

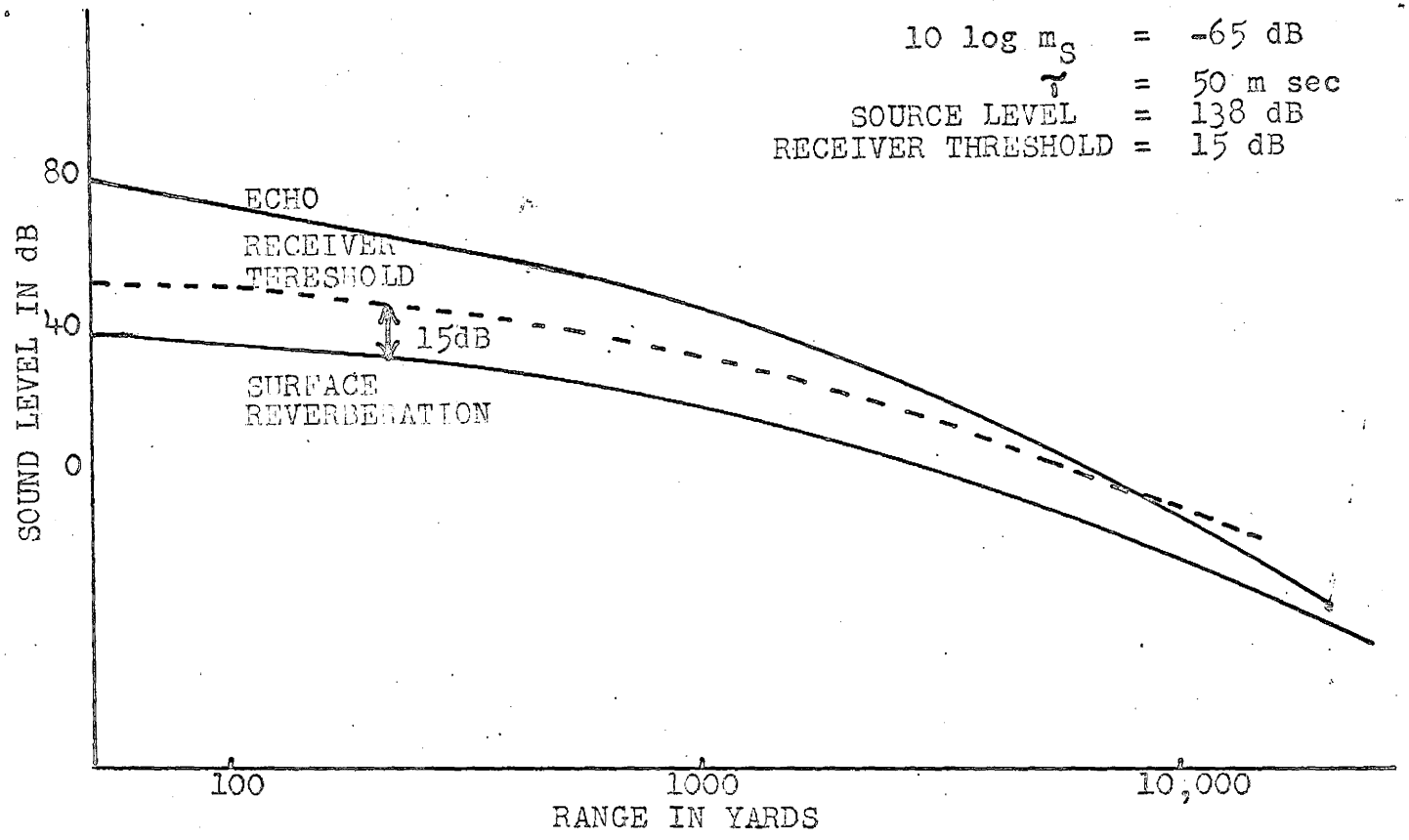

FIGURE 32 ECHO and INTERFERENCE at LOCATION 'C'